SHIP

SCIENCE & TECHNOLOGY

CIENCIA & TECNOLOGÍA DE BUQUES

ISSN 1909-8642

COTECMAR
COLOMBIA

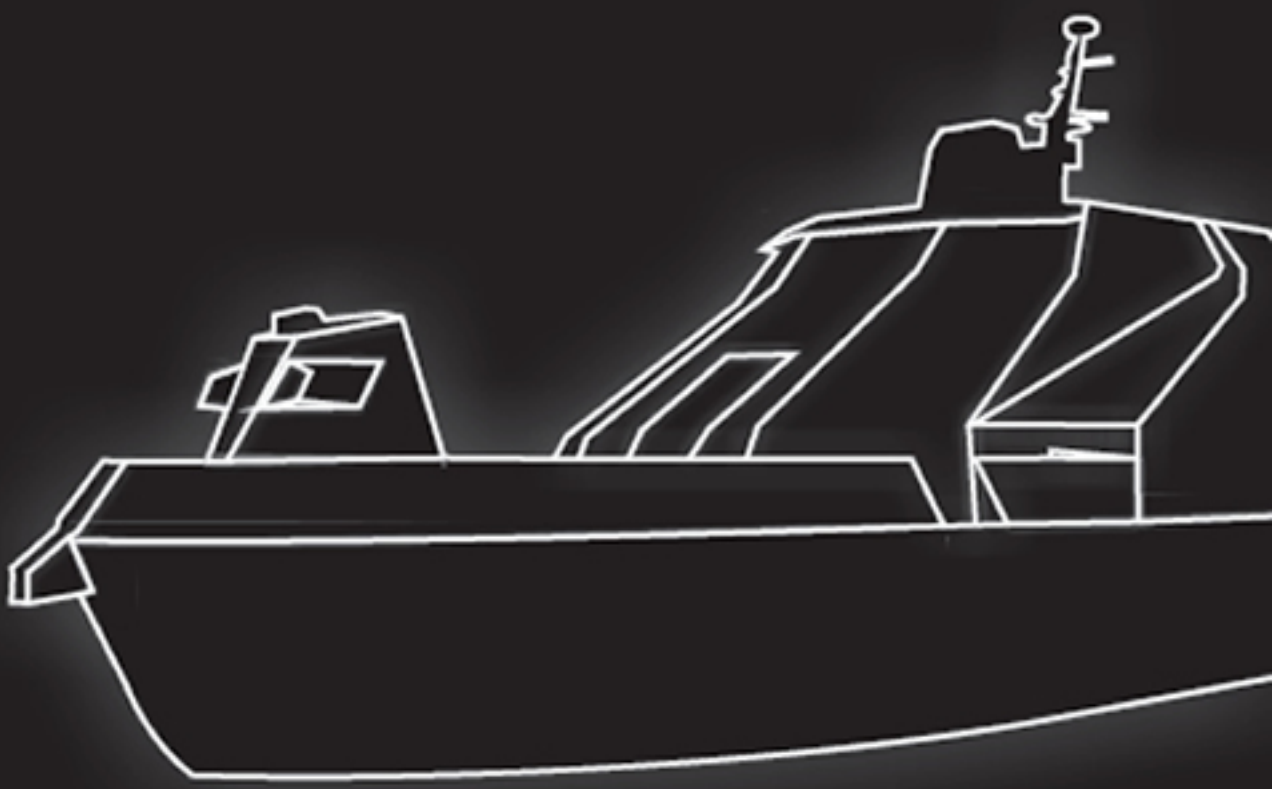

Vol. 4 - n.° 8
(1 - 84) January 2011

Cotecmar
Vol. 4 - n.° 8 - January 2011
Ship Science & Technology ISSN 1909-8642

SHIP
SCIENCE & TECHNOLOGY
CIENCIA & TECNOLOGÍA DE BUQUES

Volume 4, Number 8 | January 2011 | ISSN 1909-8642

Ship Science & Technology is a specialized journal in topics related to naval architecture, and naval, marine and ocean engineering. Every six months, the journal publishes scientific papers that constitute an original contribution in the development of the mentioned areas, resulting from research projects of the Science and Technology Corporation for the Naval, Maritime and Riverine Industries, and other institutions and researchers. It is distributed nationally and internationally by exchange or subscription.

A publication of

Corporación de Ciencia y Tecnología para el Desarrollo de la Industria Naval, Marítima y Fluvial - Cotecmar
Electronic version: www.shipjournal.co

Editorial Coordinator
Karen Domínguez Martínez. MMSc. (c)
Jimmy Saravia Arenas. MMSc. (c)

Layout and design
Mauricio Sarmiento Barreto

Printed by
C&D Publicidad & Marketing. Bogotá, D.C.

SHIP
SCIENCE & TECHNOLOGY
CIENCIA & TECNOLOGÍA DE BUQUES

Volume 4, Number 8 January 2011 ISSN 1909-8642

Scientific and Technological Research Articles
Artículos de investigación científica y tecnológica

SHIP
SCIENCE & TECHNOLOGY
CIENCIA & TECNOLOGÍA DE BUQUES

Editorial Note

Cartagena de Indias, 21 January 2011.

In 2010, the Science and Technology Corporation for the Development of the Naval, Maritime and Riverine Industry, COTECMAR accomplished ten years of existence and commitment with the development of the nation's naval, maritime, and riverine industry. Aware of the importance of working for the future, COTECMAR developed during the last year a prospective exercise to revise its Strategic Management. This activity – carried out by an interdisciplinary team of professionals in COTECMAR and from the main players of its interest groups – received methodological accompaniment from Universidad Externado de Colombia. In parallel manner, seeking to implement a support tool to the planning processes of the Corporation's science, technology, and innovation activities, a Technological Diagnostic update was conducted, which for the first time permitted determining the capacities and domain of technologies, both for its industrial activity, as well as science, technology, and innovation activities. This process was carried out jointly with the *"BioGestión"* Research Group at Universidad Nacional de Colombia.

Likewise, continuing with the objective of positioning the Corporation among the scientific community through dissemination of new knowledge, activities for the diffusion of science, technology, and innovation were promoted. These included, among others, editorial improvements to the Ship Science & Technology Journal, planning of the second International Congress on Naval Design and Engineering, the organization and execution of the first meeting of the Pan-American Advanced Studies Institute (PASI) on Dynamics and Control of Manned and Unmanned Vessels, and compliance of the agenda of diffusion events of science, technology, and innovation through ten international presentations and two participations in scientific fairs.

In this edition of Ship Science & Technology, we present partial results of two research projects conducted by COTECMAR, in collaboration with its scientific and technological partners and leveraged with resources from INDUMIL, which have allowed the Corporation and the nation to acquire new skills; these projects are Recovery of Metallic Parts by Thermal Spraying *(Recuperación de Piezas Metálicas por Proyección Térmica)* and Integrated Command and Control System for Public Forces *(Sistema Integrado de Comando y Control para las Fuerzas Públicas)*. As customary, the two articles stemming from these projects are accompanied by contributions from our collaborators throughout the nation and abroad working on issues as varied as dynamics of high-performance vessels, technologies for offshore industry and ICTs. All these articles have been subjected to an exhaustive process that guarantees compliance of scientific and editorial standards of quality, stability, visibility, and national and international recognition, seeking access to the national bibliographic index, *Publindex*, from the COLCIENCIAS Administrative Department of Science, Technology and Innovation. We hope these contents to be of interest to all our readers.

Once more, from the Ship Science & Technology journal we extend our congratulations to the whole team at the Corporation for its commitment, integrity, leadership, and continuous effort to innovate; values that have contributed along these ten years to set the bases for the development of our naval, maritime, and riverine industry.

Commander, OSCAR DARÍO TASCÓN MUÑOZ

SHIP
SCIENCE & TECHNOLOGY
CIENCIA & TECNOLOGÍA DE BUQUES

Nota Editorial

Cartagena de Indias, 21 de Enero de 2011.

En el 2010, la Corporación de Ciencia y Tecnología para el Desarrollo de la Industria Naval, Marítima y Fluvial – COTECMAR, cumplió diez años de existencia y compromiso con el desarrollo de la industria naval, marítima y fluvial del país. Consciente de la importancia de trabajar para el futuro, COTECMAR desarrolló durante el año pasado un ejercicio prospectivo para la revisión de su Direccionamiento Estratégico. Esta actividad, llevada a cabo por un equipo de profesionales interdisciplinarios de COTECMAR y de los principales actores de sus grupos de interés, tuvo el acompañamiento metodológico de la Universidad Externado de Colombia. De forma paralela, con el objetivo de implementar una herramienta de soporte a los procesos de planificación de las actividades de ciencia, tecnología e innovación de la Corporación, se realizó la actualización del Diagnóstico Tecnológico, el cual por primera vez permitió determinar las capacidades y dominio de las tecnologías, tanto para su actividad industrial como para sus actividades de ciencia, tecnología e innovación. Este proceso fue llevado a cabo en conjunto con el Grupo de Investigación "BioGestión" de la Universidad Nacional de Colombia.

De igual manera, continuando con el objetivo de posicionar a la Corporación ante la comunidad científica mediante la difusión de nuevo conocimiento, se promovieron actividades de Divulgación de Ciencia, Tecnología e Innovación. Estas incluyeron, entre otras, las mejoras editoriales a esta revista Ship Science & Technology, la planeación del segundo *Congreso Internacional de Diseño e Ingeniería Naval, la organización y ejecución del primer encuentro Panamerican Advance Studies Institute (PASI) en Dinámica y Control de Embarcaciones Tripuladas y No Tripuladas*, y el cumplimiento de la agenda de eventos de divulgación de Ciencia, Tecnología e Innovación, a través de diez ponencias internacionales y dos participaciones en ferias científicas.

En esta edición de *Ship Science & Technology* presentamos resultados parciales de dos proyectos de investigación desarrollados por COTECMAR, en colaboración con sus socios científicos y tecnológicos y apalancados con recursos de INDUMIL, los cuales le han permitido a la Corporación y al país adquirir nuevas capacidades; estos proyectos son *Recuperación de Piezas Metálicas por Proyección Térmica y Sistema Integrado de Comando y Control para las Fuerzas Pública*. Como siempre, los dos artículos producto de estos proyectos están acompañados por contribuciones de nuestros colaboradores en el país y en el exterior trabajando en temas tan variados como dinámica de embarcaciones de alto desempeño, tecnologías para la industria offshore y TICs. Todos estos artículos han sido sometidos a un exhaustivo proceso que garantiza el cumplimiento de los estándares de calidad científica y editorial, estabilidad, visibilidad y reconocimiento nacional e internacional, con miras a acceder al índice bibliográfico Nacional, Publindex, del Departamento Administrativo de Ciencia, Tecnología e Innovación – Colciencias. Esperamos que este contenido sea del interés de todos nuestros lectores.

Una vez más extendemos desde la revista *Ship Science & Technology* una felicitación a todo el equipo de la Corporación por su compromiso, su integridad, su liderazgo y su esfuerzo continuo por innovar, valores que han contribuido durante estos diez años a sentar las bases para el desarrollo de nuestra industria naval, marítima y fluvial.

Capitán de Fragata OSCAR DARÍO TASCÓN MUÑOZ

Passenger Submarine Concept Design for Oil Production Offshore Systems

Diseño conceptual de submarinos de pasajeros para sistemas oceánicos de producción petrolera

Thiago Lobão de Almeida [1]
Victor Coracini Tonacio [2]

Abstract

The paper proposes an innovative solution to transport workers of offshore oil production platforms from the coast to their units, which operate at the Pre-Salt exploration, 300 km from the coast. A passenger submarine concept design was developed, justified by the range of practical obstacles observed in the current modes of transportation, helicopters and supply boats. Requirements like operational depth (100 m), passenger capacity (250 people), and cruising speed (minimum 13.4 knots) are defined, based on estimates. Firstly, it seeks the adoption of air-independent propulsion (AIP) systems, by fuel cells (PEMFC). However, the work progress leads to an entire electric propulsion system. The internal arrangement is elaborated, regarding passenger comfort, structural constraints, allocation of batteries and ballast tanks. Then, after a hydrodynamic hull optimization, by Computational Fluid Dynamics analysis, we provide a final configuration with 100-m length and 9.7-m diameter, operational speed of 16 kt, and autonomy of 26 hours.

Key words: Passenger submarine concept design; Manpower flow in offshore systems; CFD analysis.

Resumen

El documento propone una solución innovadora para el transporte de los trabajadores de las plataformas de producción de petróleo en alta mar a sus unidades, que operan en la exploración pre-sal, a 300 kilómetros de la costa. El proyecto conceptual de un submarino de pasajeros se desarrolló, justificado por la serie de obstáculos prácticos observados en los medios de transporte actuales, helicópteros y barcos de suministro. Requisitos como la profundidad operativa (100 m), la capacidad de pasajeros (250 personas) y la velocidad de crucero (un mínimo de 13,4 nudos) se definen, con base en estimaciones. Al comienzo, se propone la adopción de sistemas de propulsión independiente del aire (AIP), por las celdas de combustible (PEMFC). Sin embargo, la evolución del trabajo conduce a un sistema de propulsión eléctrica completa. La disposición interior es elaborada con respecto a la comodidad del pasajero, las limitaciones estructurales, la asignación de las baterías y tanques de lastre. Entonces, después de una optimización del casco hidrodinámico, mediante el análisis Computacional de Dinámica de Fluidos, se presenta una configuración final con 100 m de longitud y 9,7 m de diámetro, 16 kt como la velocidad de funcionamiento y una autonomía de 26 horas.

Palabras claves: Proyecto conceptual de un submarino de pasajeros; Flujo de mano de obra en sistemas en alta mar; Análisis CFD.

Date received: November 28th, 2010 - *Fecha de recepción: 28 de noviembre de 2010*
Date Accepted: December 15th, 2010 - *Fecha de aceptación: 15 de diciembre de 2010*

[1] Universidade de São Paulo. Brazil. e-mail: thiago.lobao@poli.usp.br
[2] Universidade de São Paulo. Brazil. e-mail: vtonacio@usp.br

Introduction

Within the current Brazilian context, a unique opportunity has been noted: increased oil production since the discovery of petroleum reserves in the pre-salt area, demanding a greater flow of human resources between the coast and the offshore units.

Current Solutions

Currently, two alternatives exist, supply boats and helicopters. These possibilities, however, face a series of setbacks. For helicopters, the problems include low passenger capacity per vehicle, high variable cost, dangers of landing on platforms, and infeasibility under adverse weather conditions. For boats, the main obstacles are high discomfort, poor transition systems, risk of collisions, and climatic constraints.

Alternative Proposal

To avoid wave influences, which cause uncomfortable journeys, the possibility of adopting an underwater mode of transport, a submarine, was pondered. A range of submerged transition alternative proposals are being developed to solve the boarding issues. The main approach consists of a trail to conduct the vehicle untilthe Floating Production Storage Offload (FPSO) platform, dispensing the need toconstruct submerged complex systems like elevator cylinders.

Methodology

The spiral design for submarines waspresented by Jackson (1992). Before dimensional estimates, the analysis focuses on the conditions of null buoyancy. The spiral begins with the verification of the balance between submerged displacement, weight, and ballast. Then, the work proceeds to dimensional estimates. The definition of hull form permits estimating water resistance at a proposed speed. The analysis of a series of helices enables hull-propeller-motor interaction. Hence, the nominal engine power required is obtained. With the propulsion subsystems estimated, the internal arrangement of the hull is elaborated, analyzed in terms of weight distribution and structural aspects.

In this project, however, in which the strictly military modules are discarded and new modules for passenger accommodation have to be developed, there is no way to rely on the initial estimates of weights presented in the literature. This fact implies

Figure 1. Methodology Organizational Diagram

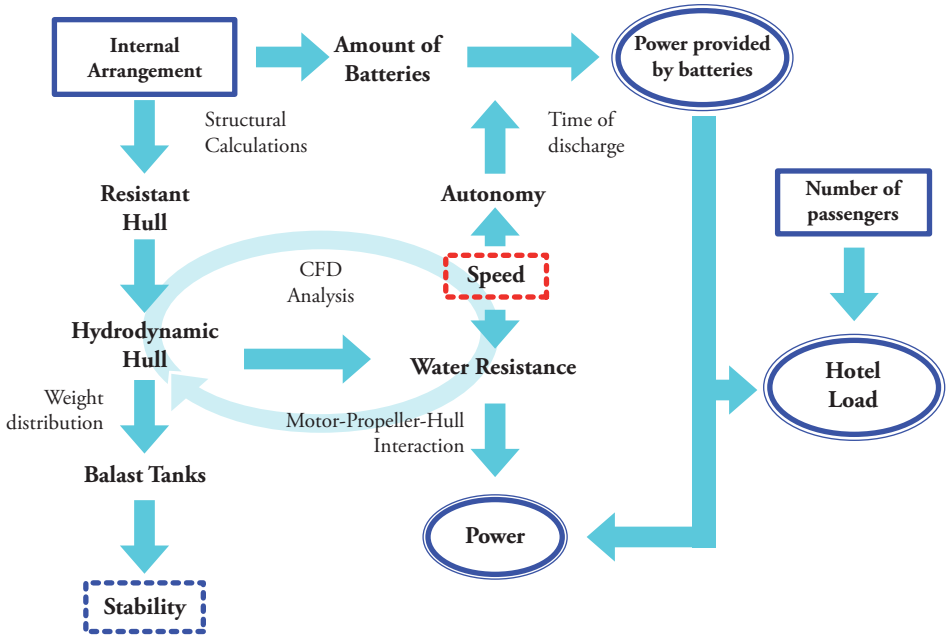

the creation of an alternative approach, represented by Figure 1. The new sequence of activities begins with the proposal of the internal arrangement, the leading element related to people transportation.

Project Requirements

The estimates related to project requirements are supported by the theory of hydrodynamics and practical context data, always following guidelines according to Brazil's current oil exploration policies. The proposals assumed to achieve the final results herein exposed are specified in detail in Tonacio & Almeida (2010).

Table 1. Project Requirements

Depth	65 m<H<200 m; 100 m adopted
Length	50 m<L<170 m
Diameter	4.5 m<D<13 m
Passenger Capacity	At least 250 people
Speed	Minimum 13.4 knt

First Spiral Design

The First Spiral Design, whose details can also be thoroughly checked in Tonacio & Almeida (2010), begins with the definition of available space for passengers along the resistant body. This first conscious calculation of the necessary area enables comparing other existent submarine hulls, seeking to select the most proper case that facilitates achieving numerical estimates (submerged volume, displacement, water resistance, and power). In this case, the Type 212 German Series stood out as the most helpful reference. Primarily, the intention of an exclusive AIP propulsion system was analyzed, looking for advantages and negative points among the different options described in the academic literature. The Polymeric Fuel Cell (PEMFC) system was recognized as the greatest opportunity for future submarine designs. Thus, a first propulsion plant using this sort of energy source (Adams, 1990) was idealized. However, the design weight distribution was compromised due to the lightweight characteristics of the PEMFC, requiring an excessive ballast cargo. In essence, the results lead to the implementation of a refining second spiral design.

Second Spiral Design

Introduction

The project's second phase sought two main objectives: to provide more comfortable and harmonious environments to passengers and to compensate for the huge and light volume destined for passengers by using a heavier propulsion alternative.

New Propulsion System

As already cited, the light PEMFC propulsion option has to be replaced by another heavier alternative, so we now propose an electric propulsion system, powered exclusively by batteries.

The search for a new engine, which keeps the innovative character sought by this project, points to a new electric motor technology, High-Temperature Superconductor (HTS). This new motor model has been destined for the marine industry and provides a weight and volume reduction of nearly 70% and 50%, respectively, in comparison with traditional electric motors.

Currently, two HTS motor configurations are being commercialized, *i.e.*, 5MW and 36.5MW motors. Considering the power resulting from the past spiral design, the first option is close to the project's necessity and can allow higher operationspeed, depending on the amount of batteries allocated. Therefore, the adoption of the HTS motor (5MW), with 23 tons and 2.5m x 1.9m x 1.9m (DxWxH) is perfectly suitable.

According to the necessity for precise maneuverability,two 360°bow thrusters installed at the bottom of the hull (one in front and another in the back) were adopted to give the submarinemore mobility, especially at the moment of the Submarine-Platform coupling. The following

illustration shows the principle of operation of the Veth-Steering Grid, the most suitable model for this objective.

Figure 2. Bow thruster´s principle of operation

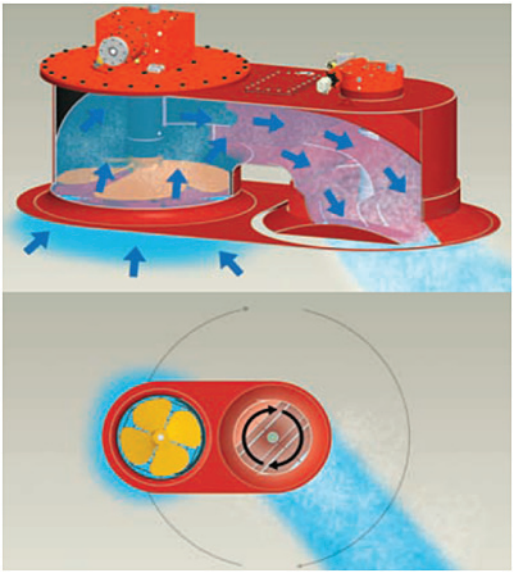

The choice of batteries mustconsider energy, access, volume, and weight aspects. The first model of energy source foundincluded lead batteries manufactured by Sepang, traditionally used in submarines. They are heavy (395 Kg), allow for top access and have an elongated format (29x30x150cm - LxWxH); thus, they are appropriate for allocation at the bottom of the PMB hull.

In certain places of this submarine, top access is not advantageous. Therefore, we looked for batteries with side access, which allow stacking. We found a new generation of lithium ion batteries (manufactured by Onyx), which are much lighter than the lead ones and carry more energy. Their format is more advantageous for the engine room. Nevertheless, it is not possible to replace lead batteries in all cases, because a lot of weight would be lost, which is not interesting for the submarine.

New Internal Arrangement

The new scheme for the internal arrangement is presented in Figure 3. It portrays the main modules, which will be presented in the subsequent sub-items.To start, it is important to highlight that a volume throughout the hull was reserved for the ballast tanks, which may be completely used or not, depending on the calculations in item 5.6 (Ballast Allocation). The Rhinocerossoftware was used in the 3D modeling, which provides the images in the next sub-items.

Accommodations and Refectories (Parallel Medium Body - PMB)

Given that one of the targets of this second phase is to increasepassenger comfort, the cabins were enlarged and spaced from each other. The booths now have dimensions of 210cm x 90cm x 135cm (LxWxH). The image in Figure 4 shows the new configuration.

The top of the corridor is wider than the past configuration to make the environment more harmonious, besides of bringing up a step that enablesaccess to the upper cabins. At first impression, it seems a waste of space, but it creates a runner for air ventilation, or ducts for electric cables, for instance. Thenarrowest part of the corridor has 60cm, on upper deck, and 80cm, on lower deck. Four refectories (Figure 5) were projected to make the passenger meals more comfortable and sociable. Next to them, 12 toilets in total were projected. The dimensions of the new accommodations arrangement require a 9-m fixed internal diameter, for the PMB cylinder, one of the inputs for the structural calculation.

Figure 3. Scheme of the new arrangement

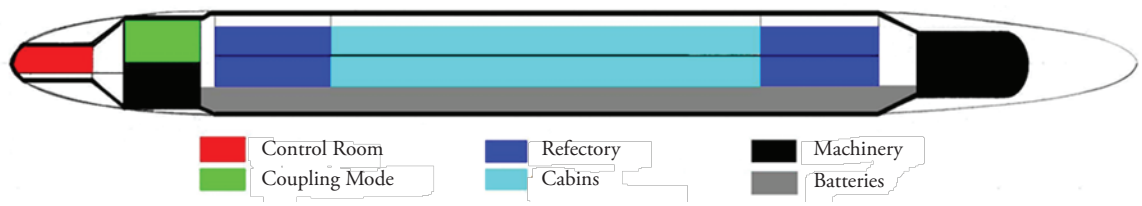

Figure 4. Inside cabins

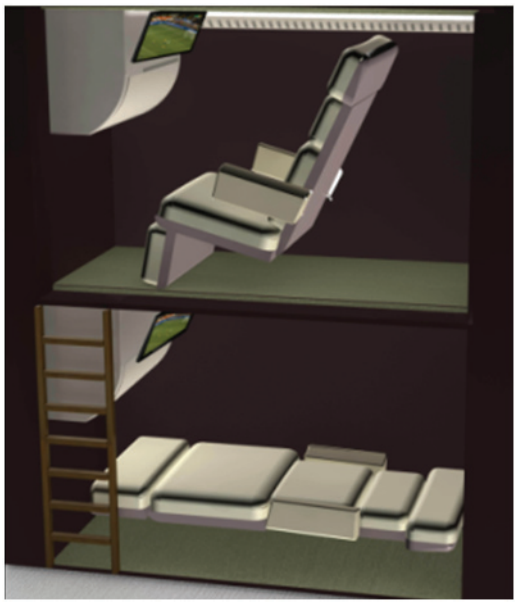

Figure 5. Refectories

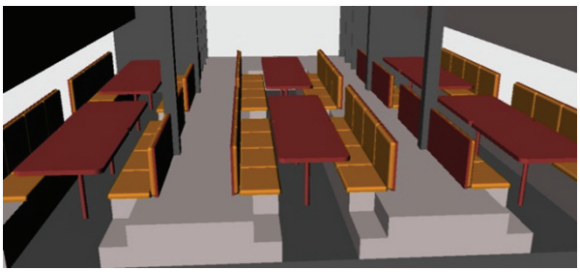

Batteries (PMB)

Most of the batteries were allocated in the bottom of the PMB hull, under the lower accommodation deck. This area is completely isolated from the passenger area, but there is a corridor in the middle of battery area that permits crew access. On both sides of the hull, there are also a few batteriesthat, like the others, are isolated from the passengers and accessible for the crew. The chemical reactions occurring inside the batteries release gases, which in large amounts are harmful to humans; thus, this area also allows implementing an exhaust system to solve this problem. Figure 6 shows battery arrangement in the PMB cross section.

Engine Room (M)

At the stern, a cylinder with 5.8m of internal diameter is projected to lodge the HTS motor, the reducer, and a considerable amount of batteries

Figure 6. Cross Section of structure

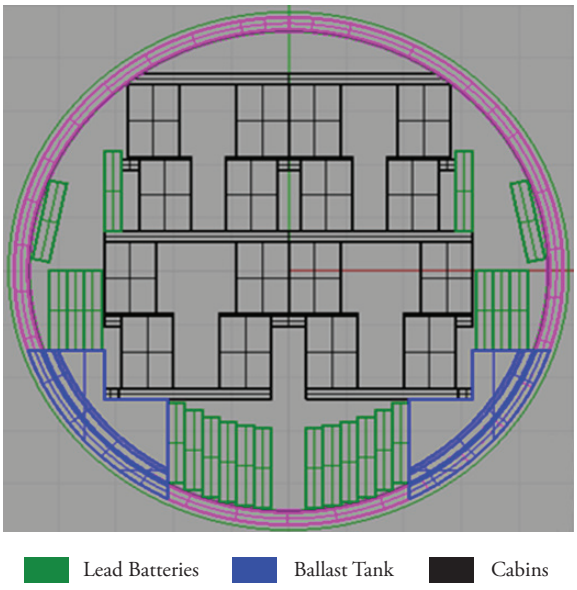

(Figure 7). In this case, batteries with side access are more advantageous than those with top access. Each of the"bow" thrusters can be accessed through this room.

Coupling Section (C)

The elevator access to transport passengers to the FPSO and vice versa will be allocated in this

Figure 7. Engine Room

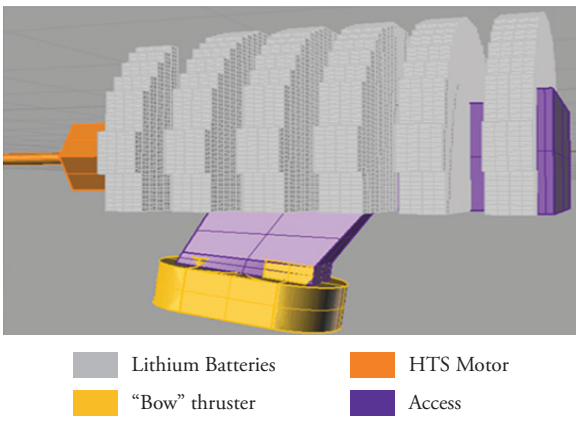

section, at the stern of the vessel (Figure 8). There are also some lockers for people to leave their luggage.

The lower deck is destined for a small engine room, with some lead batteries and the front bow thruster. This cylinder has an8-m internal diameter.

Figure 8. Coupling Module

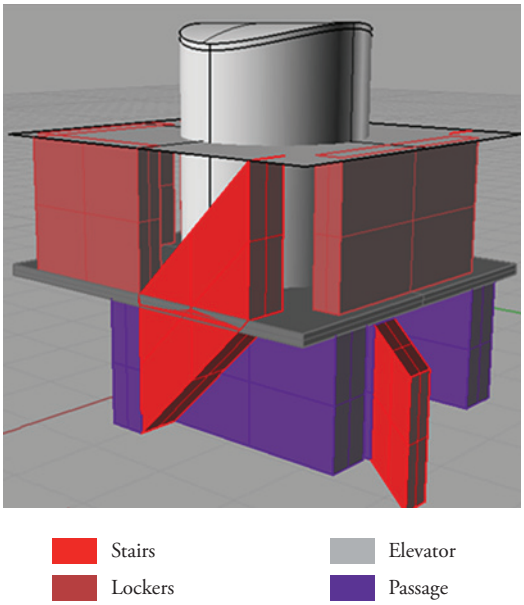

Control Room (CR)

A small, 3-m internal diameter cylinder was destined to centralize the control of the vessel at the bow extreme.

Transitions between Cylinders

The four cylinders, which are components of the resistant hull, are connected by conical transitions.

Figure 9. CR-C Transition

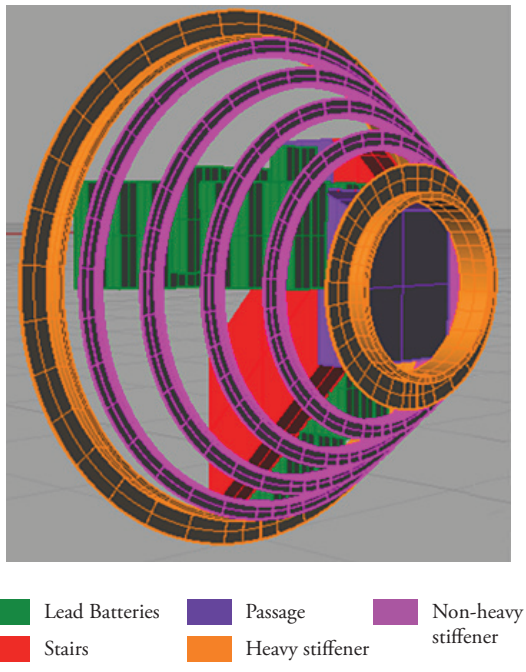

Their internal diameters mustmatch the cylinders' diameters and their lengths are determined, considering the space necessary for the stairs, which allow passage of security crew (Figure 9).

Structure

The project's scope, a passenger submarine, is determinant in the step sequence of the spiral design. Because there are no estimates or references for passenger submarines, the starting point of this project's spiral is the internal arrangement. The internal configuration described in the last sub-item will be the input for the structural calculation of the resistant hull.

Table 2 lists the internal diameter and the minimum length required by the new internal arrangement for each of the sections.

Table 2. Internal Dimensional Requirements

Module	Inner Diameter(m)	Length(m)
CR	3.0	5.4
CR-C	3.0-8.0	2.8
C	8.0	6.4
C-PMB	8.0-9.0	0.8
PMB	9.0	53.6
PMB-M	9.0-5.8	3.2
M	5.8	10.0

The shell and the non-heavy-stiffenerswill be built outside this fixed internal diameter. The heavy stiffeners sometimes enter into this space, but these occasions were carefully planned so that the internal arrangement is not compromised and the free circulation inside the vessel is maintained.

The collapse pressure is another input for structure calculations. The hydrostatic pressure the submarine's structure would not resist was defined as the double of the operational pressure, which, in the practical context, is not exceeded. The hydrostatic pressure at 110-mdepth[1] is 1.1 MPa, so

[1] Depth considering the diameter, almost 10m, under the 100-mdepth

the collapse pressure determined is 2.2 MPa.
For the selection of materials, a search of the history of submarines reveals that HY-80 steel is most commonly used, so its properties are adopted in this project: Yield strength (552 MPa), Poisson's ratio (0.3), and Modulus of Elasticity (205000MPa).

The 6th section of the ABS (*American Bureau of Shipping*, 2010) rules for underwater vehicles substantiates the structure calculation. Shell thickness, the space between stiffeners and the parameters of their cross section (T) (Figure 10) were calculated (Table 3), based on the following criteria: inter-stiffener strength, overall buckling strength, stiffener stress limits, tripping and local buckling, and inertial requirements. The group of stiffeners indicates the design of the resistant hullformat (Figure 11).

Figure 10. Stiffener Cross Section

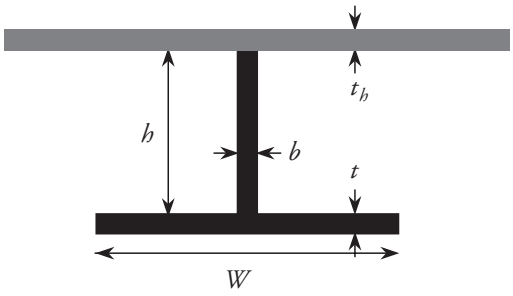

Figure 11. Resistant Hull

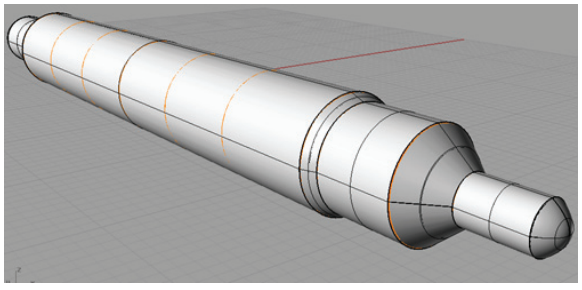

Hydrodynamic Hull Optimization

After the resistant hull is conformed, based on the structural calculations, the dimensional restrictions are determined for hydrodynamic hull optimization because, obviously, the hydrodynamic shell cannot cross inside the resistant hull.

In Jackson (1992), a study for submarine hull proposes an ideal format for good hydrodynamic performance (Figure 12). This format consists of three parts: entrance (bow), PMB, and the run (stern) (Figure 13). The PMB is a cylinder; the entrance can be calculated as an ellipsoid of revolution, and the run as a paraboloid of revolution (Figure 14). The upcoming equations and graphics refer to the bow and stern formats.

Figure 12. Hull format by Jackson (1992)

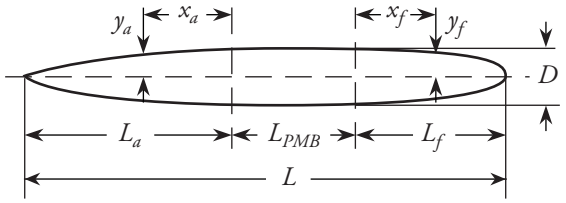

Equation for the bow format (ellipsoidal):

$$y_f = \frac{D}{2}\left[1 - \left(\frac{x_f}{L_f}\right)^{n_f}\right]^{\frac{1}{n_f}} \quad (1)$$

Equation for the run format (paraboloid):

$$y_a = \frac{D}{2}\left[1 - \left(\frac{x_a}{L_a}\right)^{n_a}\right] \quad (2)$$

Table 3. Stiffeners and Hull Specifications

Hull	Heavy stiffeners				Non-heavy stiffeners			
t_h	h	b	W	t	H	b	W	T
69	530	95	502	99	230	20	220	40

Figure 13. Entrance format by Nf (Jackson, 1992)

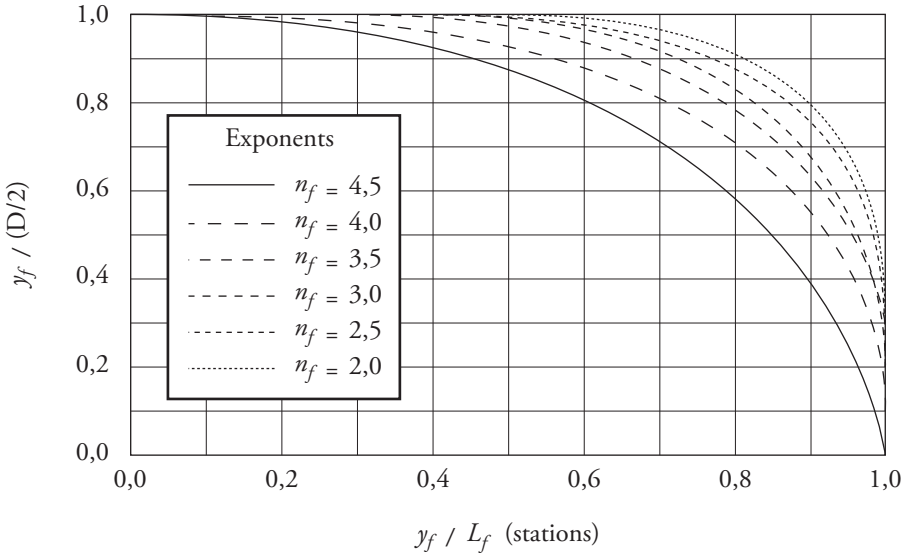

Figure 14. Run format by Na (Jackson, 1992)

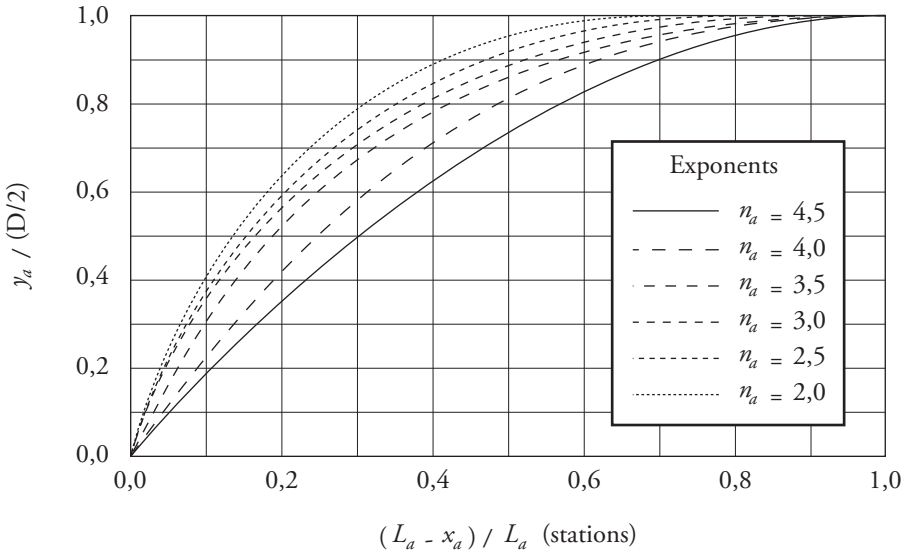

In function of the parameters presented, La, Lf, na, nf, the hull was modeled by using the Friendship® software. Friendship® provides the offset file, with the hull's quotas, and the command file and triggers Shipflow® for CFD analysis. The main analysis was made by XCHAP, more efficient and reliable when used with low input values for Reynolds coefficient. Therefore, the different hull cases under analysis were modeled in 1:20 scale (instead of Re~108, authors adopted so Re~105 for simulation). In the traditional formulation of the water resistance estimate (the following equation), the total resistant coefficient (Ct) can be split up in three components: Cf (Frictional Coefficient), Cw (Wave Generation Coefficient) and Cpv (Viscous Pressure Coefficient, which concerns the geometry of the hull, regarding the vortices generation), the most important coefficient in this analysis.

$$R_t = 0.5 \times C_t \times \rho \times WS \times V^2 \quad (3)$$

$$C_t = C_f + C_w + C_{pv} \quad (4)$$

- Cf: the value of this coefficient does not change significantly among the different analyzed models. This happens because the range of Re values is very restricted, so the logRe changes shall be ignored, what can be noticed in the ITTC (International Towing Tank Conference) Cf estimate.

- Cw: the resistance by wave generation was not considered, because the submarine is submerged at a high depth, without free-surface effects. This could be verified with a CFD analysis based on the potential approach (using the tool XPAN), which provides very small Cw values for cases deeper than 20m.

- Cpv: this coefficient will be one of the focusing parameters evaluated by the CFD analysis, since it can be extrapolated to real scale (Cpv varies according to the hull geometry).

The other parameter directly influenced by hull geometry variables is WS (wetted surface). Therefore, minimizing the product WSxCpv reveals as the main strategy to find the optimum hydrodynamically hull case. Actually, this number is not going to be used for the water resistance calculation, it is only a comparative value, a qualitative indicator.

The optimization of the hull was not automatically made. An initial configuration with the smallest WS was analyzed, from which the parameters were increased in order to improve the viscous pressure parcel. The observation of the product (WSxCpv) behavior enables the perception of which kind of geometric improvement compensates the WS increasing. As shown on the following table, the increases of the bow's length (Lf) and the stern's curvature (Na) don't optimize the hull performance. On the other hand, the parameters La and Nf, whose increases improve the performance, are going to be analyzed separately (Table 4).

To understand the bow's curvature effects, several values for Nf were tested, between 2 (the space restriction) and 3.5 (the maximum curvature analyzed by the Friendship®, from which the software doesnot run for mesh conditions). The values of the other parameters are equal to the initial configuration (Figure 15).

Figure 15. Entrance Optimization by curvature nf

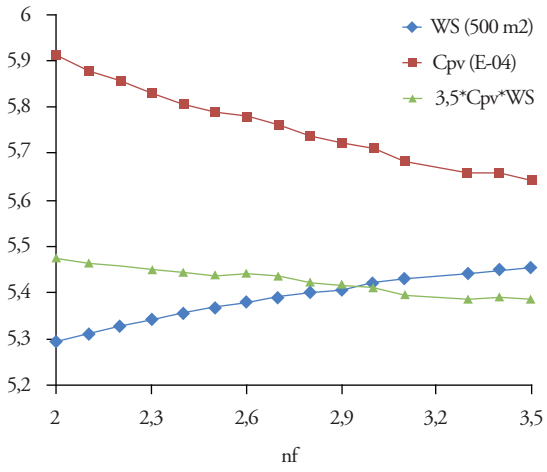

Table 4. Analysis of Hydrodynamic Parameters

Case	La(m)	na	Lf (m)	nf	WS(m2)	cf	Cpv	WS.Ct
Initial	20,3	2	18,1	2	2647,4	0,001248	0,000591	4,869
>Lf	20,3	2	18,7	2	2661,3	0,001247	0,000589	4,887
>Nf	20,3	2	18,1	2	2671,3	0,001235	0,000583	4,857
>La	21,3	2	18,1	2	2667,2	0,001244	0,000569	4,835
>Na	20,3	2	18,1	2	2666,7	0,001243	0,000645	5,036

The same analysis is made for the parameter La. Thereis an optimum value that improves the geometry decreasing the Cpv, from which the more elongated stern effects donot overcome the WS increase (Figure 16).

Figure 16. Run Optimization by length La

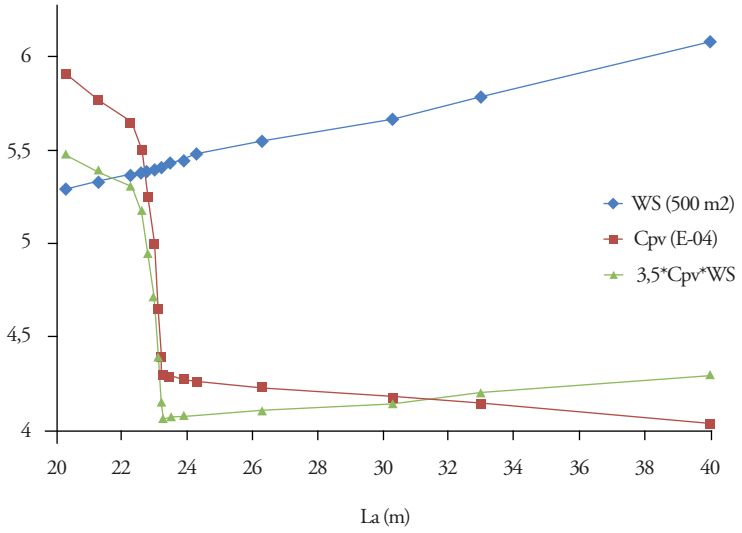

Figure 17. Final Hydrodynamic Hull

Case	La(m)	na	Lf (m)	nf	WS(m2)	cf	Cpv	WS.Ct
Best	20,25	2	18,1	3,5	2785,5	0,001168	0,000501	4,649

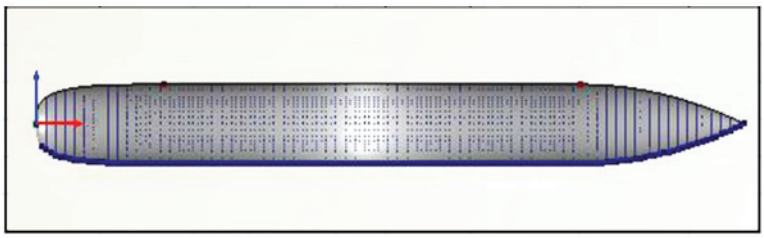

The best stern and the best bow obtained by the individual analyses are combined, culminating in the best hull geometric configuration, as expected (Figure 17).

Speed and Power

The definition of the operational speed is an iterative method because the speed determines at the same time the autonomy required, which influences battery productivity and water resistance, which is the main factor of the motor power (SHP). These two paths have to converge, respecting the amount of batteries allocated (Table 5) and the Hotel load (the power required by the crew and the auxiliary systems), estimated as 750 Kw.

Table 5. Batteries Allocated

Kind of Battery	Size (LxWxH)cm	Amount
Lead (Sepang)	29x30x150	4829
Lithium (Onyx)	60x57x19	10208

Figure 18. Methodology diagram (Speed Influence)

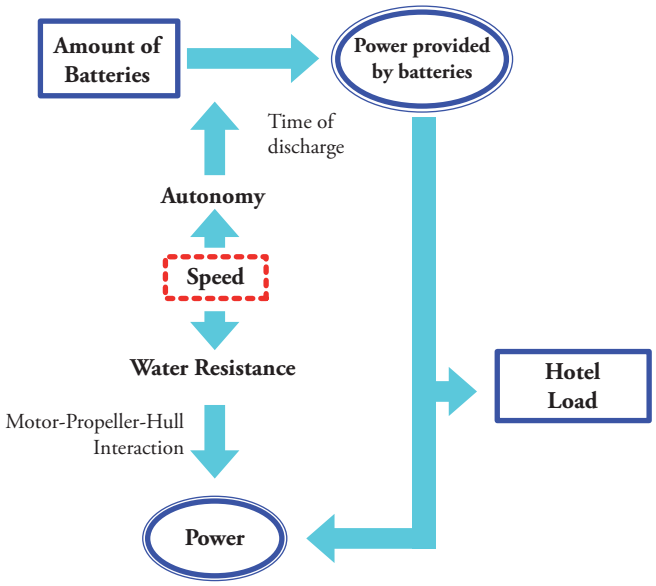

Figure 18 is a diagram of the total methodology presented in the beginning of this paper, which illustrates this moment of the project. The minimum speed required, 13.4kt, is the starting point of this cycle. Then, the speed is gradually increased to obtain the maximum speed possible,

Figure 19. Power by time of discharge (batteries)

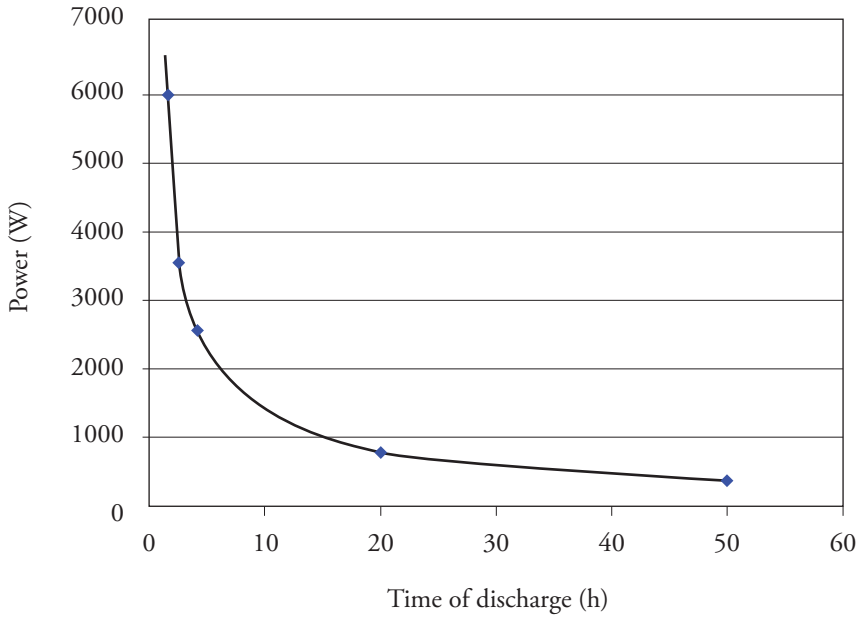

respecting the constraints.The autonomy for the respective speed is the time of battery discharge, which determines the power provided. The graphic in Figure 19 shows the power behavior of the lead battery adopted in this project.

Water Resistant

The water resistance estimate is made according to the traditional method. Because of the specificity of the submarine's design, the Ctcoefficient was calculated according to the theory described by

Jackson (1992). Ct is the sum of five components: C_f, δC_f, C_r, C_A, C_S.C_f is the friction coefficient, calculated by the formula that was agreed upon at the International Towing Tank Conference:

$$C_f = \frac{0{,}075}{(logR_n - 2)^2} \quad (5)$$

The parcel δC_f is sometimes called roughness coefficient or the correlation allowance, related to fabrication uncertainties; Arenzel and Mandel (1960) suggest 0.0004.C_r, developed from Bernoulli's conservation of energy theorem, accounts for the pressure difference along the hull;it is similar to C_{pv}

$$C_r = \frac{0{,}00789}{\frac{L}{D} - K_2} \quad (6)$$

K_2 is extracted from the following equation:

$$WS = \pi D^2 \left[\frac{L}{D} - K_2 \right] \quad (7)$$

C_S refers to the resistance of the sail, which is absent in this submarine's design. C_A is the drag coefficient of the appendages. The first approximation is adapted from Jackson's suggestion as:

$$C_A = \frac{L \times D}{1000 \times WS} \quad (8)$$

Motor-Propeller-Hull Interaction

The propeller presented by Jackson (1992) with 7 blades is very often used in submarines, so for this concept design it is going to be adopted. For the definition of the propeller's diameter, we used the ratio of 60% of the hull diameter; therefore, Dp=5.81m.

The wake and thrust coefficients(w and t, respectively) are extracted from the graphic data provided by Jackson (1992).The hull and the propeller can be combined by the relation of the thrust coefficient (Kt) provided by the propeller data (Figure 20) and provided by the following equation:

$$K_{TC} = \frac{R_T}{\rho D^{22}(1-t)(1-w)\ V^2} \times J^2 \quad (9)$$

The interception between this parabola just presented and the propeller Ktcurves, for each **P/D** relation, provides the open water efficiency (η_o) and the advance coefficient (J).

The other efficiencies included on power calculation are η_{rr}, the relative rotative efficiency, and η_h=(1-t)/(1-w), the hull efficiency. Therefore, the motor power required and the rotation are presented, respectively:

$$n\ \bar{P} = \frac{R_T \times V}{\eta_o\ \eta_h\ \eta_{rr}} \quad (10)$$

$$\frac{V(1-w)}{JD_p} \quad (11)$$

The iterative method converges to a speed of 16 kt. The principal results are demonstrated in Table 6:

Table 6. Bow Optimization

Speed	16 kt
Autonomy	26 h
Water Resistance	310.7 kN
Propeller Diameter	5.8 m
Motor Power	3001 kW
Rotation	65 Rpm

Weight distribution and Ballast Allocation

The most significant weights were calculated with high precision, as well as their centroids.

The two volumes between the hydrodynamic hull and the resistant hull, located in the bow and in the stern, are floodable, once the hydrodynamic hull cannot resist the water pressure. However, in emergency cases, when the emersion is needed, high-pressure gas isadded to these volumes, pushing the water off. They are called emersion tanks and,

Figure 18. Propeller-hull interaction graphic (Kt x J)

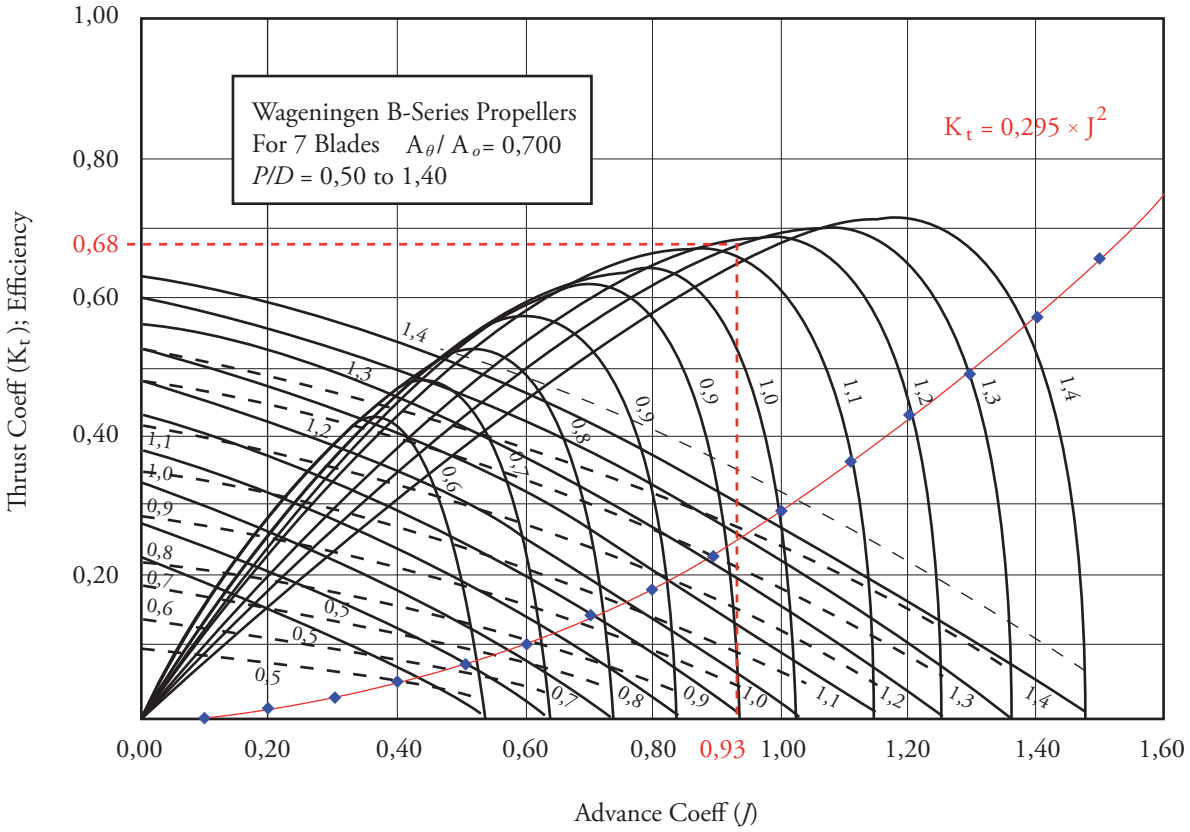

Table 7. Main modules weight distribution

Module	Weight (t)	GX(m)	GZ(m)
Res. Hull	1279	-1.06	0
Hyd. Hull (bow)	78.7	-37.27	0
Hyd. Hull (Stern)	74.1	37.07	0
Non-heavy Stiffeners	306	-2.32	0
Heavy Stiffeners	208	-2.32	0
Internal Structure	402	0	0
Batteries	2034	1.26	-1.64
Emersion tank (bow)	411	-43.08	0
Emersion tank (stern)	463	46.04	0
Motor	23	41.07	0
Displacement	6294	-1.63	0

as they are always filled, are considered weight. Weight distribution is resumed in Table 7. The centroids are referred from the middle of the PMB.

The other modules were estimated, remaining at 840t of fixed ballast. First, the main variable weights (passengers, luggage, oxygen storage in LOX tanks, fresh water) were identified, as well as their centroids, which were assumed as the same for their respective compensation tanks, in order to not cause trim. Actually, it can be noticed that these variable cargo are, comparatively with the submarine main weights, almost negligible.

For extreme load conditions, like heavy concentration of passengers frontwards or backwards, or even the emergency emersion situation, the use of trimming and regulation tanksto balance the submarine is necessary. Ballast allocation is illustrated in Figure 21.

Figure 21. Configuration of Ballast tanks

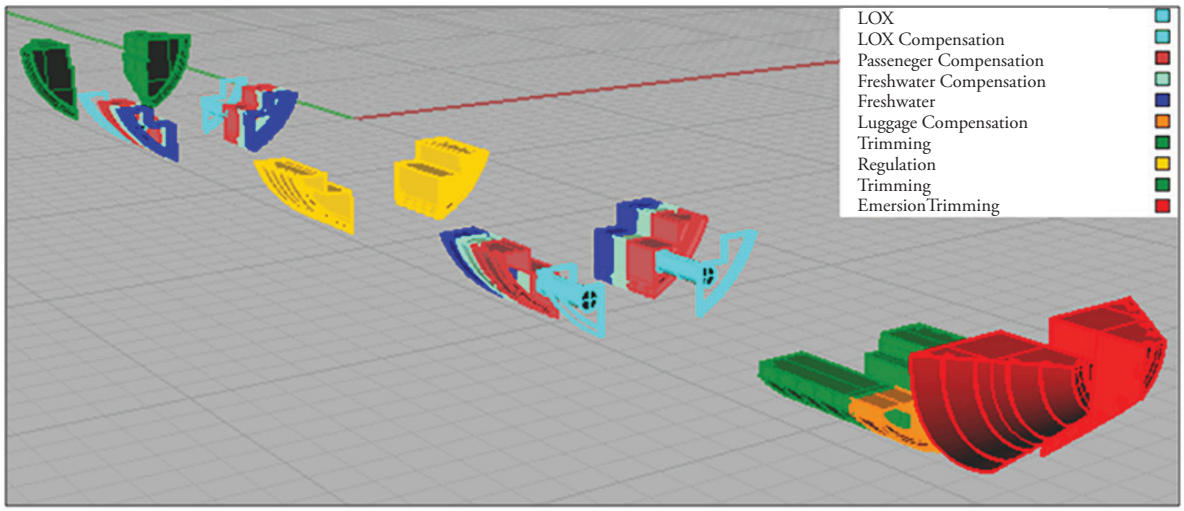

Conclusions

After this second spiral phase, the final hull presents a total length of 100m, diameter of 9.7m, displacement of 6.294 tons, values included in the range of existingsubmarine hull dimensions. Good speed and autonomy conditions, moreover, reinforce the viability intentions of the designers.

Optimizations, however, are suggested, mainly expecting to reduce fixed ballast and overall structural weight. Perhaps good initiatives can be provided by re-evaluating the operation depth or even analyzing the possibility of adopting airplane configurations for people allocation, yielding more speed with less power installed.

Bibliography

ABS (American Bureau of Shipping). *Rules for building and classing underwater vehicles, systems and hyberbaric facilities*. 2010.

ADAMS, V. W. Possible fuel cell applications for ships and submarines. *Journal of Power Resources*. 1990. Vol 29. PP. 181-192.

GABLER, U. *Submarine Design*. 1ª ed. São Paulo. AMRJ/ETCN. 1991.

JACKSON, H. A. Fundamentals of Submarine Concept Design. *SNAME Transactions*. 1992. Vol 100. pp. 419-448.

NEWMAN, J. N. Marine Hydrodynamics. The Massachusetts Institute of Technology. 1977.

PRINS, C. A., EVERARD B., Approaches to submarine design in a changing environment. *INEC*. 1996. Paper 3.

CFD modeling of 2D impact with symmetric entry

Modelado CFD del impacto 2D con entrada simétrica

Roberto Algarín [1]
Antonio Bula [2]
Oscar Tascón [3]

Abstract

The 2D impact phenomenon in calm water, considering symmetric entry with vertical velocity is studied. The analysis was performed by using commercial STAR-CCM+ computational fluid dynamics software. The results obtained from the simulations are pressure distribution and force during impact. The study was carried out for typical planning of boat sections. The results are compared with models and data obtained from some authors and they present very good agreement.

Key words: 2D Impact, CFD modeling, symmetric entry, flow separation.

Resumen

El fenómeno del impacto bidimensional en agua en calma, considerando entrada simétrica con velocidad vertical fue estudiado. El análisis se realizó usando el software comercial CFD STAR-CCM+. Los variables obtenidas de las simulaciones son la distribución de presión y fuerza durante el impacto. El estudio se desarrolló para secciones típicas de botes de planeo. Los resultados son comparados con modelos y valores obtenidos por algunos autores presentando gran similitud.

Palabras claves: impacto 2D, modelado CFD, entrada simétrica, separación del flujo.

Date received: May 20th, 2011 - *Fecha de recepción: 20 de mayo de 2010*
Date Accepted: August 31th, 2011 - *Fecha de aceptación: 31 de agosto de 2010*

[1] Department of Mechanical Engineering. Universidad del Norte. Barranquilla, Colombia. e-mail: algarinr@uninorte.edu.co, ingmec_83@yahoo.com.mx
[2] Department of Mechanical Engineering. Universidad del Norte, Barranquilla, Colombia. e-mail: abula@uninorte.edu.co
[3] Research, Development and Innovation Direction. Science and Technology Corporation for the Development of the Naval, Maritime and Riverine Industry in Colombia. Km 9, Via Mamonal. Cartagena D. T., Colombia. e-mail: otascon@cotecmar.com

Symbols

B	Beam length.
C_{fz}	Vertical force coefficient.
C_p	Pressure coefficient.
f_z^p	Vertical Force per unit length.
p	Pressure.
t	Time.
w	Vertical or Impact velocity.

Greek Symbols

τ	Time coefficient.
β	dead rise angle.
ρ	Fluid density.

Introduction

The 2D impact phenomenon has been studied through the application added mass theory, boundary valued problems and CFD applications. *Wagner (1932)*, applied added mass theory to obtain the lift force in a wedge section, as presented in Figure 1. He also evaluated the pressure distribution assuming potential flow and applying energy conservation. *Tveitnes (2001)*, also studied the impact applying added mass theory. He also calculated the lift force, and concluded that the hydrodynamic force experienced by a wedge section under symmetric entry and constant velocity entry, is generated by the variation of mass and flow moment. Moreover, the force exerted during the impact linearly increases as the section submerges and reach the flow separation at the knuckle. This separation occurs when $z/d = 2/\pi$. From that point, the moment decreases. The behavior in this zone was obtained empirically, showing that the force remains constant after certain time. The added mass and the flow moment coefficients were determined empirically as a function of the dead rise angle. *Caponnetto et al. (2003)*, generalized the impact for symmetric entry for sections with variable dead rise angle. He also evaluated the flow separation for section including knuckles. *Vorus (1996)*, studied the 2D impact with symmetric entry for a section with variable dead rise angle, solving the problem as a boundary value problem, assuming potential flow. Based on *Vorus (1996)*, *Xu et al. (1998)* analyzed the 2D impact with asymmetric entry, calculating the pressure, force and roll moment in the section. *Seif et al. (2005)* simulated the impact using CFD tools for circular and wedge sections, considering symmetric and asymmetric entry over calm water with vertical velocity. The results obtained are very close to experimental results presented in the previous studies. According to his results, the surface tension and viscosity effects can be neglected, but the gravity effect must be considered.

Mathematical Model

In order to present the results, some variables were defined according to the following equations and the geometric characteristics presented in Figure 1:

Vertical force coefficient

$$C_{fz} = \frac{f_z}{\frac{1}{2}\rho w^2 B} \tag{1}$$

Pressure coefficient

$$C_p = \frac{p}{\frac{1}{2}\rho w^2} \tag{2}$$

Time coefficient

$$\tau = \frac{wt}{\frac{1}{2}B} \tag{3}$$

Fig. 1. Geometric characteristics of the hull

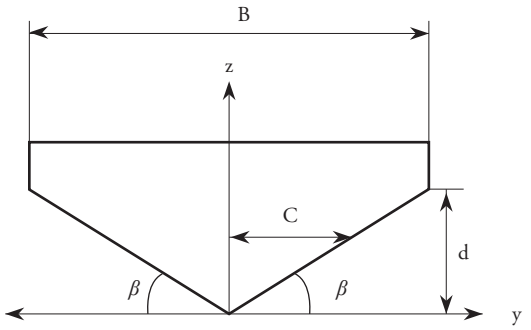

Numerical Computation

The conservation of mass and momentum equations were numerically solved. The commercial CFD software STAR-CCM+ was used as a tool to solve the differential equations that govern the phenomenon. The software uses finite volume approximation, and the equations obtained from the discretization procedure are solved using an AMG (Algebraic Multi Grid) solver. The models used to simulate the phenomenon are: multiphase mixture (water-air), inviscid flow, segregated flow and unsteady (implicit method). For the fluids, water was modeled as an incompressible liquid, while air was considered as an ideal gas. In order to confirm that the viscosity and the surface tension could be neglected, some simulations were carried. The conclusions attained are similar to *Seif et al. (2005)*, where the effects of these two variables were discarded. The ratio $w / \sqrt{gB}$ took values greater than 0.3.

The size of the computational domain was developed, changing the width and the height in order to model the impact in calm water over an infinite canal. The peak force during the impact was monitored, and the grid size was selected when the variation of the peak force was less than 1%. The final width and height of the domain were 9B to 10B, and 5B to 12.5B, respectively. The time step was also varied considering the impact velocity and it ranged between 0.008 to 0.016 d / w.

The mesh was developed using polyhedral elements, and it was divided in three regions as shown in Figure 2a. The region 1 is mainly water.

Figure 2a. Wedge Section with symmetric entry. Computational domain mesh

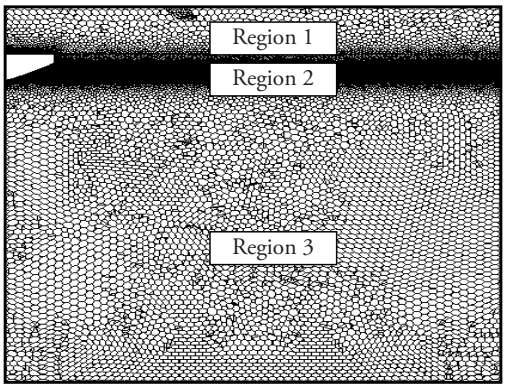

Fig. 2b. Wedge Section with symmetric entry. Mesh in the hull

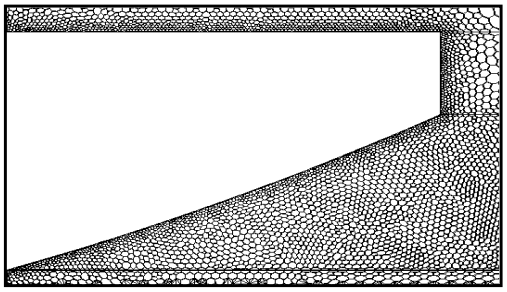

Region 2 is a phase mixture, where the hull gets in contact with the water and the air, and the free surface is generated. This area is very important for the study and because of this the mesh was refined as shown in Figure 4b. Region 3 is mainly air.

Figures 2a and 2b show the mesh after a refinement process for a convex section. The base size of the polyhedral element took values ranging between 0.15B to 0.25B. For Region 1 and 3, the values ranged between 0.045B to 0.100B. For Region 2 the values ranged from 0.0075B to 0.020B. The residuals values for the impact force and pressure keel were used as the stop criteria, and the magnitude of the global residual was limited to10-8, while the maximum numbers of inner iterations in each time step was limited to 30.

Results and Discussion

The boundary conditions for the symmetric entry are: pressure outlet at the top, velocity entry at the bottom, symmetry axis of the section, and wall over the hull.

Figure 3 presents the vertical force coefficient variation for a wedge section with different dead rise angles. The results are compared with *Tveitnes (2001) and Caponnetto et al. (2003)*. The values attained are similar to Tveitnes (2001), presenting a 5% maximum error in the peak force. From Figure 3, it is noticed that $z / d = 0$ represents the instant when the impact begins. From that point, the vertical force presents a linear behavior increasing up to the point where flow separates from the knuckle,

approximately at $z / d = 2 / \pi$. After that, the pressure and force decrease to a minimum value.

Figure 3a. Impact of wedge section, C_{fz} vs z/d (β=10°)

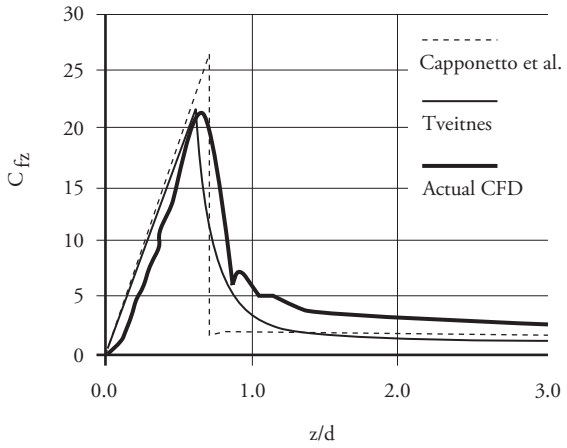

Figure 3b. Impact of wedge section, C_{fz} vs z/d (β=20°)

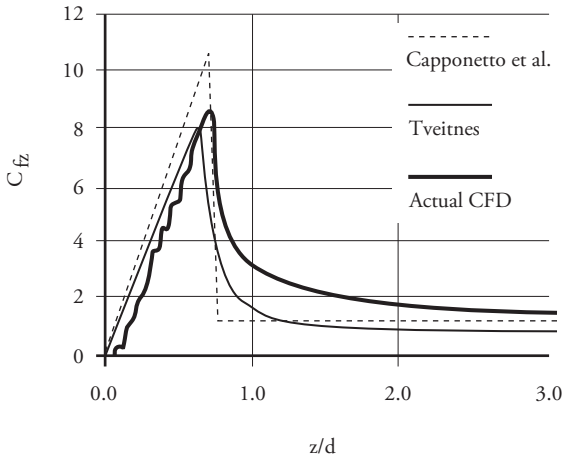

Figure 3c. Impact of wedge section, C_{fz} vs z/d (β=30°)

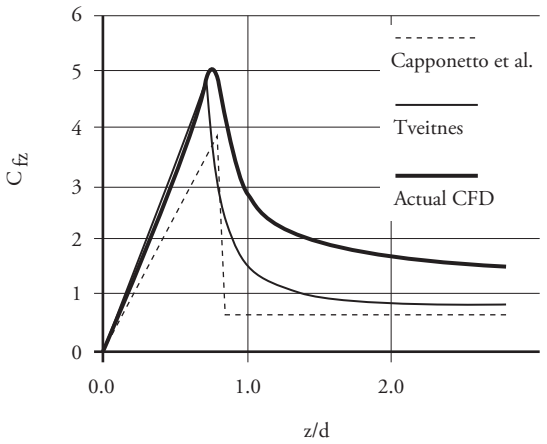

Figure 4 presents the pressure coefficient distribution for a wedge section with different dead rise angles. The results attained compare very well to the results presented by *Wagner (1932)* and *Caponnetto et al. (2003)*. The maximum error on the keel pressure is 12% respect to *Caponnetto et al. (2003)*. The trend shows that the pressure coefficient has a higher value close to the final contact point over the hull. Usually, the hydrodynamic pressure is smaller in the keel , at $y / c = 0$, and increases as it moves away from this point. At the final contact point $y / c = 1$, the pressure decreases once again.
For a circular section with radius $R=5.5m$ and entry velocity of 10 m/s, the vertical force coefficient was calculated, and the results are presented in Figure 5. It is shown that hydrodynamic force is maximum when the impact begins, $z/R=0$, and decreases as the section is submerged. The results present a maximum error measured at the peak force, close to 4% when compared to *Campbell and Weinberg (1980)*.

Figure 6 presents concave and convex sections studied by Vorus (1996). Figs. 7 and 8 show the vertical force coefficient and keel pressure coefficient variation with the time for the concave section. The force and pressure coefficients increase when the section submerges up to the point where the flow separates at the knuckle. After this point, both coefficients decrease.

Figures 9 and 10 show the force coefficient at the hull and keel pressure coefficient variation with the time for the convex section. Both coefficients present a trend similar to the concave section. The force increase as the section submerges up to the point where the flow separates at the knuckle, while the peak pressure occurs when impact begins and decrease as the section submerges.

Figures 7 to 10 present a good agreement for the pressure and force distribution before flow separation. Respect to *Caponnetto et al. (2003)*, the maximum error in the peak force is 9% and of the pressure peak is 8%. Respect to *Vorus (1996)*, the main difference is after the flow separates from the knuckle where the simulations show higher value for pressure and force, and the error presents values similar to *Caponnetto et al. (2003)*.

Figure 4. Impact of wedge section Cp vs y/c

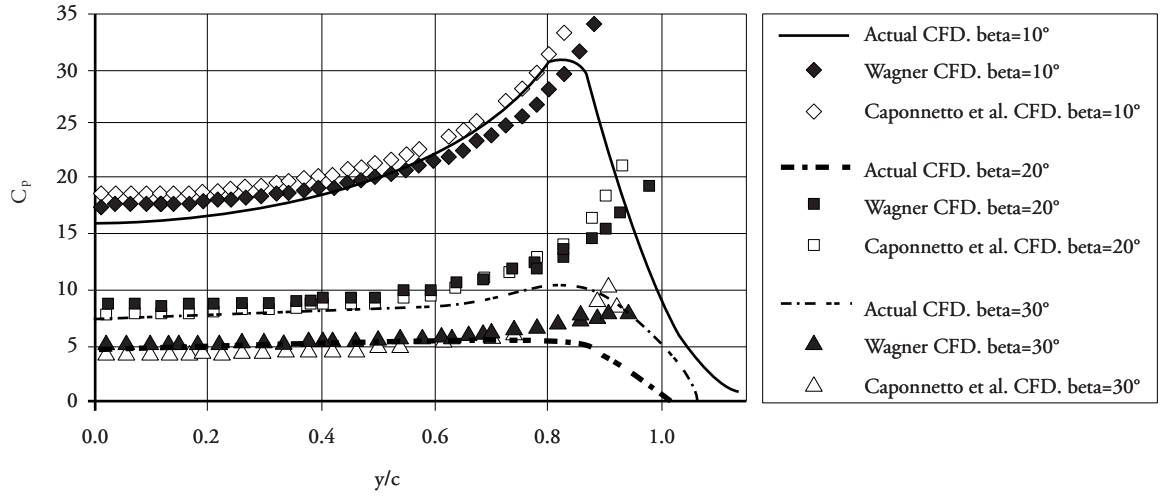

Figure 5. C_{fz} vs z/R, circular section

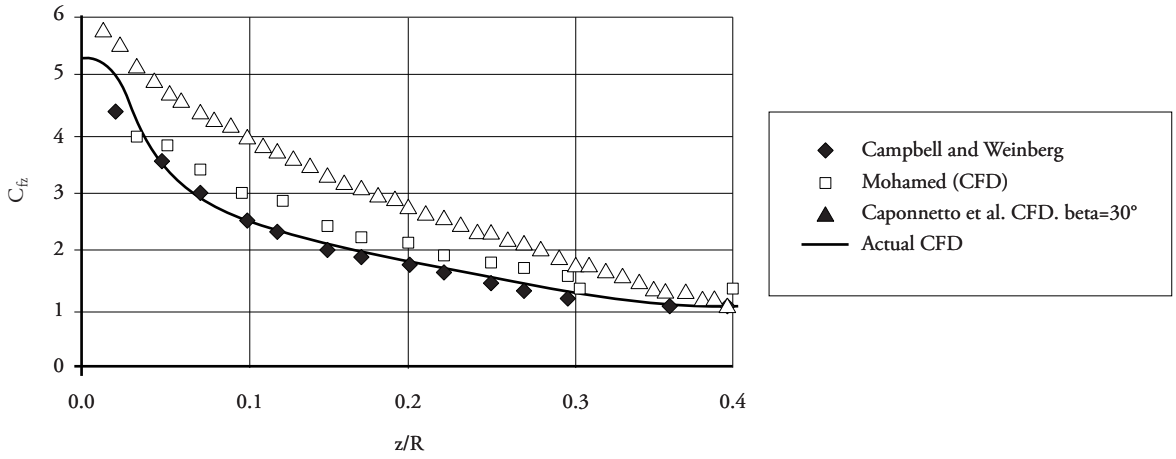

Figure 6. Sections evaluated by Vorus (1996)

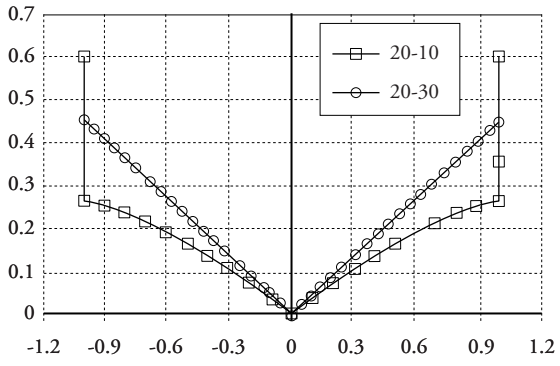

Figure 7. C_{fz} vs τ, Section 20-10 (Vorus, 1996)

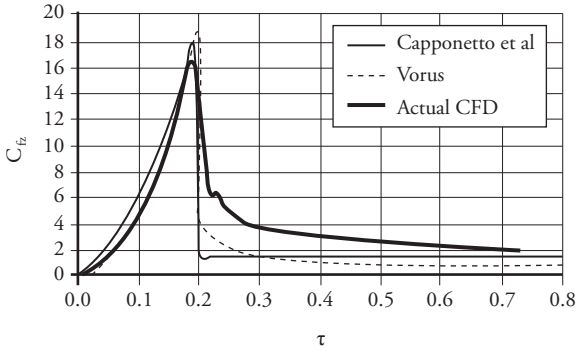

Conclusions

The 2D impact was modeled with symmetric entry of wedge sections with variable dead rise angle with CFD software STAR CCM+. The results obtained for the force and pressure coefficient present a good agreement compared to the values reported by *Wagner (1932)*, *Caponnetto et al. (2003), Tveitnes*

(2001), Vorus (1996) and *Campbell and Weinberg (1980).a*a

Fig. 8. C_{fz} vs τ, Section 20-10 (Vorus, 1996)

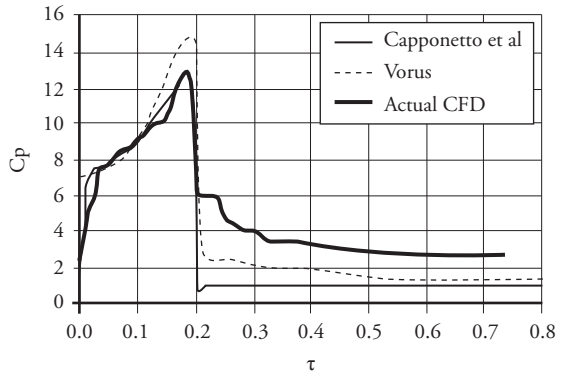

Fig. 9. C_{fz} vs τ, Section 20-30 (Vorus, 1996)

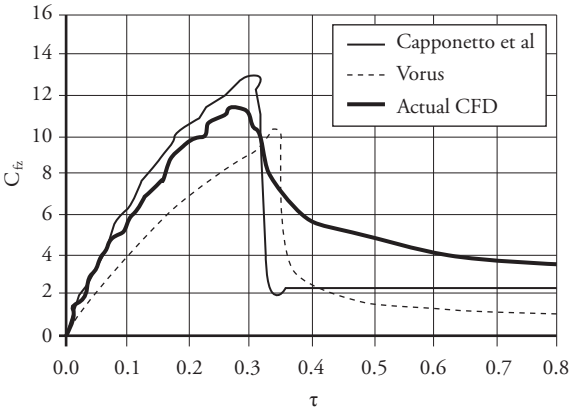

Fig. 10. Cp vs τ, Section 20-30 (Vorus, 1996)

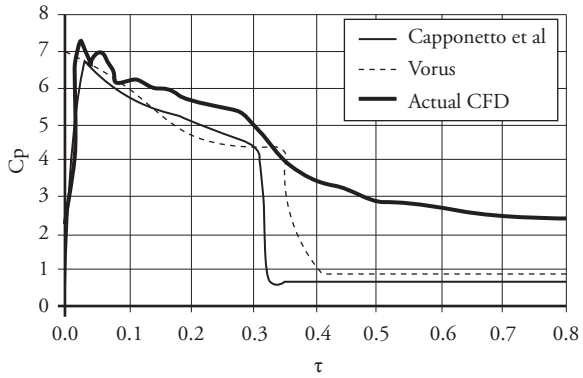

References

CAMPBELL, I.M.C. and WEINBERG, P. A., *"Measurement of parameters affecting slamming,"* Wolfson Unit, University of Southampton, Report No. 440, 1980.

CAPONNETTO, M., SÖDING, H., AZCUETA, R. (2003): *"Motion Simulations for Planing Boats in Waves"*, Ship Technology Research, Vol 50, pp. 182-196.

SEIF, M.S., MOUSAVIRAAD, S.M., SADDATHOSSEINI, S.H. & BERTRAM, V., *Numerical Modeling of 2-D Water Impact in One degree of Freedom*. En: Síntesis Tecnológica. Noviembre, 2005, vol 2, no 2, p. 79-83.

TVEITNES, T. *Application of Added Mass theory in planing* [Ph.D. Thesis]. Glasgow: University of Glasgow. Departamento de Arquitectura Naval y Ingeniería Marina, 2001, 339p.

VORUS, W. S. *A flat cylinder theory for vessel impact and steady planing resistance*. En:Journal of Ship Research. Junio, 1996, vol 40, no 2, p. 89-106.

WAGNER, H. *Über stoss – und Gleitvorgänge an der Oberfläshe von Flüssigkeiten*. En: Zeitschrift für Angewandte Mathematik und Mechanik. Agosto, 1932, vol 12, no 4, p. 193-215.

XU, L., TROESCH, A.W., and VORUS, W.S. *Asymmetric Vessel Impact and Planing Hydrodynamics*. En:Journal of Ship Research, Septiembre,1998, vol 42, no 3, p. 187-198.

Electric Arc Spray Coatings for the Naval Industry

Recubrimientos producidos por Proyección Térmica por Arco para aplicaciones en la industria naval

Laura Marcela Dimate Castellanos [1]
José Alfredo Morales Torres [2]
Jhon Jairo Olaya Florez [3]

Abstract

Carbon and stainless steel, as well as Fe-Nb-Cr-W coatings were deposited on steel substrates by using electric arc spray, and its possibility of applying such coatings in the naval industry was analyzed. In order to achieve this, the coating microstructure was characterized before and after the corrosion, abrasive wear, and thermal barrier tests. Corrosion resistance was analyzed via potenciodynamic polarization test using a NaCl electrolyte at 3%; abrasive wear resistance was measured by using a three-component system following ASTM G-65 recommendations, while quality control as thermal barriers was studied by using EIS tests. Scanning Electron Microscopy, optical microscopy and X-ray diffraction were used to characterize the microstructure of the coatings.

Key words: Electric arc spray, abrasive wear, thermal barrier, corrosion.

Resumen

Recubrimientos de acero al carbono, inoxidables y aleaciones de Fe-Nb-Cr-W fueron depositados sobre sustratos de acero mediante la técnica de proyección térmica por arco y se estudió la capacidad de dichos recubrimientos para ser aplicados en la industria naval. Para ello, se caracterizó la microestructura antes y después de los ensayos de corrosión, desgaste y térmicos en los recubrimientos producidos. La resistencia a la corrosión fue evaluada mediante ensayos electroquímicos de polarización potenciodinámica utilizando un electrolito de NaCl al 3%, la resistencia al desgaste abrasivo fue medida usando un sistema de tres cuerpos siguiendo las recomendaciones de la norma ASTM G-65 y para estudiar el estado y control de calidad de las barreras térmicas se utilizó la técnica de espectroscopia de impedancia electroquímica.

Palabras claves: Proyección térmica por arco, desgaste abrasivo, barrera térmica, corrosión.

Date received: September 24th, 2010 - *Fecha de recepción: 24 de septiembre de 2010*
Date Accepted: October 29th, 2010 - *Fecha de aceptación: 29 de octubre de 2010*

[1] Universidad Nacional de Colombia. Departamento de Ingeniería Mecánica y Mecatrónica. Colombia. E-mail: lauramdimate@hotmail.com
[2] Corporación de Ciencia y Tecnología para el Desarrollo de la Industria Naval, Marítima y Fluvial - Cotecmar. E-mail: amorales@cotecmar.com
[3] Universidad Nacional de Colombia. Departamento de Ingeniería Mecánica y Mecatrónica. Colombia. E-mail: jjolaya@unal.edu.co

Introduction

Thermal spray as a recovery process has its origin early in the 20th century with the invention of the Schoop-Günther metallization process in 1917 [1]. This process was first applied to materials with low melting points, such as Tin or Lead, and was later extended to refractory metals and ceramics. It is one of the most versatile techniques for the application of coating materials used in protecting mechanical components from abrasive wear, adhesion, erosion, corrosion (such as that caused by sea water), and fatigue [2]. In the electric arc process, two wires from the coating material to be deposited are conducted simultaneously to a point of contact, where a gas is sprayed to project the liquid metal as molten droplets onto the coating surface [3]. Electric arc thermal spraying is one of the most economic techniques to apply corrosion resistant metal coatings with high-quality adherence and chemical composition [4]. Low energy costs and high production rates makes this technique competitive, compared with other projection systems such as plasma and flame thermal spray [5.6]. Furthermore, the parameters used in the electric arc thermal spray system (voltage, current, air pressure and projection distance) can be optimized for specific applications [7].

Given that marine components like engines are frequently exposed to highly corrosive environments, cyclical loads, and wear during operation, state-of-the-arttechnology materials like nanocomposites or materials commonly used in the shipping industry like stainless and carbon steels is proposed. By using these materials, it is possible to recover mechanical pieces, which have spare parts that may not be serially manufactured or that may have been discontinued, as well as protecting parts that are constantly subject to aggressive environments to ensure greater durability and performance. In this paper, thermal spray coatings for applications in the naval industry are investigated. Consequently, herein, we present coatings for resistance to abrasive wear and corrosion with thermal barrier properties of Fe 25Cr 5B 6Mo 15W 3Mg 4C 12Ni 2Si (nanocomposite 140 MXC), Fe 0.8Mn 0.2Si 0.15C (530 AS) and Fe 13Cr 1Mn 1Si 0,3C (560 AS). These coatings were applied by electric arc spraying on SAE 4340 and 1045 steel substrates for the 140MXC and 530 AS coatings, and over SAEI 316L substrates for the AS 560 coatings.

Experimental Methods

Coating deposition

Table 1 summarizes the coatings applied over each substrate, their chemical composition, and the characterization studies performed. For wear and corrosion tests, 20x20x5-mm size samples were used, except for the 316L steel where samples were 20x20x2 mm in size. To study thermal properties, 23.8-mm diameter and 2-mm thickness samples were used. For these studies, the substrate surface was first prepared by using an abrasive wheel. The coatings were then immediately deposited to prevent oxidation of the sample surface. Subsequently, a 95Ni5Al base coating was deposited, providing adequate surface roughness to improve adhesion of the system.

Finally, the coatings were deposited by using the following parameters: primary air pressure at 50 psi, voltage at 29 V, current at 220 A and projection distance at 200 mm perpendicular to the sample surface. All coatings were applied by using a EuTronic Arc Spray 4 system.

Characterization

Thermal spray coatings were structurally studied by using X-ray diffraction (XRD) with Pro Panalytical X-pert equipment, operating at 45 kV and 40 mA. The measurement of thickness and qualitative porosity was carried out with a Leco convex lens optical microscope via cross-section metallography. The coatings were studied at the surface by using a scanning electron microscopy (SEM) FEI QUANTA 200 system, in a high-vacuum environment at 30 kV. Chemical analysis was performed before and after electrochemical tests with the same SEM equipment in EDS mode at 20 kV.

Table 1. Coatings applied over each substrate

SUBSTRATE	COATINGS		
	140 MXC Fe 25Cr 5B 6Mo 15W 3Mg 4C 12Nb 2Si	**530 AS** Fe 0.15C 0.8Mn 0.2Si	**560 AS** Fe 13Cr 1Mn 1Si 0.3C
4340 STEEL Fe 1.65Ni 0.7Cr 0.2Mo 0.4C 0.6Mn	Abrasive wear Corrosion	Corrosion	
1045 STEEL Fe 0.45C 0.3Si0.8Mn	Corrosion	Abrasive wear Corrosion	
316L STEEL Fe 0.03C 13Ni 2.3Mo 17.5Cr			Abrasive wear Corrosion
1020 STEEL Fe 0.2C 0.6Mn 0.04 P 0.05S		Thermal Barrier	

Microhardness tests

A Knoop microhardness test was conducted over the three coatings, with a 50-g load; using a Leco M-400-G2 hardness tester. Measurements were made with a depth profile from the surface of the coating into the substrate.

Wear tests

Wear tests were performed using equipment meeting ASTM G65 standards, which determines abrasive wear by contact between dry sand and a rubber wheel against the sample material [8]. The sample weight loss is reported in units of volume (mm^3). The test parameters were set at: 130 N load, time 1 min, sand flow at 300-400 g/min and 200 rpm of the wheel.

Electrochemical tests

Potentiodynamic tests were performed by using a GamryReference 600 Potentiostat/Galvanostat/ ZRA system with a high-purity graphite counter-electrode and a saturated calomel electrode (SCE) as reference, following ASTM G5 standard recommendations [9]. The area exposed to this solution was 0.79 cm^2 within an electrolyte at 3% NaCl. The sweep was carried out between -0.3 and 1.0V with respect to the potential rest, at a scanning rate of 0.5 mV/s.

Study of Thermal Properties

The coatings were subjected to thermal treatments at 600, 800, and 1000°C for 4hrs and at 1000°C for 24hrs. Afterwards, electrochemical tests were performed by electrochemical impedance spectroscopy at room temperature, using a 0.01-M electrolyte ($K_3Fe(CN)_6$)/$K_4Fe(CN)•3H_2O$) [10]. Prior to the measurement, a 45-minute wait was established to allow for stabilization of the open circuit potential and to ensure the penetration of the electrolyte through the open pores. The area exposed to this solution was 0.79 cm^2; electrochemical impedance spectroscopy measurements were performed with initial and final frequencies of 10 mHz and 100 kHz, respectively, with a 10-mV perturbation. Subsequently, the coatings were studied via SEM to observe the microstructural changes and XRD to determine the oxides formed.

Results And Discussion

Microstructure and Chemical Analysis

Figure 1 shows the micrographs of each of the surface coatings studied. In general, coating surfaces presented lenticular structures and splat formation, as expected for these coatings. Likewise, low roughness values were observed in the coatings,

Figure 1. SEM micrographs at 500 X of coatings (a) 140 MXC, (b) 530 AS, (c) 560 AS

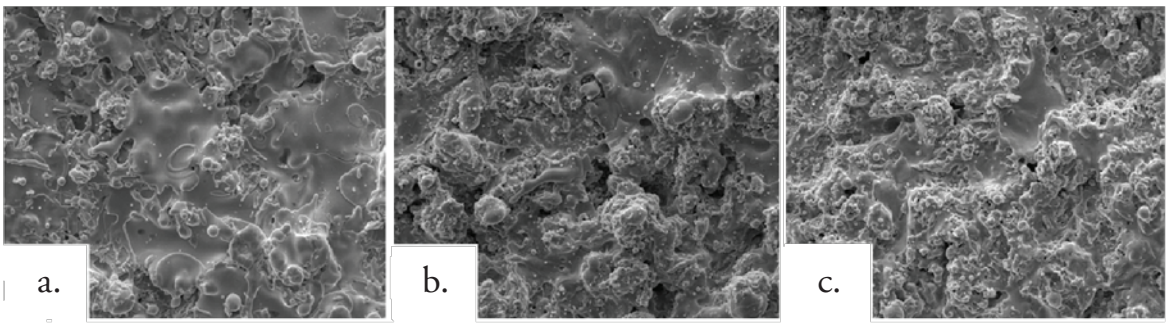

with low oxide content and porosity. Thereafter, roughness was measured with a diamond edge profilometer, obtaining roughness values of Ra = 5.1, 5.44 and 6.23 µm for 140 MXC, 530 AS, and 560 AS coatings, respectively. To measure thickness, cross sections were performed and samples were observed with an optical micrograph; 10 measurements were made to obtain the average thickness. In the micrographs, fewer pores and oxides were observed present in the 140 MXC coating than in the 530 AS and 560 AS coatings, agreeing with the manufacturer's specifications. The XRD spectra of 140 MXC nanocomposite are presented in Figure 8, but an A wire coating spectra was first registered, where only Fe was found; this suggests that the amorphous phase to form the nanocomposite is found in the powder, we also observed CrO2. Figure 10 shows XRD spectra for the 530 AS coating. This coating revealed the presence of Fe and FeO and Fe2O3 oxides, which are probably formed when the particles melt and react with the surrounding environment before depositing over the substrate and solidifying. In turn, on the 560 AS coating (Figure 12) it was noted that Fe3O4 oxide and Fe-Cr compounds were formed.

Measurement of microhardness

Results of the Knoop hardness test are shown in Figure 2. The highest hardness was observed in the nanocomposite, possibly due to the presence of hard tungsten-, niobium- and chromium-based elements [11]. An increase in hardness in the 560 AS coating was observed because of the presence of the martensite phase [12], while for the half-carbon coating, the lowest microhardness was observed because of the absence of alloying elements and the amount of oxides formed [13.14], which produces a coating not suitable for applications where the part will be subjected to wear, *i.e.*, recommended for applications in cases of dimensional recovery.

Figure 2. Microhardness values of 140 MXC and 530 AS coatings and 4340 and 1045 steel substrates

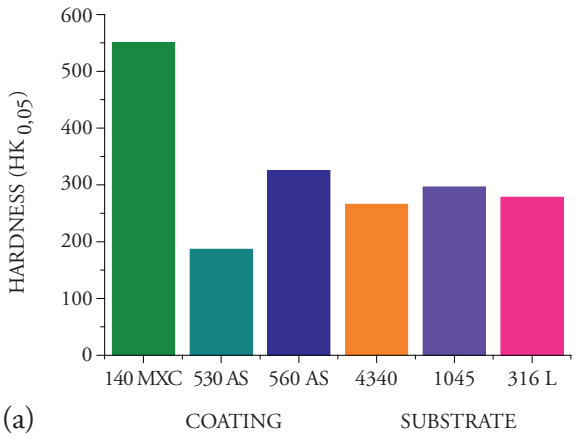

Abrasive Wear Tests

Volume loss values obtained are presented in Figure 3. In the case of the 560 AS coating, the abrasive wear test was not performed because sample thickness was not sufficient to be mounted on the sample-holder of the abrasive wear equipment. The 140 MXC coatings lost less volume during the test, agreeing with the highest hardness values. This may be possible due to the formation of a microstructure with good mechanical properties, based of an amorphous matrix composed of chromium, niobium, and molybdenum elements, and nanostructured structures without preferred

Figure 3. Volume loss of the 140 MXC and 530 AS coatings, and the 4340 and 1045 substrates

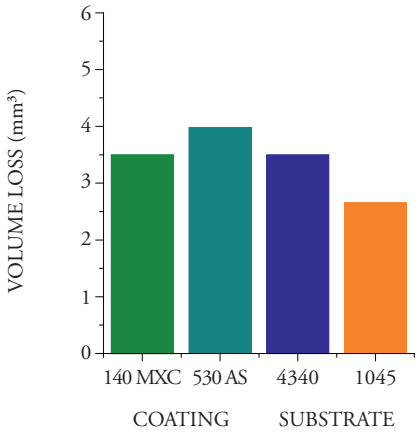

Figure 4. Potentiodynamic polarization curves of the 140 MXC and 530 AS coatings and 4340 and 1045 substrates

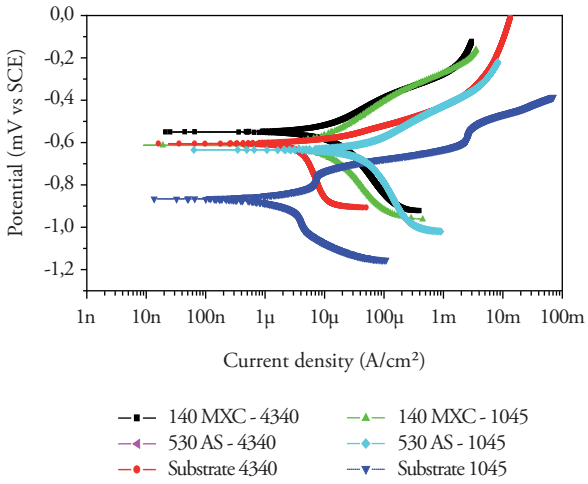

orientation [13]. These measurements should be confirmed via transmission electron microscopy. After these tests, samples were analyzed via SEM, where signs of wear mechanisms and plastic deformation were observed. When the chemical composition was determined, silicon, oxygen and carbon traces were observed; the first due to the silicon sand introduced by the abrasive material of the experiment, and the other elements probably due to the interaction of the coating with the surrounding environment.

Potentiodynamic Polarization

Figure 4 shows the Tafel polarization curves of the 140 MXC and 530 AS coatings. To observe the effect of substrate resistance against corrosion, 140 MXC and 530 AS coatings were deposited onto two substrates (SAE 1045 and 4340 steel).

For these coatings, an improvement in the resistance corrosion for both substrates was observed, that is, the corrosion potential values are more positive and present lower corrosion resistance values. These observations are consistent with the chemical composition, given that the presence of niobium and chromium, even in small quantities, improves corrosion resistance [15]. The 530 AS coating was also deposited onto the two substrates. In this case, corrosion resistance showed improvement when applied over the 1045 substrate, but when applied over a SAE 4340 steel substrate, no improvement in the electrochemical behavior was observed; thus,

Figure 5. Potentiodynamic polarization curves of a 560 AS coating and 316L substrate

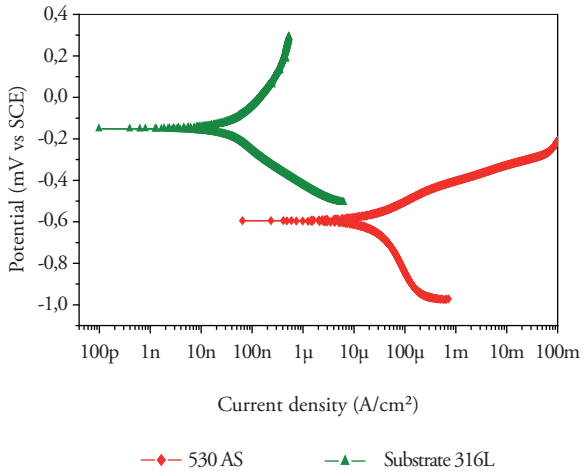

manifesting the importance of substrate selection. Figure 5 shows the Potentiodynamic polarization curves of the 560 AS coating deposited over the 316L stainless steel. It was observed that the substrate had better corrosion resistance behavior without the coating, possibly due to the martensitic nature of the stainless coating while the substrate is totally austenitic. An insulating layer forms on the surface of a 316 austenitic stainless steel, which makes the steel passive; thereby improving corrosion resistance [16]. For this reason, this system is recommended for applications where corrosion and wear act synergistically.

Thermal barrier behavior

The micrographs in Figure 6 show the degradation of coatings due to heat treatment at 1000°C over 4 h [17], which is evident when compared to Figure 1. (see page 12).

Figure 6. SEM micrographs at 1600 X after heat treatment at 1000 °C during 4 h of the coatings (a) 140 MXC (b), 530 AS, and (c) 560 AS

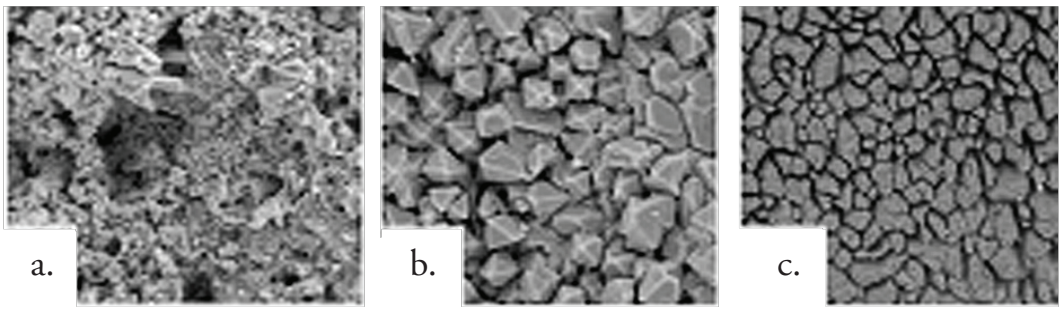

Figure 8 shows the Bode plot of the 140 MXC coating after heat treatment. A significant increase in the impedance modulus was observed in the samples under heat treatment when compared to the untreated coating. In turn, an increase in the impedance of the system was observed after isothermal oxidation, which can be related to thermal degradation after the onset of oxides. After a 4-h exposure at 800°C, the results describe some variations; for example, overlapping the curve at 1000°C during 24 h at low frequencies. Nonetheless, it was expected that under high-temperature treatment over long periods of time, an increase in the concentration of oxides would be observed. However, this tendency was not observed. The XRD spectra in Figure 9 shows that at 800°C, there was the highest concentration of oxides, such as chromium oxide (Cr_2O_3) with rhombohedral crystal structure, manganese oxide (MnO) with a face-centered cubic structure, and molybdenum oxide (MoO_3) with a monoclinic structure, which may act as a thermal barrier. Samples subjected to treatment at 1000°C for 4 and 24 h presented ferrous oxides, which are not

Figure 7. Bode-plots for EIS data of the 140 MXC coating at 25°C and at 600°C, 800°C and 1000°C during 4 h, and 1000°C during 24 h

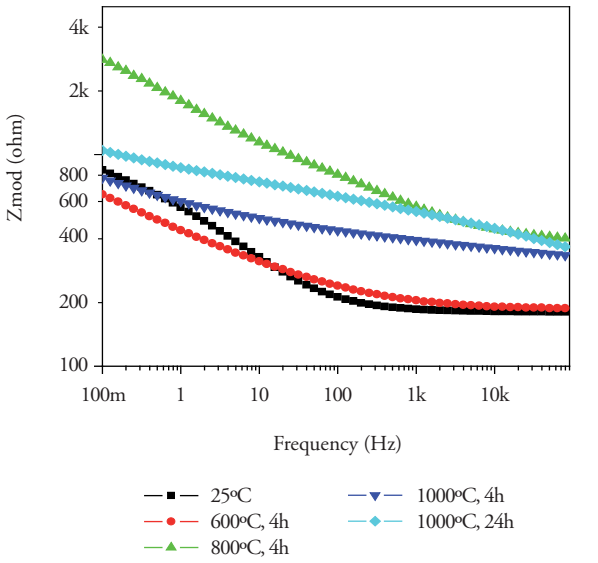

Figure 8. XRD pattern from the 140 MXC coating at 25°C and at 600°C, 800°C and 1000°C during 4 h and 1000°C during 24 h

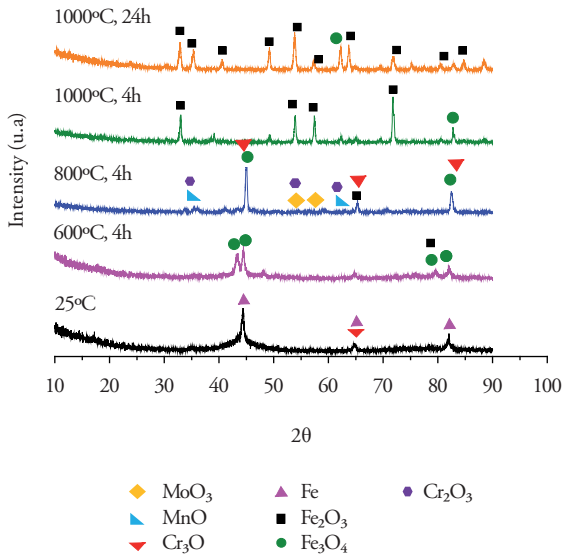

Figure 9. Bode-plots for EIS data of the 530 AS coating at 25°C and at 600°C, 800°C and 1000°C during 4 h, and 1000°C during 24 h

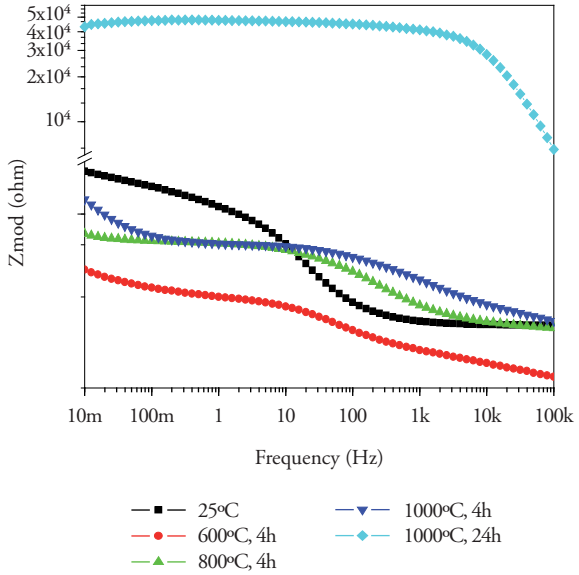

Figure 10. Bode-plots for EIS data of the 530 AS coating at 25°C and at 600°C, 800°C and 1000°C during 4 h, and 1000°C during 24 h

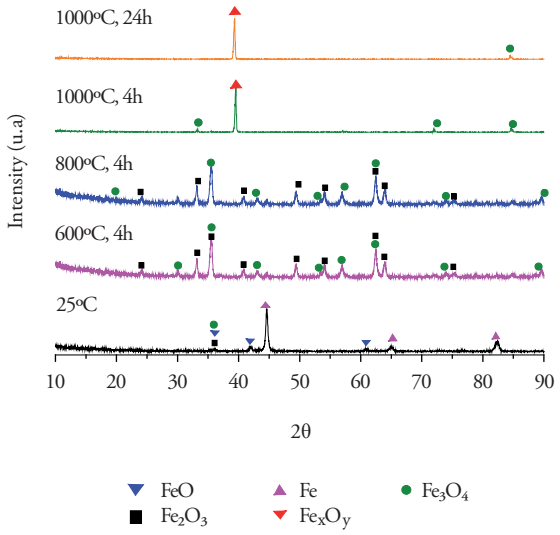

recommended for insulation applications [18]. Figure 9 shows the Bode plot of the 530 AS coating, showing that impedance is significantly higher for heat treatment at 1000°C for 24 h, which suggest a high rate of oxide formation [19]. The XRD spectra for the 530 AS coating (Figure 10) show the formation of Fe_2O_3 at room temperature [18].

Figure 11 shows a Bode plot of the 560 AS coating. Overlapping of the curves at lower frequency values is observed in more aggressive treatments. In turn, treatment at 800°C decreases impedance values drastically, suggesting oxide formation.

Figure 11. Bode-plots for the EIS data of the 560 AS coating at 25°C and at 600°C, 800°C and 1000°C during 4 h, and 1000°C 24 h

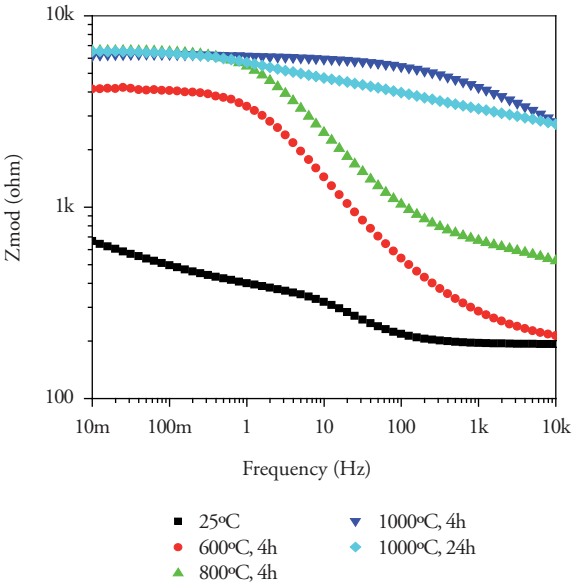

Figure 12. XRD pattern from a 560 AS coating at 25°C and at 600°C, 800°C and 1000°C during 4 h, and 1000°C 24 h

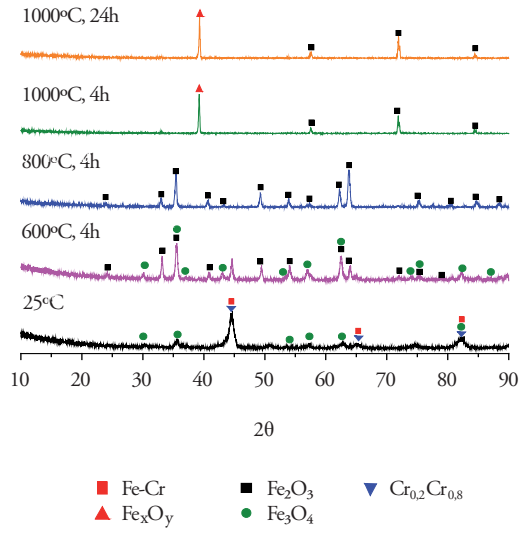

Figure 12 shows the XRD spectra of a 560 AS coating. No significant increase in the oxide phase formation is noted with increasing temperatures. However, the chromium phases, an essential element of this coating, are only observed in the coating without heat treatment [20]. For temperatures above 800°C the presence of Fe_2O_3 oxide is well observed, and for treatments below this temperature Fe_3O_4 and Fe_2O_3 oxides were present [21].

Conclusions

In general, the coatings used in this work can improve resistance to corrosion and abrasive wear of carbon steel substrates; however, the efficiency of such protection depends largely on the defects of the microstructure of the coating, as well as the corrosive and wear environment. Moreover, the coatings studied are a viable alternative for applications in the ship building industry, and the coating should be chosen given the stress and conditions to which the piece will be subjected. The conclusions drawn from the microstructural characterization, the thermal evaluation, and resistance to corrosion and wear of the coatings produced are presented as follows.

With regards to the tests performed on trademark 140 MXC, 530 AS, and 560 AS coatings applied via electric arc thermal spraying technique on substrates used in the ship building industry; it was found that the coating with best performance, that is, the coating with the best combination of properties in terms of corrosion resistance, microhardness, abrasive wear resistance, and thermal barrier properties was 140 MXC, followed by 560 AS and, finally, 530 AS. The importance of the substrate for corrosion testing was determined, for it is important to use stainless steel materials which have a passivation layer that improves the electrochemical behavior of the system as a whole. Regarding the properties of the coatings as thermal insulators, more tests are required to determine the feasibility of nanocomposite 140 MXC coatings at temperatures below 800°C. The 530 and 560 AS coatings were discarded for thermal applications.

References

1. LASHRERAS E., MARÍA J. (1978). *"Tecnología del acero"*. Ediciones Cedel. Tercera edición, Barcelona. España.

2. GEDZEVICIUS I., VALIULIS A. (2006). *"Analysis of wire arc spraying process variables on coatings properties"*. Journal of Materials Processing Technology.

3. Handbook of Hard Coatings. Tomo 3. Thermal Spraying and Detonation Gun Processes. (2003).

4. MARULANDA, J. (2000). *"El Rociado Térmico y sus Aplicaciones"*. Publicación Universitaria.

5. DOBLER K. (2006). *"Reconditioning Power Generation Components with Thermal Spray Welding Journal"*.

6. Department of the Army. U.S. Army Corps of Engineers. Thermal spraying: New construction and Maintenance. EM 1110-2-3401. Washington, DC 20314-1000. (2005).

7. COOKE K., OLIVER G., BUCHANAN V., PALMER N. (2007). *"Optimisation of the electric wire arc-spraying process for improved wear resistance of sugar mill roller shells"*. Surface & Coatings Technology 202 185–188.

8. ASTM Designation: G65. Standard Test Method for Measuring Abrasion Using the Dry Sand/Rubber Wheel Apparatus. (2001).

9. ASTM G5 – 94. Standard Reference Test Method for Making Potentiostatic and Potentiodynamic Anodic Polarization Measurements. (2004).

10. GARCÍA J., SALAZAR A., MÚNEZ C.J., UTRILLA V. y POZA P. (2005). *"Análisis de la degradación de recubrimientos de barrera térmica por espectroscopía de impedancia electroquímica"*. Revista Cerámica y Vidrio, 232-239.

11. GEORGIEVA, THORPE P., YANSKI R., SEAL A. (2006). *"Nanocomposite materials: an innovative turnover for the wire arc spraying technology"*. University of Central Florida, Mechanical, Materials and Aerospace Engineering Department.

12. KRAUSS G. (1989). *"Heat Treatment and Processing Principles"*. Eds, ASM International.

13. SMITH W. (1993). *"Structure and Properties of Engineering Alloys"*. Mc Graw Hill International Editions.

14. JANDIN G., LIAO H., FENG Z.Q., CODDET C. (2003). *"Correlations between operating conditions, microstructure and mechanical properties of twin wire arc sprayed steel coatings"*. Materials Science and Engineering A349 298/305.

15. ZHOU Z., WANG L., WANG F., LIU Y. (2009). *"Formation and corrosion behavior of Fe-based amorphous metallic coatings prepared by detonation gun spraying"*. Transactions of Nonferrous Metals Society of China. S634-s638.

16. ASM Handbook, Volume 1, Properties and Selection: Irons, Steels, and High Performance Alloys. (2005).

17. ABEDINI A., POURMOUSA A., CHANDRA S., MOSTAGHIMI J. (2006). *"Effect of substrate temperature on the properties of coatings and splats deposited by wire arc spraying"*. Surface & Coatings Technology 201 3350–3358.

18. SONGA S.-H., XIAO P., WENG L.-Q. (2005). *"Evaluation of microstructural evolution in thermal barrier coatings during thermal cycling using impedance spectroscopy"*. Journal of the European Ceramic Society 1167–1173. 25.

19. CULHAA O., TOPARLIA M., SAHINB S., AKSOYA T.. (2008). *"Characterization and determination of FexB layers mechanical properties"*. Journal of Materials Processing Technology 206 231–240.

20. JIN G., XU B.S, WANG H. D, LI Q. F, WEI S.C. (2007). *"Microstructure and tribological properties of stainless steel coatings sprayed by two methods based on spraying"*. Surface & Coatings Technology 201 5261–5263.

21. AMOKRANE M., BOUNARB N., BENABBASB A., ATIA A. (2008). *"Study of microstructure, phases and microhardness of metallic coatings deposited by flame thermal spray"*. Journal of Materials Processing Technology 200 410–415.

Aid in the Design of Antenna Arrays with Electronic Phase Steering using Matlab®

Ayuda al diseño de arrays de antenas con direccionamiento electrónico de haz empleando MATLAB®.

Francisco José Gil Navia [1]

Abstract

Antenna arrays have been used since the 1950s in multiple applications; however, it was not until recent years that, given progress in digital technologies, this application has become the fastest and most varied development in the radar world. The main motivation for their development is that they permit electronic phase steering that implies extreme phase agility, while also being tolerant to failure because of the amount of elements that comprise them. They also permit the reduction of side lobes by controlling the amplitude of each element.

Because it is a currently applied technology, but with many aspects under development, it is necessary to enter this field and generate the required tools including those for computer assisted prototyping. Because of the aforementioned, this work sought to use Matlab® to create virtual prototypes of arrays that permit visualizing an approach to their real behavior stemming from certain parameters.

Key words: Antenna arrays, electronic phase steering, MATLAB.

Resumen

Los arrays de antenas han sido empleados desde los años cincuenta en múltiples aplicaciones, sin embargo no ha sido hasta años recientes que, gracias a los adelantos en tecnologías digitales, se ha logrado convertir esta aplicación en la de más rápido y variado desarrollo dentro del mundo radar. La principal motivación para su desarrollo es que permiten el direccionamiento electrónico de haz que implica una agilidad de haz extrema, además son muy tolerantes a fallos por la cantidad de elementos que los componen. También permiten la reducción de lóbulos laterales por medio del control de la amplitud de cada elemento.

Por ser una tecnología aplicada actualmente pero con muchos aspectos en desarrollo se hace necesario adentrarse en este campo y generar las herramientas necesarias incluyendo aquellas de prototipado mediante computador. Por lo anterior en este trabajo se pretende emplear Matlab® para crear prototipos virtuales de arrays que permitiría visualizar una aproximación al comportamiento real de los mismos a partir de ciertos parámetros.

Palabras claves: Arrays de antenas, Direccionamiento electrónico de haz, MATLAB.

Date received: September 10th, 2010 - *Fecha de recepción: 10 de septiembre de 2010*
Date Accepted: November 1st, 2010 - *Fecha de aceptación: 1 de Noviembre de 2010*

[1] Departamento de Armas y Electrónica de la Armada Nacional, Fuerza Naval de Caribe, Base Naval 1. Colombia.
E-mail: francisco.gil@armada.mil.co

General considerations on Arrays with Electronic Phase Steering

Antenna arrays with electronic phase steering are antenna groups arranged in space in such a way that they permit obtaining a desired radiation pattern. In practical applications, the elements tend to be in linear or plane arrangement, in regular polygonal or circular form; additionally, these can also form crosses or diamond shapes amongst themselves. The spacing between elements is normally uniform. Also, active and passive elements are combined [2].

Types of Electronically Guided Arrays

There are two basic types, passive and active.

Passive Arrays

Consists of a sole transmitter whose signal is distributed to the different elements with the signal phase being modified in each element via a phase shifter [3].

Active Arrays

Consist of individual transmission and reception modules. Each module has a phase shifter, a high-power amplifier (HPA), a duplexer, which permits communicating between signal transmission and reception, a protection system that keeps transmission residue from filtering into the reception, and a low-noise amplifier for the receptor.

In both cases, the phase shifters are controlled via a beam steering controller (BSC).

Advantages of Arrays with Electronic Phase Steering

Extreme phase agility (in the order of milliseconds) permits performing multiple simultaneous tasks like monitoring several simultaneous targets or monitoring and searching at the same time. This is accomplished through spatial, temporal, or spectral multiplexing, or all of them [4].

Besides, it saves energy and the complex systems that involve the antena addressing using servomotors. It also present little or no aperture blockage.

Another important advantage is that they permit accomplishing lower RCS on the platform on which they are mounted [2].

Additional advantages of Active Arrays

Because the transmitter high-power amplifiers and the receptor low-noise amplifiers are near the antenna, la signal-noise ratio will always be lower.

Figure 1. Block diagram of a passive and active phased array

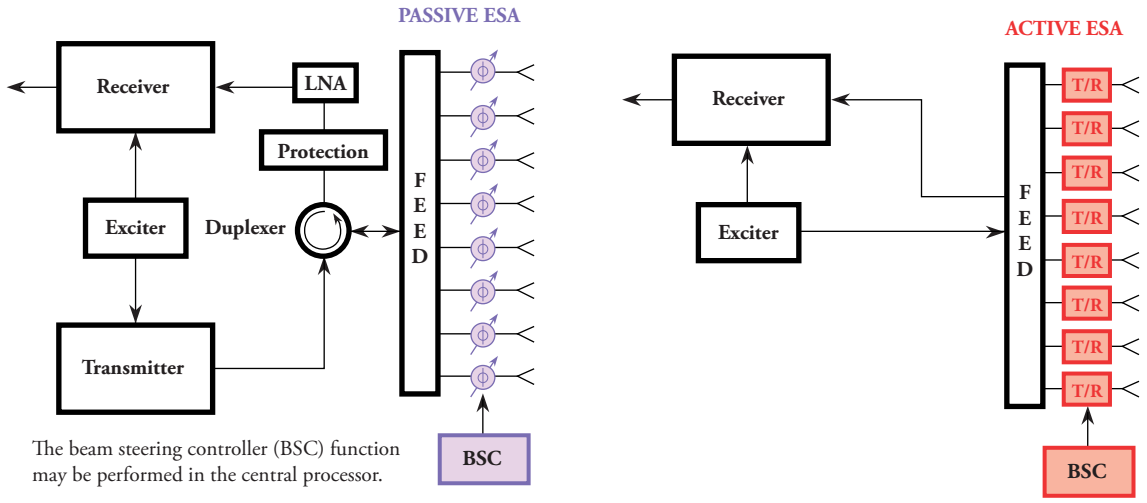

Permit controlling the lighting function, which permits reduction of side lobes.

Permit the generation of different phases pointing in different directions to different frequencies through the partition of the array into sub-arrays [2].

Limitations of Arrays With Electronic Phase Steering

The greater the pointing angle, with respect to the center, the lower the gain in the main phase and greater level of side lobes. As a general rule, the maximum pointing angle is ±60°.

The high cost, each transmission receptor module costs around US$2000. An array can have between 1000 and 2000 modules, which may mean a cost of up to 4-million US$ [2].

Electric Field of an Antenna Array

An array is formed by two or more radiators. These radiators are called elements. These elements may be of any type: dipoles, dishes, slots etc.

The electric field formed by array of "n" elements, in each "i" far field point with (Θ_i,) direction, is the sum of the individual electric fields of each element in that point.

$$E(\Theta_i,\phi_i) = \sum_{m=1}^{n} E_m(\Theta_i,\phi_i) \quad (1)$$

In the far field, it may be considered that the lines between each element and the point are parallel and, hence, the θ and φ angles are equal.

Also, the phase with which each signal reaches the point in space will be different. This can be found by calculating the difference of the distance travelled by the signal transmitted by each element to reach each point, obtaining the point product between the "q" propagation direction and the "d" distance vector for each emitter with respect to the point of reference. [6]

$$\Delta r_{ni} = \vec{d_i} \cdot \vec{q_i} \quad (2)$$

Assuming that the electromagnetic waves propagate in cosine form and that the phase of a signal originating at the point of reference reaches the far field with zero phase, it is possible to determine the "ψ_{ni}" phase with which all the signals arrive from their very wavelengths and the Δr_{ni} distance.

$$\psi_{ni}(\Theta,\phi) = \frac{2\pi * \Delta r_{ni}}{\lambda} \quad (3)$$

If we now incorporate the "I_n" illumination function represented by the signal width for each of the elements, we have the magnitude of the electric field in each direction (θ,φ).

$$E_i(\Theta,\phi) = \sum_{m=1}^{n} I_n * \cos(\psi_{ni}(\Theta,\phi)) \quad (4)$$

$$\vec{P} = \vec{E} \; X \; \vec{E^*} \quad (5)$$

$$S = \frac{Pt}{4*\pi} \quad (6)$$

Power and Power Density

From equation (4), and using equations (5) and (6), we calculate the magnitude of the power density in each "i" point – knowing that the direction is the same as that of the propagation vector, hence.

$$\overrightarrow{P_i(\Theta,\phi)} = |E_i^2| \cdot \vec{q_i} \quad (7)$$

$$\overrightarrow{S_i(\theta,\phi)} = \overrightarrow{P_i(\Theta,\phi)} \quad (8)$$

Electronic Phase Steering

Electronic phase steering[1] is accomplished by changing the initial phase with which the signal is transmitted in each element. This gap is done by successively delaying the signal between the adjacent elements. The "$\Delta\psi$" gap between the

[1] Set of particles with common origin, which propagate without dispersion.
Microsoft® Encarta® 2008. © 1993-2007 Microsoft Corporation. All rights reserved.

adjacent elements is proportional to the "d" distance between the elements. This means that the electric field generated by the array in the different directions would be given by.

$$E_i(\Theta,\phi) = \sum_{m=1}^{n} I_n * \cos(\psi_{ni0}(\Theta,\phi) - \Delta\psi) \quad (9)$$

Where $\psi ni0\ \Theta$ is the phase with which the signal arrives without delaying it, to the point in the far field.

If we wish to vary the pointing angle of the main phase in a "β" angle, a delay must be applied to the signal that produces a phase variation according to the following relation:

$$\Delta\psi = \frac{2\pi\, d \sin\beta}{\lambda} \quad (10)$$

Where "λ" is the signal wavelength.

Granularity of the Phase Shifters

Given that the phase variation in the different elements of the array is done with phase shifter elements that operate discretely through a binary control, the capacity of pointing the phase in a determined direction without degrading the radiation pattern (dimensions of main lobe and height of side lobes) depend on the amount of bits permitted by the phase shifter and the number of elements of the array. The minimum leap in angular phase units that each phase shifter can perform in function of the amount of bits available is denominated granularity and is given by equation (11) [4].

$$\Delta\psi_{\min} = \frac{2*\pi}{2^b}\ \text{rad} \quad (11)$$

Measurable Parameters

Width of the Main Lobe

Obtained by measuring the angle formed from the origin by the points of media power of the radiation pattern.

Level of Side Lobes

In practice, there is commitment among the level of the side lobes, the width of the main lobe, and the directivity. The most accepted means to assess the level of side lobes is by comparing the highest of these, on the logarithmic scale, with the main lobe.

Aspects not considered

For effects of this work, we will not bear in mind the mutual impedance between elements and polarization.

The Program

The program was developed in Matlab®, including the graphic user interface (GUI) through which the data are introduced and from which it is executed.

The software has a friendly interface that allow the data ingress to it's performance. The data to be introduced, shown in Figure 2, are:

Other data

For effects of this work, we will not bear in mind the mutual impedance between elements and polarization.

Number of samples per pi radians arc: The number of samples in the whole sphere is $2*S^2$.

Lobe discriminating threshold: This control permits adjusting a threshold that will allow adequate discrimination of the lobes for each particular case. This is implemented because in some cases the lowest level where the lobes are differentiated are too high and, hence, the program can assume that two different lobes are only one, producing errors. The most recommended value is 0.005.

Physical Configuration of the Antenna

- Number of rows of the array.

Figure 2. Screen deployed by the GUI for the introduction of data and execution of the program

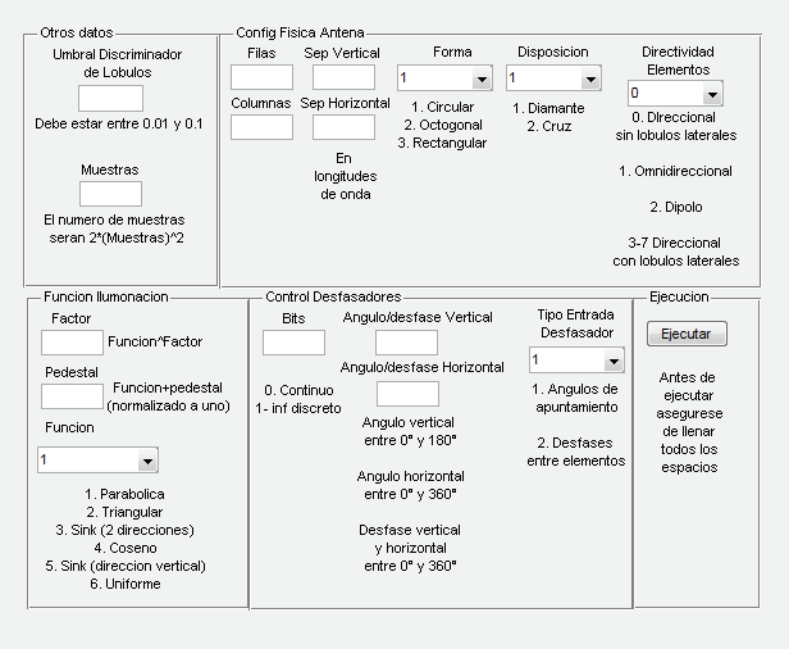

- Number of columns of the array.
- Vertical separation between rows.
- Horizontal separation between columns.
- Shape of the array; it can be (1) circular, (2) octagonal, or (3) rectangular.
- Disposition of the elements within the array; it can be in (1) diamond or in (2) cross.
- Directivity of the individual antennas; can be selected between (0) directional antenna without side lobes, (1) omnidirectional antenna, (2) dipole antenna, or (3,4,5,6, or 7) directional antennas with side lobes.

Lighting Function

The function can be selected from the following: (1) parabolic, (2) triangular, (3) sink, (4) cosine, or (5) uniform. In addition, it may be defined to what power the function selected is raised except for the uniform function that can only be raised to the first power.

The pedestal of the lighting function permits adding a reference value for the function greater than zero.

Phase Shifters

These permit selecting if the phase shifter is analogous (continuous) or digital (discrete); it also permits data input in two ways. In the first, the phase pointing angle is input in spherical coordinates (θ,φ). In the second form, the degrees of gap between consecutive elements are input.

Execution

This triggers the execution of the whole program. Be sure to have input all the data before executing the program; on the contrary, error will be produced.

Graphics

The results are deployed through graphics that can be manipulated by users.

Power in spherical coordinates (Θ,Φ) projected on a plane

This graphic permits better visualizing the peak powers for each of the lobes and permits more

easily locating the spherical coordinates of said points. It has the disadvantage of distorting the radiation pattern, given that a three-dimensional volumetric form is being represented on a plane.

Directivity of a sole element

This graphic permits visualizing the radiation pattern of a sole element.

Figure 3. Projection of the array normalized power over a plane of (θ,φ) coordinates

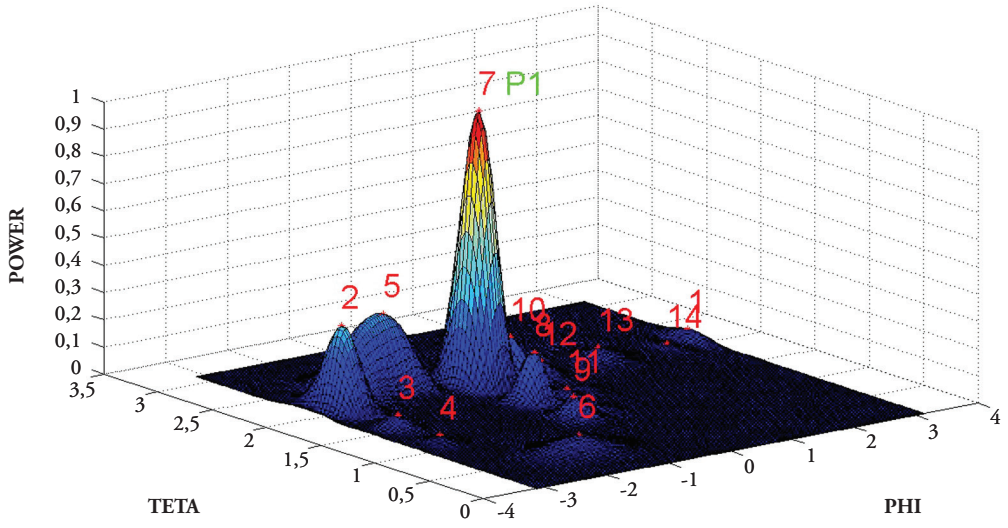

Radiation pattern of the Array

The radiation pattern permits visualizing the location of each of the lobes in three dimensions, numbering

Figure 4. Directivity of a sole element in 3d

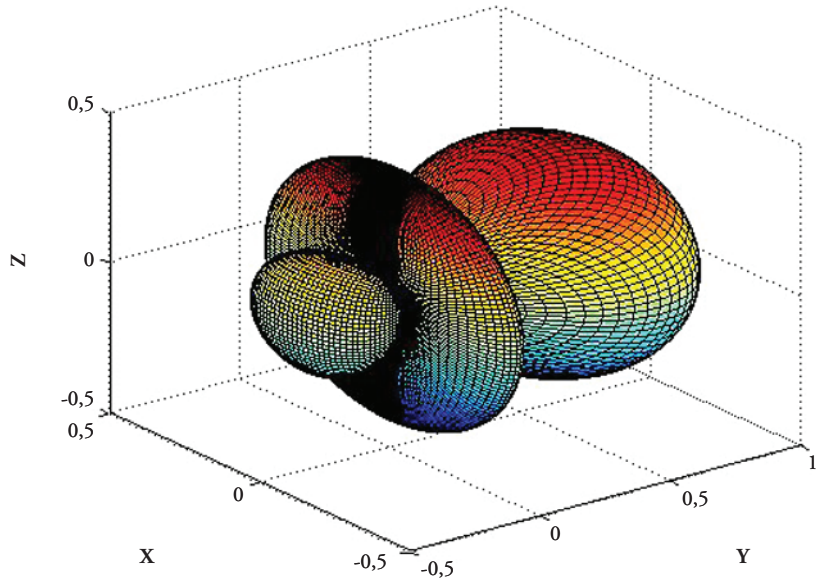

them in such a manner that they can be compared with the measurements. Additionally, the main lobe is distinguished with the green letter "P", followed by a number that indicates, in case of more than one main lobe, the corresponding lobe.

Array in space

It permits visualizing the shape, number of elements, and their disposition in space.

Figure 5. Radiation diagram of the array normalized to one

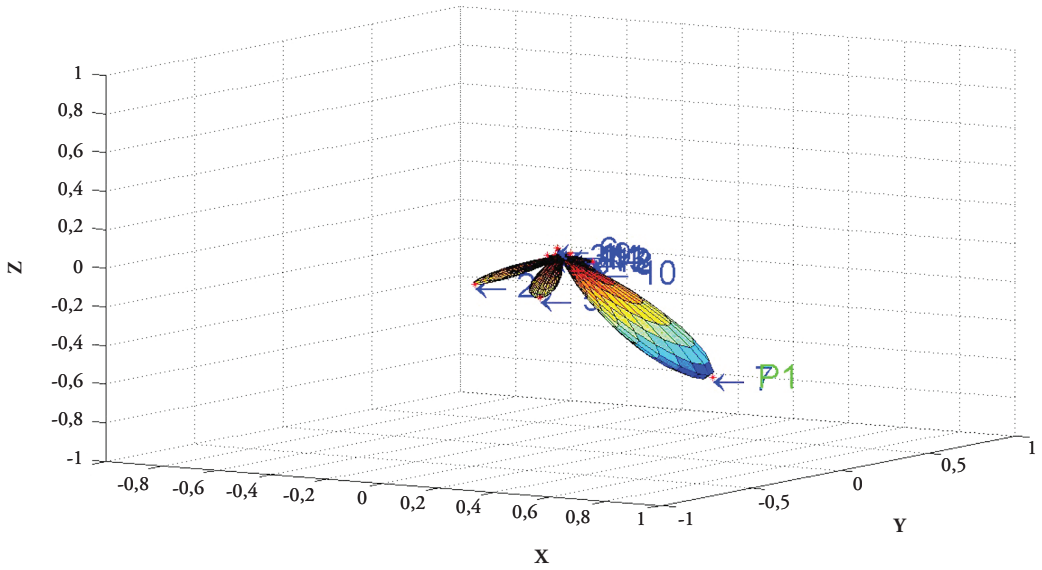

Lighting Function

This permits graphically visualizing the lighting function of the array. The surface of colors represents the values of the lighting function for each element.

Figure 6. Array in space

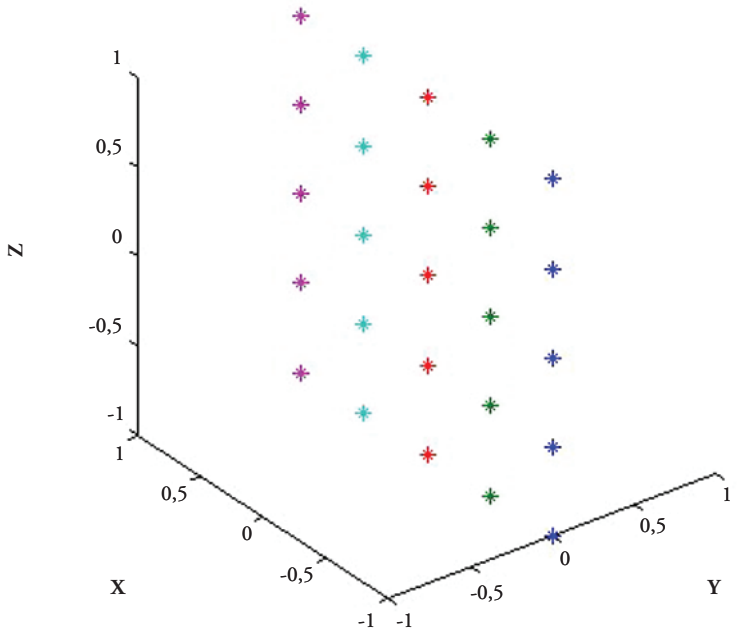

Initial Phase of the elements of the Array

It permits seeing graphically the initial phase of the array elements. The values of the initial phase form a surface of colors whose values are interpolated on the coordinate called "phase".

Figure 7. Lighting function of the Array

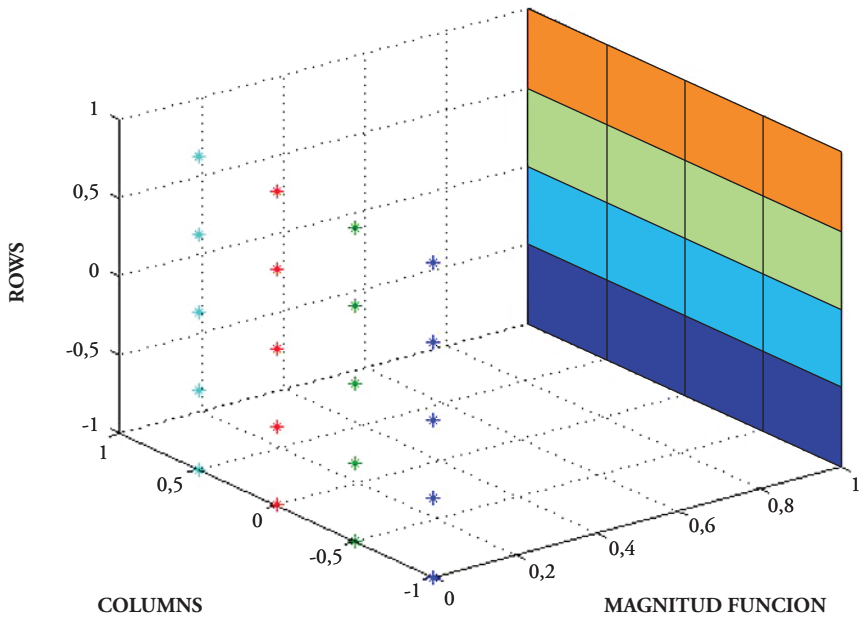

Results

The linear antenna is the base for the design of planar arrays, given that they represent the simplicity of performing analysis in two dimensions rather than three. For this case, we take a linear

Figure 8. Initial phase of the array elements

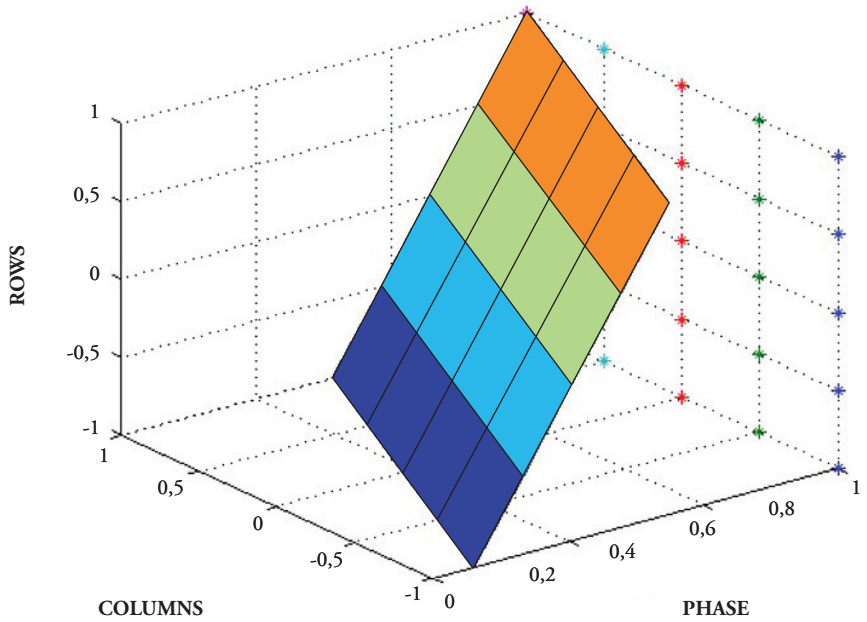

antenna of three omnidirectional elements; each separated from the other by half a wavelength, with a constant lighting function in all and a zero pointing angle.

Width of the Main Lobe in function of the pointing angle

To test the functioning of the program, two references are taken. The first is the approach made by M. Skollnick, in chapter 9.5 of "Introduction To Radar Systems" where it is suggested that the width of the θ_B lobe of a linear antenna uniformly illuminated and with a half wavelength gap between elements, it is approximately:

$$\theta_B \approx \frac{0.866\lambda}{Ndcos\,\theta_0} * \frac{180}{\pi} \qquad (12)$$

Where N is the number of elements.

The second test is made by taking the Matlab® "linear_array.m" function as reference, introduced by Bassem R. Mahafza in the work "Radar Systems Analysis and Design Using Matlab®" where the radiation pattern can be observed for a linear antenna.

The parameters measured to test the functioning are: width of the main lobe measured in degrees, the peak power in each of the lobes normalized to one, and the pointing angle for each lobe. For this, the measurements for the pointing angles of the main lobe are taken from 0 to 90°, in 10° leaps, measured from the perpendicular to the antenna. The following are the results obtained:

As noted in Figure 9, the results obtained by the three methods are very close up to a 30° pointing angle, even similar up to a 60° angle. As of 60°, it can be noted how the approximation proposed by Skollnick increases exponentially. The author clarifies in his work that the approximation operates for angles below 60°. Regarding the results of the "linear_ array .m" function, compared to those of the "3D" program, it may be observed that they are almost identical. It is worth clarifying that both methods reach their respective results via different methods. The "linear_array.m" function employs the discrete fast Fourier transform, from

Figure 9. Width of the main lobe in function of the pointing angle

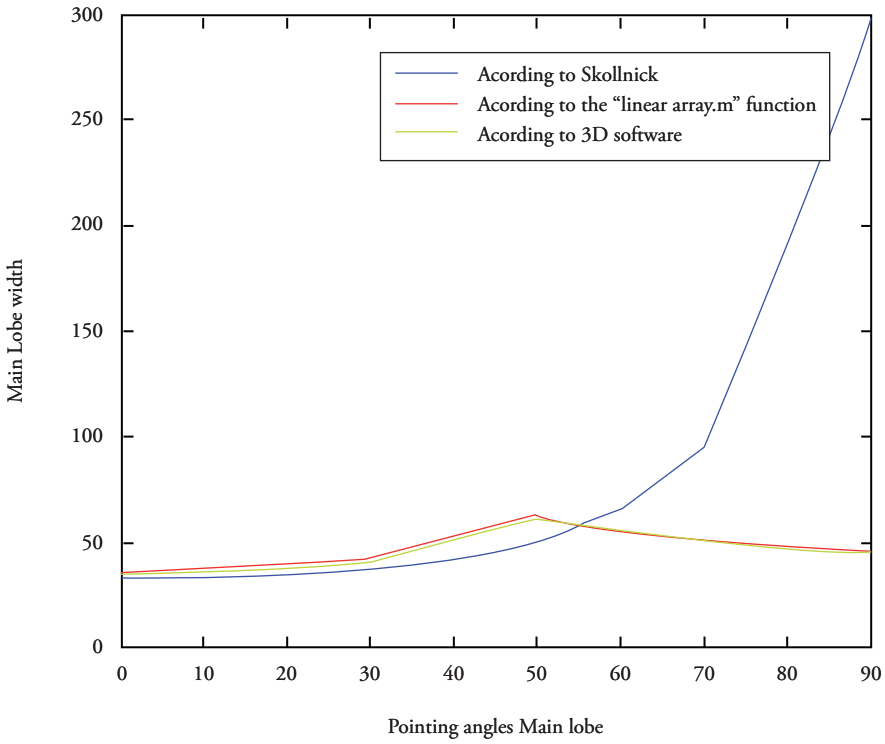

the lighting function, while the "3D" program employs the sum of all the electric fields in each point.

Peak Power normalized to one in function of the Pointing Angle

The magnitude of the peak power in each of the lobes is normalized and is compared with respect to the peak power of the main lobe. This is a very useful parameter to determine the relationship between the main lobe and the side lobes. As can be observed in Figure 10, the data taken in the "linear_ array .m" and the "3D" program are almost identical.

Figure 10. Peak power normalized to one, from each lobe, in function of the pointing angle

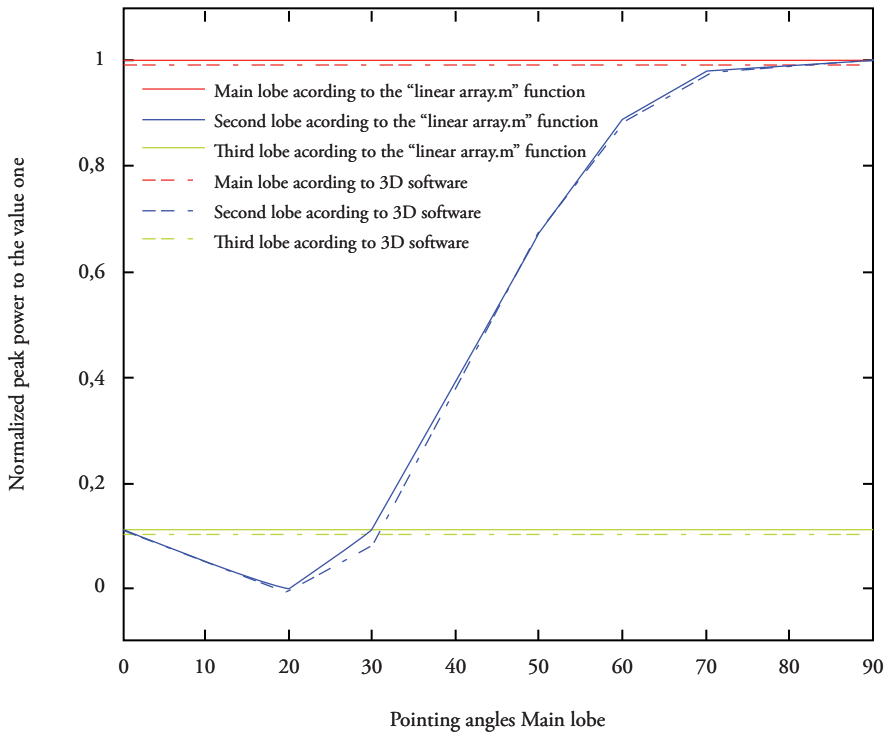

Pointing Angle of each lobe

By measuring the pointing angle of each lobe, we can confirm that the main lobe points in the desired direction. In addition to visualizing that the results obtained by both methods are quite similar.

Distance between elements

This parameter is especially important in the design of arrays because the separation of the elements permits narrower phases but generates greater height in the side lobes. The optimal spacing should produce narrow phase widths and small side lobes with a minimum of elements. It is also necessary to determine what will be the maximum pointing angle we want to achieve, given that with greater pointing angle greater side lobes and less width of the main lobe.

This ratio is suggested by Stimson G. [3] with the following equation.

$$d_{max} = \frac{\lambda}{1+sen\beta} \qquad (13)$$

Where d_{max} is the maximum gap between elements, and β is the maximum pointing angle sought. Figure 12 shows the solution to the equation for

Figure 11. Pointing angle of each lobe in function of the pointing angle of the main lobe

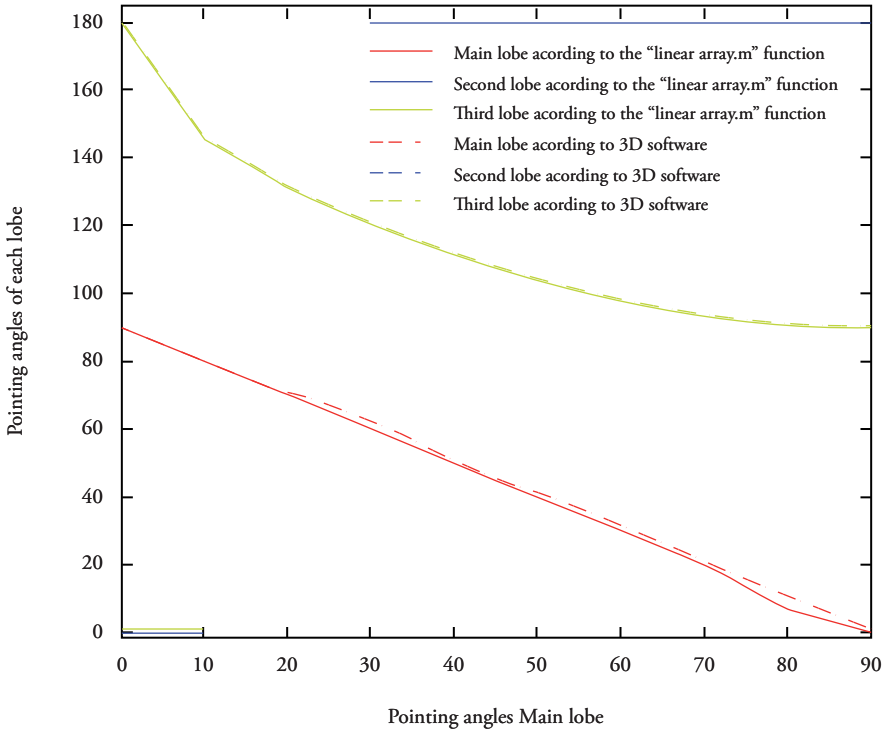

pointing angles between 0° and 90°. From the graphic, it may be deduced that for gap separations below 0.5 wavelengths, the maximum pointing angle is not limited, and that for gaps greater

Figure 12. Maximum pointing angle in function of the distance between elements

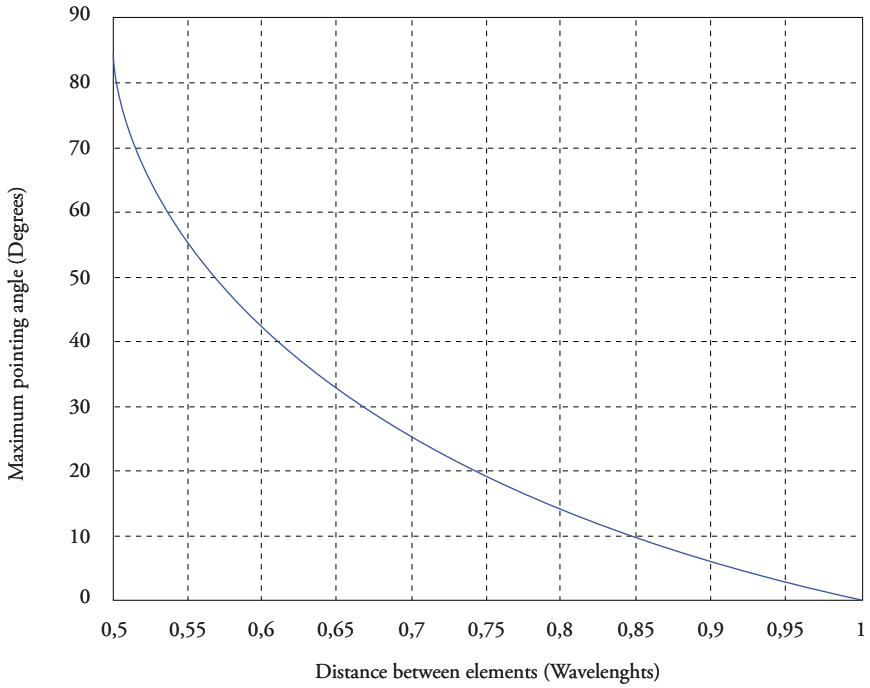

than a wavelength, there will always be side lobes important for pointing angles different to zero.

Figure 13 shows the results of the measurements of the amplitudes of the biggest side lobes for the different gaps between elements pointing the phase in different directions. It may be confirmed that the when the gap is greater between elements, the big side lobes appear in the smaller pointing angles.

Note that for 0.5 wavelength gaps, and pointing angles above 70° there are big side lobes, implying that the rule exposed by Stimson is not fulfilled. However, we were able to show that upon increasing the antenna length, the maximum pointing angle for gaps of 0.5 wavelengths increases with a tendency to reaching 90°, suggesting that the equation exposed by Stimson supposes an antenna of infinite length in which case the condition would be fulfilled.

Plannar Antenna

For planar antennas, proceed to verify their performance by varying length and effective area of the antenna, shape of the array, disposition of the elements in the array, the directivity of each element, distance between elements, the lighting function, granularity, and the pointing angle. The parameters to be measured will be: the percentage of power concentrated in each lobe, the peak power of each lobe, the ratio in decibels of the side lobes with respect to the main lobe, the directive gain, measurements in degrees, at points of half power, from the main lobe in the vertical and horizontal senses, and the solid angle formed by these measurements.

Length and effective area of the Antenna

According to theory, as the length of the antenna is increased with respect to the wave length, the main lobe will become narrower. To confirm that the program behaves according to these parameters, measurements will taken for rectangular arrays conformed of 2x2 to 11x11 omnidirectional elements, with vertical and horizontal gaps of 0.5 wavelengths between elements, uniform lighting

Figure 13. Amplitude of the biggest lateral lobe in function of the gap between elements and the pointing angle

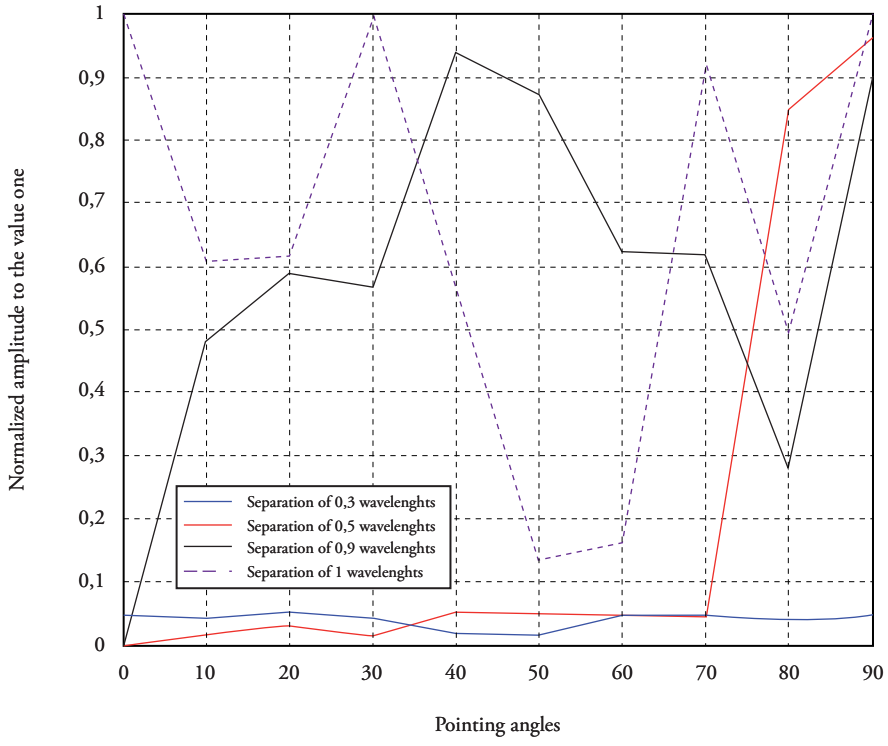

function, disposition in cross shape, and a 0° pointing angle. Antenna length is given by the number of elements and the gap between them. As noted in Figure 14, the condition posed is fulfilled, given that the greater antenna length will make the main lobe narrower. Analogically, it is shown that the condition is fulfilled for the physical aperture of the antenna, having to diminish the solid angle of the main lobe when increasing the area of the antenna, as observed in Figure 15.

The Lighting Function

This parameter is quite important in regards to the

Figure 14. Width/height of the main lobe in function of the length of the array. Gap of 0.5 wavelengths between elements. The nxn numbers indicate the rows and columns conforming the array

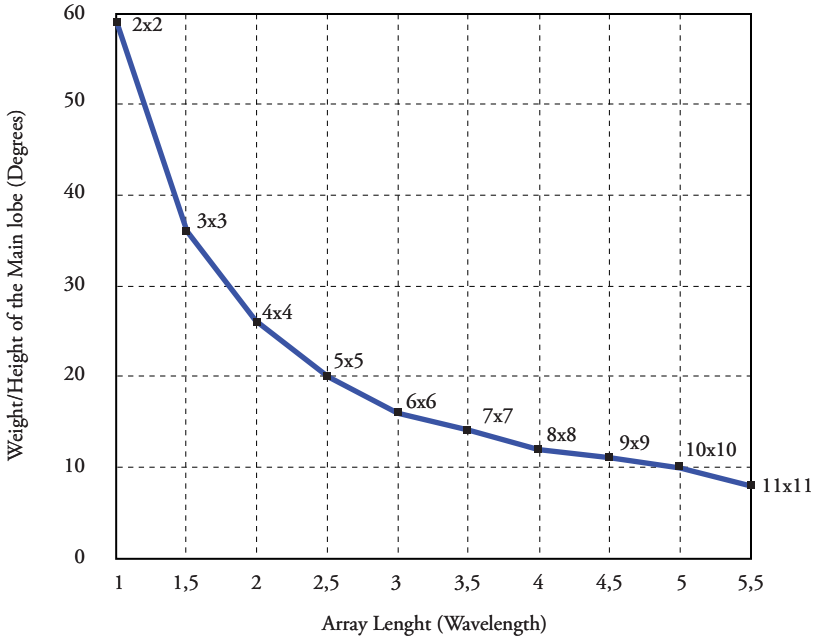

Figure 15. Solid angle of the main lobe in function of the physical aperture of the array. Separation between elements at 0.5 wavelengths. The nxn numbers indicate the rows and columns conforming the array

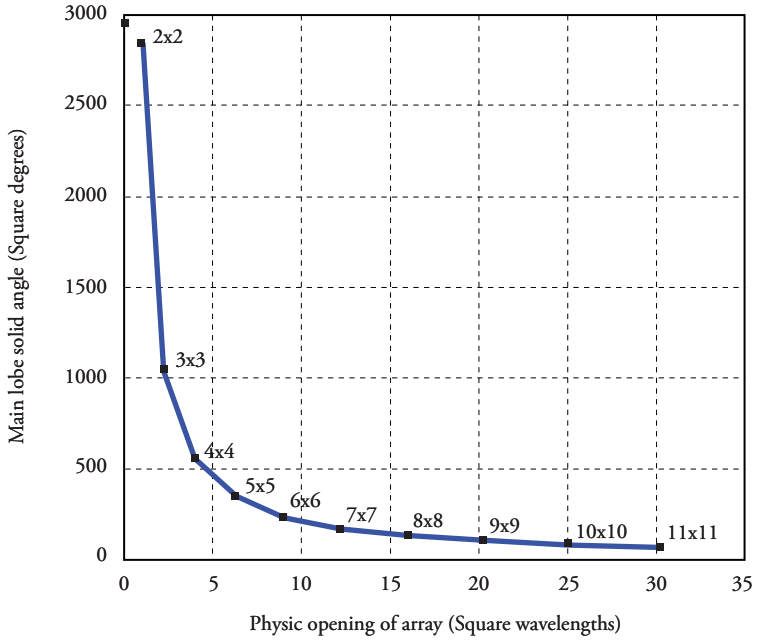

suppression of side lobes. It consists in controlling the signal width of each element. Knowing that the radiation pattern in the far field is an approximation to the Fourier transform of lighting function, we can then approach the shape of the radiation pattern by controlling the lighting function.

To test the functioning, use an array of 10 x 10 elements, in circular shape, with gap of 0.5 wavelengths, with different pointing degrees and alternating the lighting function among uniform, triangular, parabolic, cosine, and sink. In each case, evaluate the width of the main lobe and the height of the biggest secondary lobe.

Upon observing Figure 16, it may be deduced that the best lighting function to accomplish a narrow phase width is a "sink" function and the worst is the triangular function.

Upon observing Figure 17, it may be deduced that the best lighting function to accomplish small side lobes is the triangular function and the worst is the "sink" function. From the two previous deductions, we may state that there is a commitment between the width of the main lobe and the height of the side lobes, which besides depending on the gap between elements, also depends on the lighting function.

Figure 16. Width of the main lobe in function of the pointing angle for different lighting functions

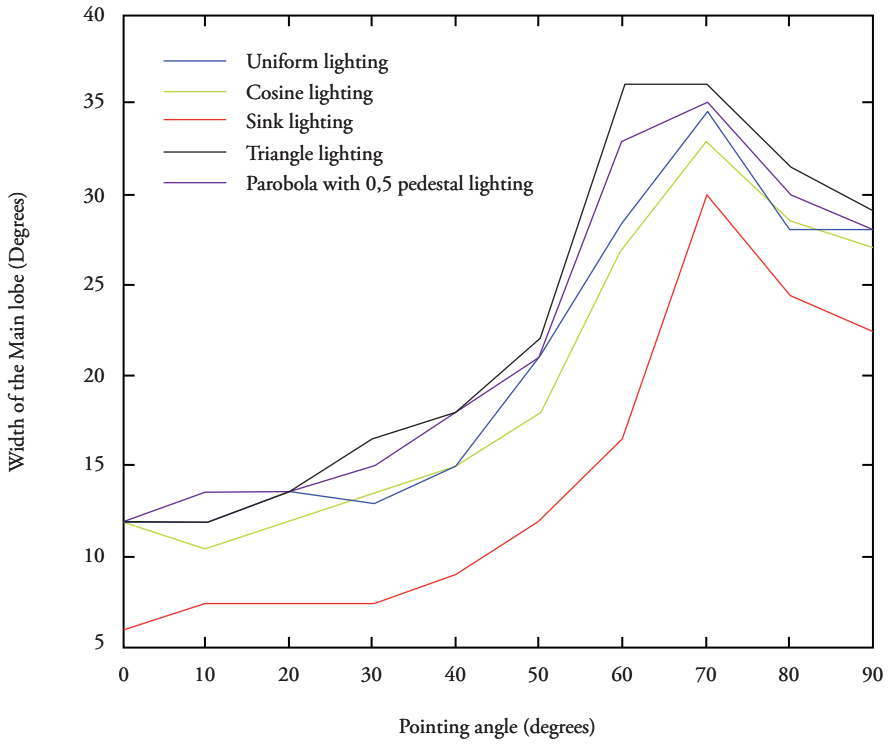

The selection of the lighting function will then depend on the specific requirements of the particular application.

Granularity and the Pointing Angle

This parameter permits visualizing the effect the phase shifters of binary or digital functioning have on phase pointing. For such, we will use an array of 5 x 5 elements, of rectangular shape, with uniform lighting function, gap between elements of 0.5 wavelengths, employing phase shifters from 1 to 5 bits for the different pointing angles. The width of the main lobe and the amplitude of the biggest secondary lobe will be measured to test the functioning.

Figure 17. Amplitude of the biggest lateral lobe lateral in function of the pointing angle for different lighting functions

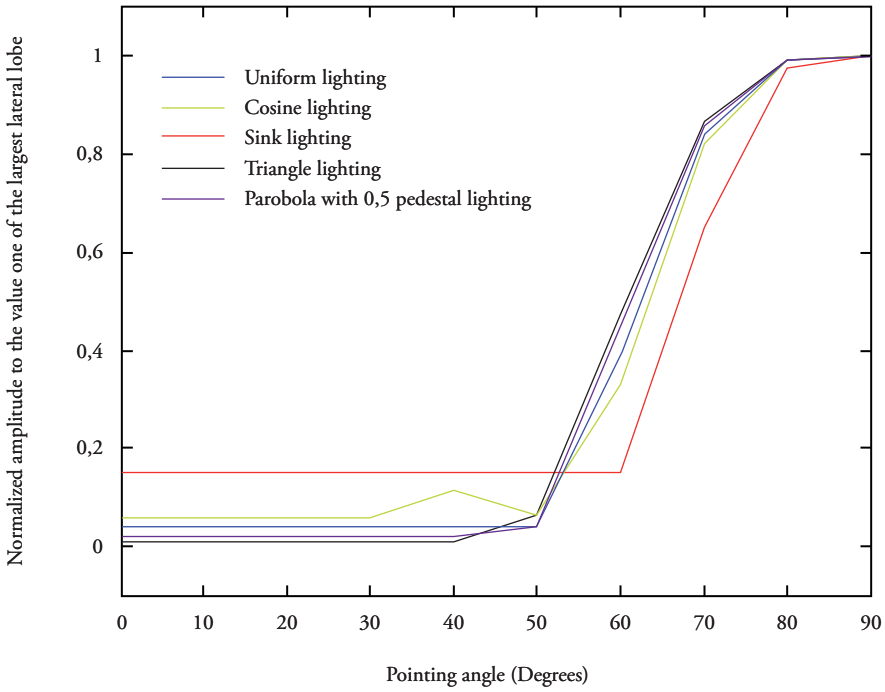

Figure 18. Width of the main lobe in function of the pointing angle for phase shifters with different numbers of bits

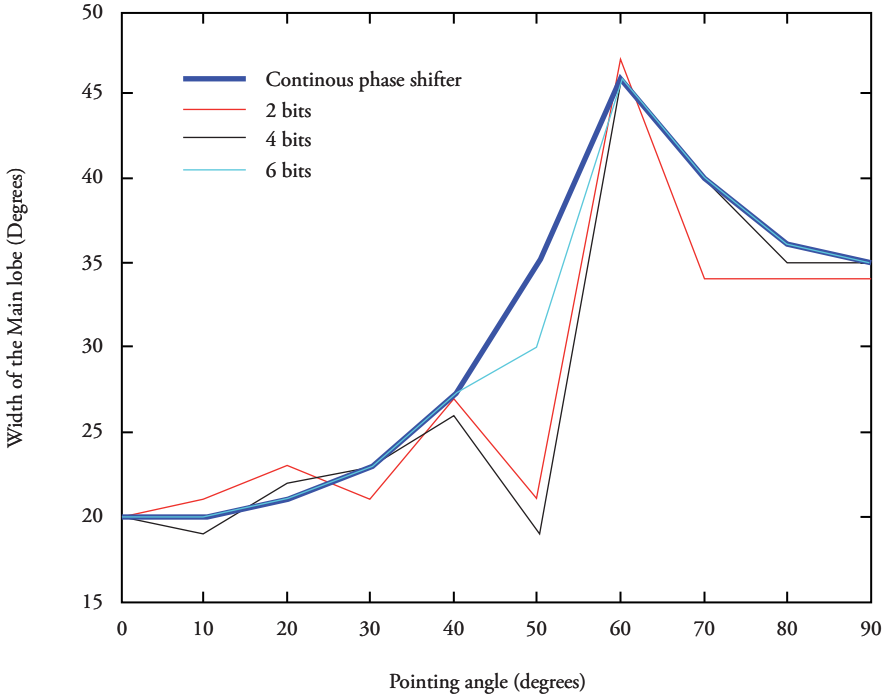

As noted in Figures 18 and 19, as the number of bits of the phase shifter is increased, the performance of the array appears more like when a continuous phase shifter is used. Observe how the side lobes

Figure 19. Width of the main lobe in function of the pointing angle for phase shifters with different numbers of bits

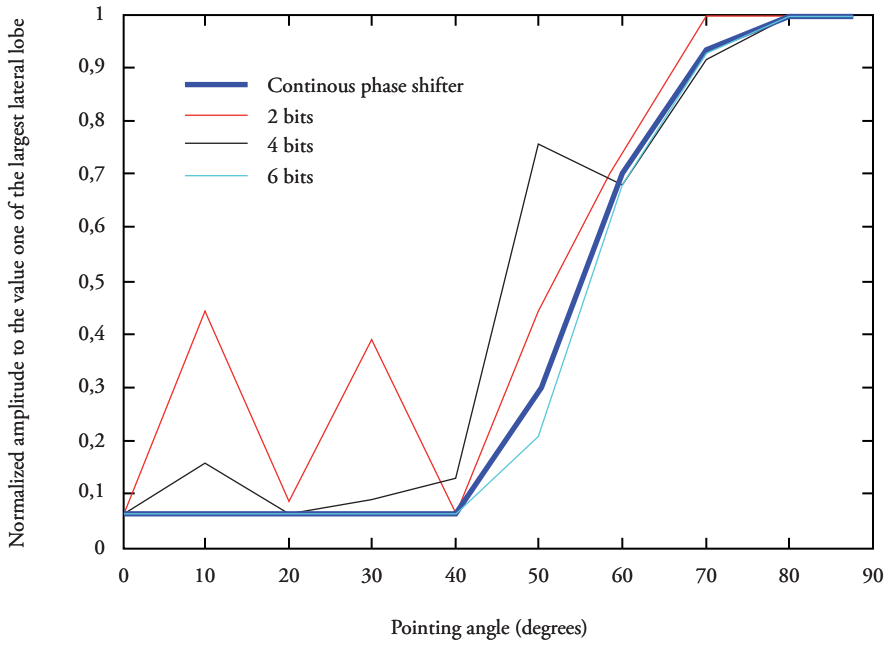

are increased while the main lobe is broadened or narrowed when trying to point the phase in certain directions with a limited number of bits (red line = 2 bits). It is also noted that by using 6 bits, the response of the side lobes and the main lobe is quite similar to that of the continuous phase shifter.

Directivity of each Element

This parameter permits employing elements with distinct radiation patterns; this serves to visualize the functioning of more realistic arrays and will permit – in case of having the measurements – incorporating data of real elements and, thus, visualizing how said elements would behave in distinct dispositions.

Shape and disposition of the Elements in the Array

These two aspects that can be manipulated in the program represent a good number of possibilities and their effect on the performance of the array is quite complex; thereby, they will not be used in this work as proof. However, given that they are enabled within the program, they permit future research on the theme.

Problem of exercise

To show the use of the program as a tool for the design of an active phased array, a hypothetical design problem is posed and a solution is sought.

Let us suppose that we need to design an active phased array antenna for a radar that must comply with the following specifications: Electronically steer the phase in vertical sense with a beam 3° in width and 3 decibels in the horizontal and 15° in the vertical, able to have a pointing angle of ± 50° in vertical sense, operate in the G band, employ the least possible elements and be the smallest possible size, have small side lobes and be steerable in elevation in 3-degree steps without important degradation of its radiation pattern.

Employing the approach suggested by Skollnik in [2], which indicates that for an array of "N" elements with a gap of 0.5 λ between elements, the width of the main lobe in "θ_{3dB}" half power is:

$$\theta_{3dB} = \frac{102}{N} [grados] \quad (14)$$

The number of elements that would be necessary to comply with the required widths of the main lobe may be estimated, both in the vertical and horizontal sense.

$$N_{horizontal} = \frac{102}{3°} = 34 \quad (15)$$

$$N_{vertical} = \frac{102}{15°} = 6.8 \approx 7 \quad (16)$$

Then, an array is constructed with 7 x 34 elements, initially with cross-shaped disposition and rectangular shape, uniform lighting function, gap between elements of 0.5 wavelengths, and continuous phase shifters. Given the lack of knowledge of the radiation pattern of the elements, these are presumed omnidirectional. Thereafter, the configuration is modified in function of the results obtained increasing the antenna length by adding another element and vertically increasing the distance between elements up to 0.521 wavelengths; this with the purpose of diminishing the height of the main lobe. It is noted that height diminishes but without complying with the required specifications. Because of the aforementioned, we proceed to add another element in vertical sense until completing 10 rows; additionally, the distance between elements is increased in horizontal sense up to 0.9 wavelengths and the number of elements is decreased to 19 per row, seeking to maintain the antenna length; bearing in mind that electronic phase steering is not required in the horizontal sense.

The results obtained indicate that to accomplish the required specifications, a configuration of

Figure 20a. Height of the main lobe in function of the pointing angle for distinct array configurations

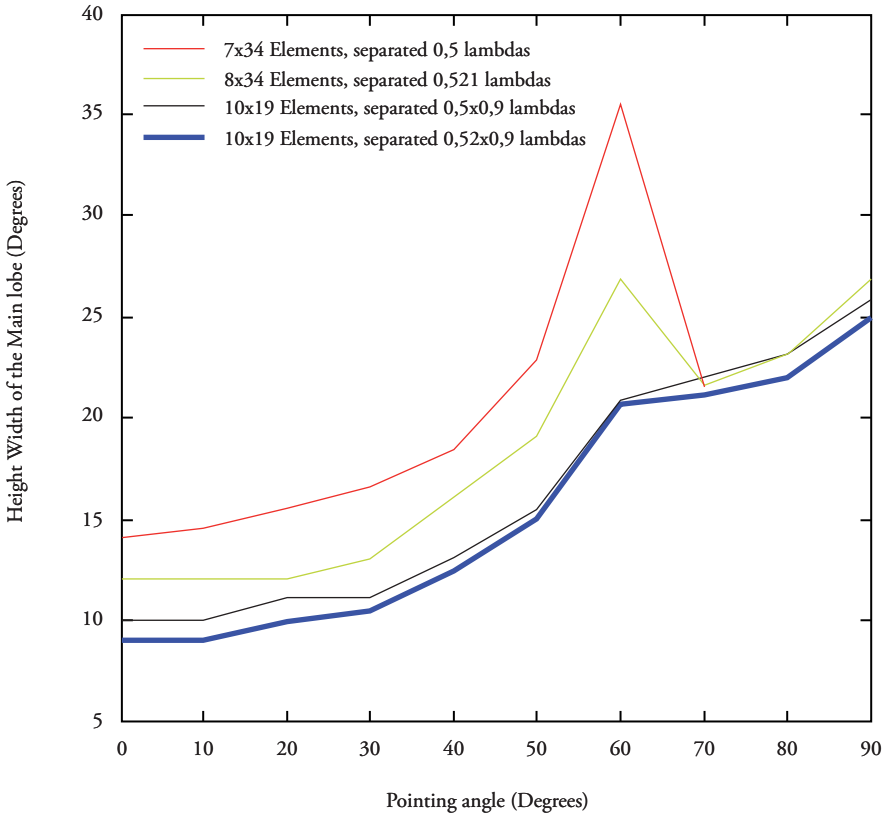

Figure 20b. Peak power normalized of the biggest lateral lobe in function of the pointing angle for distinct array configurations

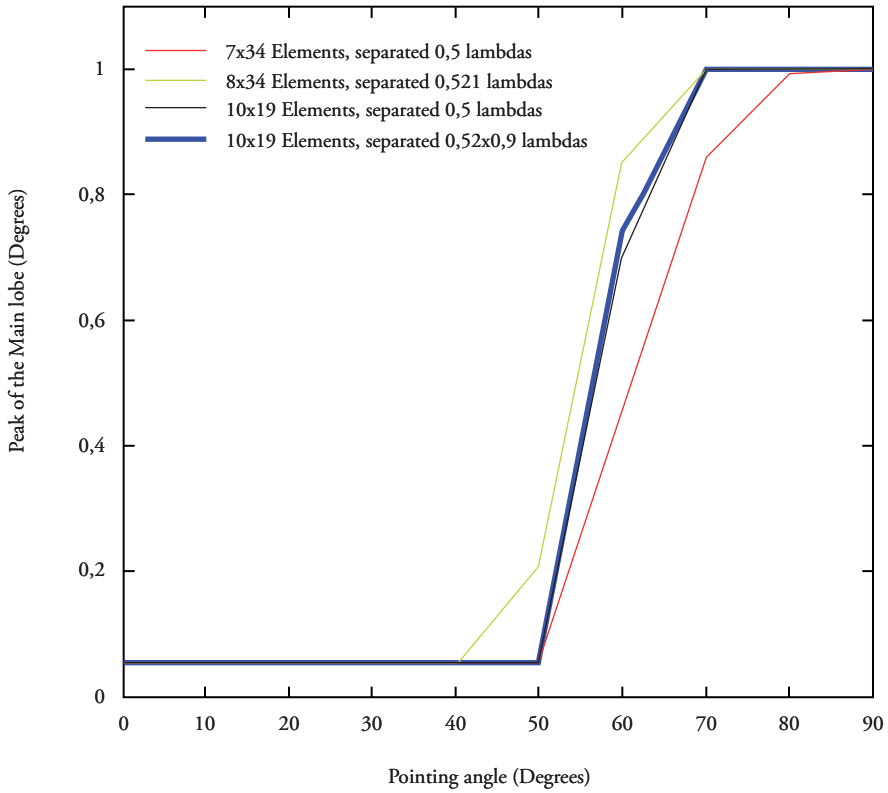

Figure 21a. Height of the main lobe in function of the pointing angle for an array of 10 x 19 elements with gaps of 0.5 x 0.9 wavelengths with phase shifters of "n" bits

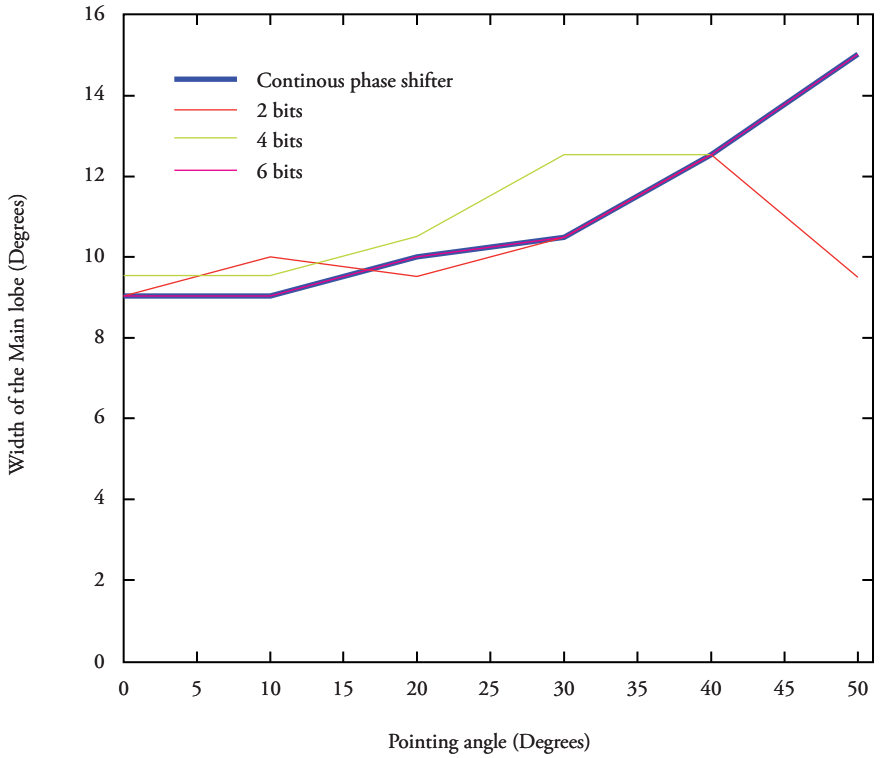

Figure 21b. Peak power normalized of the biggest lateral lobe, in function of the pointing angle for an array of 10 x 19 elements with gaps of 0.5 x 0.9 wavelengths with phase shifters of "n" bits

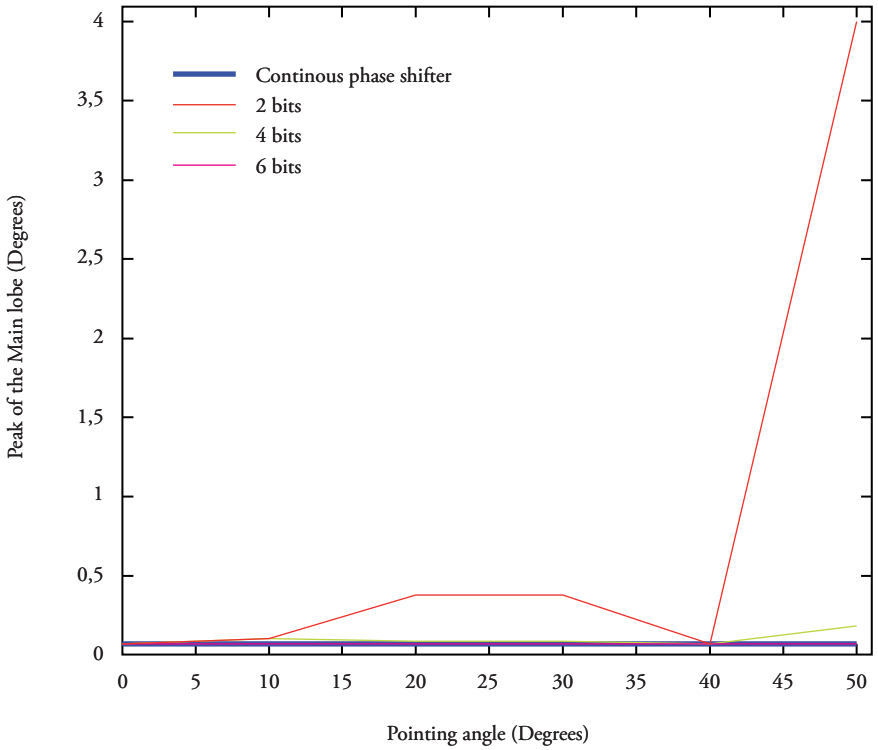

10x19 elements is required with vertical gap of 0.52 wavelengths and horizontal gap of 0.9 wavelengths. These results correspond to the blue line in Figure 20.

Now the required granularity configuration will be sought, taking values from 2 bits until reaching a number where results are accomplished within the parameters.

The results observed in Figure 21 indicate that phase shifters are required with 4 bits to accomplish satisfactory performance.

Conclusions

It is useful to model the theoretical functioning of a phased array by employing computer tools like Matlab®, given that it represents savings in costs during the initial stages of the design, permitting the visualization of problems and prevention of errors prior to the physical construction of prototypes.

Phased-active arrays are the present and future of radiofrequency antennas because they offer great advantages, among which the most important are the extreme agility to steer the phase, which permits almost instantaneous spatial multiplexing.

As conclusion of the proof, it may be stated that the measurements made with the "3D" program adjust to the models used as reference, which are presumed approximate to the reality given the trajectory of its authors. Hence, the model employed is suitable to model antenna arrays.

Bibliography

[1] KRAUS JOHN D., MARTHEFKA RONALD J. *Antennas for all applications*, third edition .Chapter 4 Point source.P72-86. Chapter 5 Arrays of point sources. P 90-159.

[2] SKOLLNICK, MERRILL L. *Introduction to radar systems*, third edition. Mc Graw Hill. Chapter 9. The Radar Antenna. 9.5

Electronically Steered Phased Array Antennas. P559-566. 9.6 Phase Shifters. P567-580. 9.8 Radiators for Phased Arrays. P589-593. 9.9 Architectures for Phased arrays. P594-614. 9.14. Cost of Phased Array Radar. P646-650. 9.16 Systems Aspects of Phased Array Radars. P658-660.

[3] STIMSON GEORGE W. *Air-Born Radar*, Second edition. Science Publishers INC. Part IX Advanced Concepts. Chapter 37. Electronically Steered array antennas. P473-479. Chapter 38. ESA design. P481-498.

[4] EDDE, BYRON. *Radar Principles Technologies and Applications*. Practice Hall PTR. Chapter 9 Radar Antennas. 9-2 Arrays of discrete elements- Principles. P422-426. 9-8 Electronically Phased steered Arrays. P450-460.

[5] BASSEM R. MAHAFZA. *Radar Systems Analysis and Design using Matlab®*, Second Edition. Chapman & Hall/CRC. 2005.

Design methodology of a military messaging system

Metodología de diseño de un sistema de mensajería militar

Gustavo Pérez V. [1]
Stefany Marrugo Ll. [2]

Abstract

The paper describes the design methodology of a military messaging system. The system's design is characterized by its coherence among security, transmission medium, and design protocol, which allow added value in the strategic operations center. The system allows using a selected data base for subsequent applications of operations research tools and simulation. The system was designed with a low bandwidth communications network (HF / VHF / UHF and satellite phone calls) as the transmission media. The messaging system security is based on a public key cryptographic system. The paper also shows some of the test results of the system's functionality.

Key words: Military Messaging System, strategic Messaging System, Messaging System design, design methodology, communications network.

Resumen

El documento describe la metodología de diseño de un sistema de mensajería militar. El diseño del sistema está caracterizado por su coherencia entre la seguridad, el medio de transmisión y el protocolo de diseño, lo que permite obtener valor agregado en el centro estratégico de operaciones. El sistema permite utilizar una base de información seleccionada, para posteriormente aplicarle herramientas de investigación de operaciones y simulación. El sistema fue diseñado tomando una red de comunicaciones de bajo ancho de banda (HF/VHF/UHF y telefonía satelital), como medio de transmisión. La seguridad del sistema de mensajería está basada en un sistema criptográfico de clave pública. El documento muestra además, algunos de los resultados obtenidos en las pruebas de funcionalidad del sistema.

Palabras claves: Sistema de mensajería militar, Sistema estratégico de mensajería, diseño de sistema de mensajería, metodología de diseño, redes de comunicación.

Date received: November 19th, 2010. - *Fecha de recepción: 19 de Noviembre de 2010.*
Date Accepted: December 14th, 2010. - *Fecha de aceptación: 14 de Diciembre de 2010.*

[1] Corporación de Ciencia y Tecnología para el Desarrollo de la Industria Naval, Marítima y Fluvial - Cotecmar.
E-mail: smarrugo@cotecmar.com
[2] Corporación de Ciencia y Tecnología para el Desarrollo de la Industria Naval, Marítima y Fluvial - Cotecmar.
E-mail: gustavoperezv@gmail.com

Introduction

Among the projects executed by the R&D plus innovation direction at COTECMAR, prototype was developed of a Messaging system for the exchange of short information and with non-synchronic character between tactical units in the field of operations and the strategic Command and Control Center.

The Messaging system is a comprehensive part of a set of sub-systems that make up the Command and Control Main System, and it is supported by different technologies and existing communication infrastructures to carry out its purposes.

The objective of this document is to describe the design methodology of the Messaging System developed by clearly showing the advantages obtained by making a coherent design of all the components of said system, which was elaborated by bearing in mind the requirements from Command and Control and the restrictions in the means available, seeking to satisfy and provide the necessary connectivity (via different transmission media), interoperability, and security in the transportation of information.

Theoretical Framework

The need for a reliable communications system is ever-more important in military operations, given that the potential effectiveness of combat systems supporting the mission depends to a greater extent on adequate coordination. Also, implementing the concepts posed by the Network Centric Warfare (NCW) according to which the complete availability of information at the indicated time and place is the most relevant factor, relying fully on a communications infrastructure with sufficient capacities for transportation of information (*Snyder, 1993*).

Although telecommunications are frequently characterized through attributes like bandwidth, data transference rate, or error rate, its main value within the Command and Control context is derived from the possibility of establishing connectivity not merely among the commanders involved in the mission, but also among the different participants who are under their charge and the network of sensors or devices supporting the acquisition of relevant information for the purposes of the operation. Additionally, the exchange of information on a safe communications infrastructure is an indispensable requirement in the military setting, to the point that the interception of communication can mean the difference between victory and defeat (*Hutcherson, 1994*).

A messaging system is a form of text-based communication, in real or differed time, between two or more individuals (units or entities). The text is sent through devices connected to a network.

Currently, it is common to find messaging systems on the internet, offering easily accessed specific services, most of which are based on TCP/IP.

For the specific military case, messaging is the main path of data communication between Command and Control center and the operational tactical units.

"The implementation of communication networks in military settings confronts important challenges that must be considered before reaching a practical application. In the first place, diverse types of airborne units exist, like airplanes and helicopters, which are in the combat space, implying different degrees of mobility that must be managed. Meanwhile, land or naval units face variable environmental settings that affect in different ways the propagation of radio-frequency signals. These conditions faced by the tactical units translate into limited bandwidths, intermittent connections, and a high probability of delay in information transmissions, situations that must be considered when implementing a data communications system" (*Michael J. Ryan, 2002*).

A messaging system seeking to satisfy military needs must comply with the following general requirements:

- Privacy.
- Authenticity.

- Certification.
- Integrity.
- Non-repudiation.
- Availability

The communications system developed is able to facilitate interconnection through the communication networks that are currently part of the existing technological infrastructure, adequately integrate their functionality, and satisfy the requirements of the joint operations undertaken. Additionally, the communications system permits data exchange via different transmission media and among equipment from different manufacturers, guaranteeing the system's interoperability.

Design Methodology

In general, the design of the components of the messaging system was carried out in parallel manner. However, each component was developed by following a particular methodology.

To develop the architecture for the information system, an incremental debugging scheme was used based on the architecture centered design method (ACDM), developed by Anthony Lattanze at Carnegie Mellon University, and architecture points of view were those elaborated by Nick Rozanski and Eoin Woods.

For the communications design protocol, we kept in mind criteria like: security, bandwidth restrictions and data optimization (selection of particular data of the operation under execution), which would permit assigning greater added value to the Command and Control system. Likewise, we considered the design of the architecture of the Command and Control system for information access, bearing in mind security mechanisms. The design protocol was based on the methodology described in the book "Design and Validation of Computer Protocols" (*Gerard J.Holzmann, 1991*).

Software design was carried out by using the Rational Unified Process (RUP) methodology, which is a software development process and along with the Unified Modeling Language (UML) constitutes the standard methodology most often used for analysis, implementation, and documentation of systems aimed at objects. The messaging system developed comprises six different applications that interoperate bearing in mind the protocol and security criteria, bandwidth restrictions, and data optimization previously proposed. Four of these applications were developed in Visual C++ language and two others in Visual C#.

The methodology employed in designing the system's security was based on public code cryptography (elliptic curves, due to code size), both for data messages and for network administration messages. During the design of the system's security, we kept in mind aspects like: the confidence ratio based on the levels of the staff that plan the operations and the processes of Authentication, Authorization, and user access to the network, with encrypted mechanisms.

The messaging system developed is formed by different network elements, which are:

- The tactical units
- The access nodes
- The messaging node
- The security node
- The Command and Control node (SIC2)

These network elements develop specific functions within the messaging system to permit safe and reliable exchange of information, so that said information is transmitted exactly to where it is required and at the moment requested.

The Messaging System permits data exchange via different transmission media and among equipment from different manufacturers, guaranteeing interoperability of the system.

Due to security reasons, the System will provide access to the messaging services according to parameters of authentication, authorization, and certification, which must be configured and negotiated in each case in the security node.

The messaging node implements all the necessary functionality for message management and

permits their exchange between the tactical units and the SIC2 node, for which adequate formats and technologies have been established to permit proper information exchange.

The access node is in charge of carrying out gateway functions among the different communication technologies integrated in Command and Control systems. There will be as many as it is convenient to reach the territorial coverage of the theaters of operations.

For the tactical units, two types of applications were developed, depending on the means of communication: one for radio-communications and another for IP communications. The radio-communications application accesses the network through the access node.

The following figure shows a general scheme of the messaging system developed.

Figure 1. Messaging system general scheme

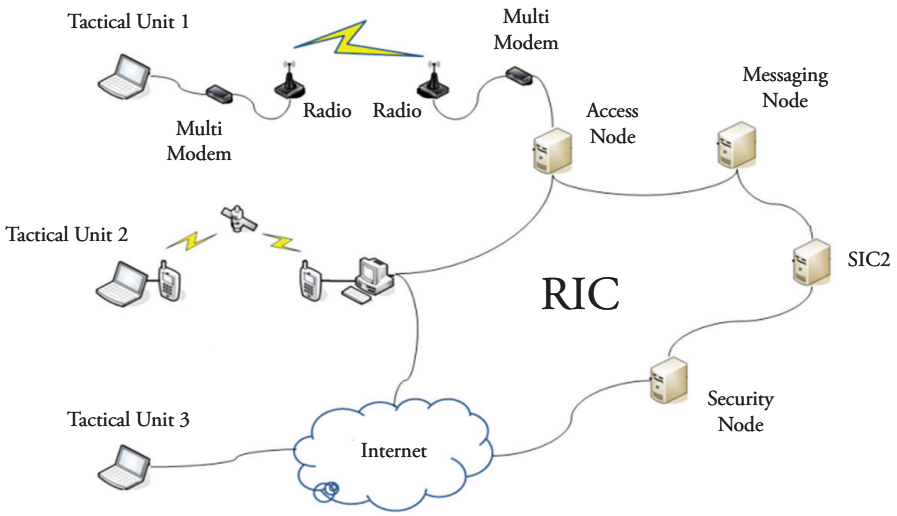

Theoretical Framework

The first step in the process of the design protocol is to analyze the operational setting and establish the set of communication requirements. The requirements are established in general terms including the following:

- Global operational setting (peace/exercise/war).
- Number of platforms (with prevision for additional participants).
- Deployment of the platforms.
- Data to be transmitted and received by each platform (or group of platforms if this is how matters are facilitated) and their characteristics in terms of:
  - ✓ Type of platform.
  - ✓ Quantity.
  - ✓ Security, including requirements of privacy, authenticity, integrity, and non-repudiation.
  - ✓ Type of message.
  - ✓ Network administration messages

For proper network operation, it is essential to have coordinated use of cryptography; hence, the availability of the codes is totally indispensable for communications to be possible.

Information exchange in the system

The system's technical functions encompass network management and exchange of tactical information related to the following 11 tasks of operational aspects; these technical functions are:

- Information exchange of the System and of

Network management.
- Precise Identification and Location of Participants (PILP).
- Air surveillance.
- Surface surveillance (Maritime).
- Submarine surveillance (Maritime).
- Land surveillance.
- Electromagnetic surveillance.
- Electronic warfare (EW)/ Intelligence.
- Mission management.
- Control.
- Information management.

Types of Messages

The types of messages derived from the design protocol are:

Table 1. Types of existing messages in the protocol of the messaging system prototype

Type	Name of Message
01	Position of Vessels, Submarines, and Boats
02	Position of Airplanes and Helicopters
03	Position of land units
04	Contact report
05	Code request
06	Code delivery
07	Chat
08	Chat reception
09	Connection request
10	Connection data
11	Connection report
12	Table of processes
13	Publication of Tactical unit IP codes
14	Delivery of configuration
15	Disconnection
16	Verification of tactical unit IP status
17	Response of verification of status
18	Publication of tactical unit Radio codes
19	Verification of tactical unit Radio status
20	Response to initial broadcast

These messages contain the following information: A clearly transmitted heading (without cryptography) and encrypted data.

It is important to highlight that the data in each type of message were carefully selected to provide the basic information according to the type of message and additional data that permit feeding operational analyses and simulation processes in the operations center, which gives added value to the system developed.

Identification of Vocabulary Format of Protocol Messages

According to protocol services, all the information needs are gathered in the following types of messages:
- Link control messages
- Participant identification and location messages
- Contact messages
- Tactical unit configuration messages
- Informal messages (chat)

Message data may be "Free Text" or "Fixed Format". Free Text messages are primarily used for chatting, although other types of data may also be exchanged as long as the participants agree on the format.

Fixed Format messages, as the name indicates, have a defined format, onto which information may only be introduced in the fields disposed for such purpose.

The message label indicates its function.

These 20 types of messages (see Table 2) gather the information necessary to obtain the tactical panorama in the Command and Control node, according to the strategic level this implies.

Guidelines for Message Exchange

To control the exchange of messages, privacy, integrity, authenticity, and non-repudiation services must be implemented, requiring the following guidelines:

Table 2. Message labels

TYPE	NAME OF MESSAGE	TYPE OF OPERATION
01	Position of Vessels, Submarines, and Boats	Participant identification and location messages
02	Position of Airplanes and Helicopters	Participant identification and location messages
03	Position of land units	Participant identification and location messages
04	Contact report	Contact messages
05	Code request	Link control messages
06	Code delivery	Link control messages
07	Chat	Informal messages
08	Chat reception	Informal messages
09	Connection request	Link control messages
10	Connection data	Link control messages
11	Connection report	Link control messages
12	Table of processes	Link control messages
13	Publication of Tactical unit IP codes	Link control messages
14	Delivery of configuration	Tactical unit configuration messages
15	Disconnection	Link control messages
16	Verification of tactical unit IP status	Link control messages
17	Response of status verification	Link control messages
18	Publication of tactical unit Radio codes	Link control messages
19	Verification of tactical unit Radio status	Link control messages
20	Response to initial broadcast	Link control messages

a. Privacy is implemented through cryptographic procedures of the data transmitted; these procedures will be performed via code mechanisms through elliptic curves.

b. Every station on the network must generate its own private code, and through a procedure it must generate a public code that stems from the product of its own private code and the ellipsis point; thereafter, it must publish such in the security node delivering it certified.

c. Every station requiring delivery of a message must have a public code from the addressee, which is sent by the security node at the moment of the connection and, with a procedure generate the private code of the communication that results from its own private code, the addressee's public code, and the point of the curve, to proceed to encrypt with AES.

d. The authenticity is made on the security node and it is conducted through an encrypted message that the security node can decrypt if and only if the originator is whom it says it is.

e. Integrity is given if the decrypted message has a coherent meaning inasmuch as the cryptogram is related to all the contents of the message.

f. The functionality of "non-repudiation" is given through the messaging node, which registers all the events of all the communications of the system.

g. The transmitting station must codify the data by using the code resulting from the point of curve *p*, and the code from addressee *Kb*; for its part, the addressee does the same to determine the code with the same point on curve *p* and the code from originator *Ka*, then encrypts using symmetric AES.

$$Mns\ Ak = A\ \{Ka*(p*Kb)\} \quad (1)$$

$$Msg\ Bk = B\ \{Kb*(p*Kb)\} \quad (2)$$

h. The transmitting unit encrypts the message with the code resulting from its own code, the addressee's code, and the ellipsis point, and it is directed to the messaging node for its distribution.

i. The messaging node receives the message and stores it encrypted and when the addressee unit is connected it proceeds to send the message, which is already encrypted with the addressee code.

j. The tactical nodes send the encrypted messages with the addressee code, through the messaging node.

k. At the start of a communication, every station must carry out an identification and authentication procedure on the security node.

l. The messaging node must lead to registering communication with the following data: Type of message, identification of originator, identification of addressee, group date hour sent, group date hour delivered to the addressee, the code gram and the verification digit of "pending".

m. Messages of interactive communications (chat) are considered informal, but are also controlled by the messaging node.

n. Every tactical unit, when started, sends a verification message to the security node to corroborate the status of its publication of codes.

o. The security node responds to the verification message affirmatively or negatively, depending on whether it has or not published the valid code.

p. The tactical units may request disconnection from the network at any time, an important situation to keep the system from sending messages, but have them stored by the messaging node.

q. When a tactical unit is going to start operating or has any novelty in its configuration, it must send a configuration message to the Command and Control node. The message includes the relevant aspects of the conditions in which the unit operates.

r. The staff preparing the order of operations must generate and publish the codes of all the units participating in such. This is done through the message "publication of codes", which is sent to the security node with the code destined for said purpose.

s. Upon a message of publication of codes, the security node respond with a message "connection data" that contains the table of public codes, including the published code, and the table of identification of all the units reporting.

t. The tactical units once configured and with its codes reported, may request connection to the network through the message "connection request" sent to the security node.

u. The security node, after authenticating it, responds to this last message by sending it a message with the updated tables of public codes and identification.

v. Likewise, every time a unit requests connection, the security node will send a message "connection report" to the "Command and Control" and "messaging" nodes. This message contains the identification of individuals connecting, their IP (in case it is

a tactical unit via radio, will place the IP of the corresponding access node) and the tables of public codes and identifies.

For the protocol of the messaging system a strategic level has been considered so that the types of messages that should be transmitted are only those referring to the tactical panorama, given that this strategic level merely requires supervision functions and not direct command, although if the command is executed such must be executed through the chain of command and not directly.

System's Security

To design the system's security, we adopted a public code cryptography scheme to ensure the data transmitted from and to the systems, minimizing exposure of sensitive information and, thus, avoiding the possibility of communications in transit of being intercepted and decoded.

The security implemented for the prototype of the messaging system developed, although based on public code cryptographic security, is able to protect the whole system, given that to perform any process within the system, it is necessary to conduct a series of validations, authentications, authorizations.

Description of the Security System

The security of the messaging system is based on that all processes are authenticated, authorized, and certified by an ECDH public code cryptographic system.

Verification processes made in the security system are:

- In case a user is completely new for the system, that user must register (publish codes) before accessing the system's functionalities, through a confidence mechanism.
- Access to the Messaging System is restricted by the use of codes assigned to users. Only units previously authenticated and authorized may enter the system.
- Access of these units to work operations on the system will be according to the roles, permits, and profiles previously established. Authenticated users must be authorized according to the profiles, roles, and permits defined.
- To access the system, the established digital signatures must be used to guarantee the integrity of a message and, thus, be able to associate it with the author to ensure that the contents have not been modified and its origin is validated.

In the messaging system developed, the security node is in charge of performing all these validations. Once the unit is authenticated, it is removed from the system and notification is sent to all the active elements on the network, reporting the event. All the messages (notifications) will be encrypted.

Encrypting algorithm used

The elliptic curve cryptography (ECC) used in the messaging system is defined as a variant of asymmetrical or public code cryptography based on the mathematics of elliptic curves. Its authors argue that ECC could be quicker and may use shorter codes than ancient methods -like RSA - while providing an equivalent level of security. The use of elliptic curves in cryptography was proposed independently by Neal Koblitz and Victor Miller in 1985.

Asymmetrical or public code cryptography systems use two distinct codes: one may be public, the other is private. Possessing the public code does not provide sufficient information to determine the private code. These types of systems are based on the difficulty in finding the solution to certain mathematical problems. One of these problems is the so-called discrete logarithm. Finding the value of b given equation ab = c, when a and c are known values, may be a problem of exponential complexity for certain large-size finite groups; while the inverse problem, discrete exponentiation,

can be efficiently evaluated by using, for example, binary exponentiation.

An elliptic curve is a flat curve defined by an equation in the form of:

$$y^2 = x^3 + ax + b \tag{3}$$

With the set of points G that form the curve (*i.e.*, all the solutions of the equation plus a point O, called point on the infinite) plus an additive + operation, an abelian group is formed. If coordinates x and y are chosen from a finite field, then we are in the presence of a finite abelian group. The problem of the discrete logarithm on this set of points (PLDCE) is thought to be more difficult to solve than that corresponding to the finite fields (PLD). Thus, the lengths of codes in elliptic curve cryptography can be shorter with a comparable level of security.

The following shows a brief mathematical introduction to the algorithm:

Let p > 3 prime. The elliptic curve

$$Ey^2 = x^3 + ax + b \tag{4}$$

over Z_p is the set of solutions (x, y) $\in Z_p \times Z_p$ in the congruence

$$y^2 = x^3 + ax + b \pmod{p} \tag{5}$$

Where $a,b \in Z_p$ are constants so that

$$4a^3 + 27b^2 \neq 0 \pmod{p} \tag{6}$$

An additive operation is defined as follows: Considering that $P = (x_1, y_1)$ and $Q = (x_2,y_2)$ are points on E and O is a point on the infinite. If $x_2 = x_1$ and $y_2 = -y_1$, then $P + Q = O$; on the contrary $P + Q = (x_3, y_3)$, where $x3 = \lambda_2 - x_1 - x_2$, $y_3 = \lambda(x_1 - x_3) - y_1$, and

$$\lambda = \begin{cases} \dfrac{y_2 - y_1}{x_2 - x_1} \\ \dfrac{3x_1^2 + a}{2y_1} \end{cases} \tag{7}$$

Finally, we define

$$P + O = O + P = P \forall P \in E \tag{8}$$

With this we may show that E is an abelian group with element identity O. It is worth noting that the inverse of (x, y) (written as -(x, y) given that the operation is additive) is (x, -y), for all $(x, y) \in E$.

According to the Hasse theorem, the number of points #E contained in E is close to p. More precisely, the following inequality is satisfied:

$$p + 1 - 2\sqrt{p} \leq \#E \leq p + 1 + 2\sqrt{p} \tag{9}$$

Given that it is known that any prime order group is cyclical, what is required is to find a subgroup of E in the order of q (q prime) to have an isomorphism with Z_p where the problem of the discrete logarithm is untreatable. In this instance, being α a generator of the cyclical group (which could be any element of the group different from O, the identity), we may calculate the "powers" of α (which are written as multiples of α because the operation of the group is additive).

Algorithm of Code Generation

In the cryptographic use, a specific base point G is selected and published to use with the curve *E(q)*. A random integer k is chosen as private code, and then the value $P = k*G$ is shown as public code (note that the supposed difficulty of the PLDCE implies that k is difficult to deduct from P). If the tactical unit A (TUA) and the tactical unit B (TUB) have private codes *kA* and *kB*, and the public codes PA and PB, then TUA could calculate $kA*PB = (kA*kB)*G$; and TUB can obtain the same value given that $kB*PA = (kB*kA)*G$.

This permits establishing a "secret" value that both TUA and TUB can easily calculate, but that is very complicated to derive by a third party. Additionally, TUB cannot learn anything new on kA during this transaction, so that code used by TUA continues being private.

The methods used in practice to encrypt messages based on this secret value consist in adaptations of older cryptosystems from discrete logarithms originally designed to be used in other groups. Among those we could include Diffie-Hellman, ElGamal, and DSA.

Performing the necessary operations to execute this system is slower than for a factorization system or full-module discrete logarithm of the same size. In any case, the authors of ECC systems believe that the PLDCE is significantly more complicated than the factorization problems or of PLD and, thus, the same security may be obtained via shorter code lengths by using ECC, to the point that it may be faster than, for example, RSA. The results published until now tend to confirm this, although some experts remain skeptical.

Elliptic curve cryptography has been broadly recognized as the strongest algorithm for a given code length, for which it may be useful on links with very limited bandwidth requirements.

NIST and ANSI X9 have established minimum requirements of code size of 1024 bits for RSA and DSA and 160 bits for ECC, corresponding to an 80-bit code symmetrical block. NIST has published a list of recommended elliptic curves of five different code sizes (80, 112, 128, 192, and 256). In general, the ECC over a binary group requires an asymmetrical code double the size of that corresponding to a symmetrical code.

Analysis of Confidence

Certicom is the main commercial company for ECC; this organization has 130 patents and has issued licenses on technology to the National Security Agency (NSA) for 25 million dollars. Certicom has also sponsored several challenges to the ECC algorithm. The most complex solved, until now, is a 109-bit code, which was broken by a team of researchers in early 2003. The team that broke the code used a parallel massive attack based on the 'birthday attack', through more than 10,000 Pentium-type PCs working continuously during 540 days. It is estimated that the minimum code length recommended for ECC (163 bits) would require 108 times the resources used to solve the problem with 109 bits.

Communications Network

The need to offer a reliable and efficient communications system is ever-more important in military operations, given that the different systems supporting a mission depend greatly on a communications infrastructure with enough capacity for transport of information that guarantees the availability of such at the indicated time and place.

The messaging system developed contemplates data exchange by networks with different transmission media, from high and low bandwidth, considering security mechanisms like information encryption, for information transference through an asynchronous communications mechanism where data transmission takes place in deferred time and in real time.

The data communications system is supported by the current network infrastructure, which defines characteristics for information transference and integration of services, aspects that should be kept in mind to obtain the maximum advantage from the resources offered by said network. Likewise, the system is supported on the RF communication systems (tactical radios), which should guarantee the necessary measures to maintain the operational channel.

Description of the Communications Network

The networks available for the development of the messaging system were:

- IP network with repeaters located in high places, with incomplete coverage of the possible theaters of operations.
- VSAT network with fixed and mobile land stations to cover theaters of operations outside the prior coverage.
- Low orbit satellite telephone network to complement the coverage previously exposed.

These networks imply an availability of restricted bandwidth, which was proven through experimentation. For VHF and UHF with a 25-KHz theoretical bandwidth, we accomplished a velocity of 2.4 kbps in the tests and bearing in mind these results, we measure performances. With low orbit satellite telephone service we experimented with IRIDIUM in two services: short bus data and data kit, obtaining the following performance: a velocity of 9.6 kbps with some restrictions:

1. Necessity for clear skies and without obstacles.
2. We noted low availability, especially in jungle zones.

It is worth noting how limited the bandwidth is for any of the means used by the tactical units to transmit information; thereby, becoming a limiting factor of the design.

Coherence among designs

To view the coherence among the most important components of the messaging system developed, the following figure shows the interrelation among them and their spiral development, to accomplish optimization of the system.

Figure 2. Spiral design diagram

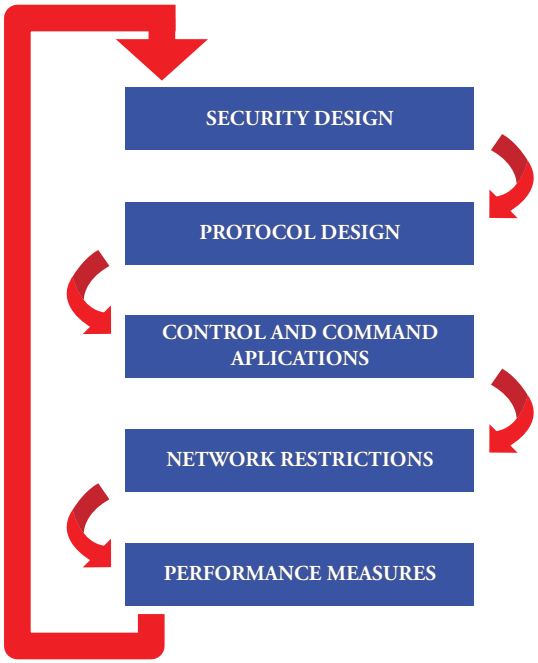

Figure 3. Tactical panorama

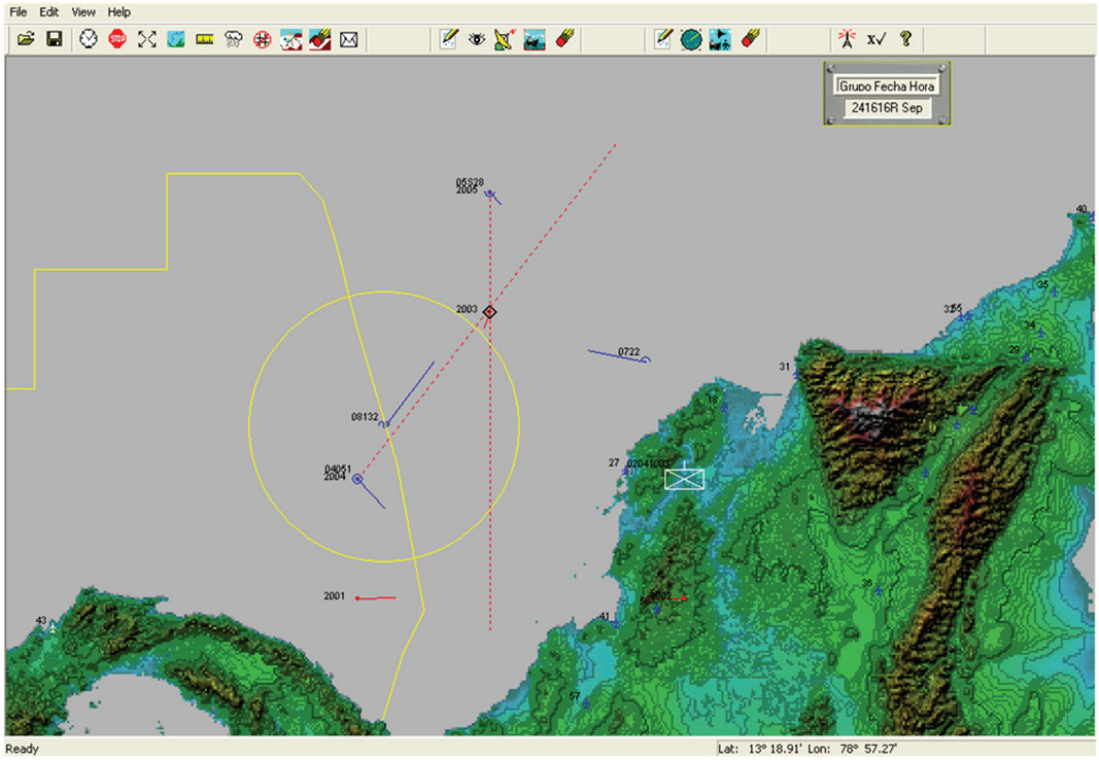

Figure 2 shows how the designs of the system's components create relationships of interdependence and as they advance on the spiral, the system's performance improves, adjusted to the restrictions established.

Results

Figure 3 shows a tactical panorama for a situation of intervention among a vessel, a submarine, an airplane, a helicopter (identified in blue) and an army company (identified in white) from the same forces.

The operation is of maritime interdiction in which the units have made their reports of position and configuration to the Command and Control node. Additionally, they have made contact reports, thus:

- An Electronic Support Measure (ESM) detection report from the submarine (this detection appears in red dotted line in Figure 3).
- An ESM detection report from the surface unit, correlated with the prior report.

The surface unit launched the helicopter to intercept the contact identified in the Command and Control center, from the ESM correlation.

The prediction of the reach of the helicopter radar may be noted in Figure 3, as made at the Command and Control center, with a 50% probability of detection, taking as a base the data from the configuration report, which includes the characteristics of its search radar and the characteristics of the target sought.

Another important factor is that position simulations are made (in function of time) in the Command and Control center, both of its units and of the contacts, guaranteeing a very good approximation to what will happen in real time.

Conclusions

Herein, we introduced the design of a messaging system, characterized by the coherence among its components, designed to obtain the tactical panorama in a strategic center.

Through this development, we showed that it is possible to have a military messaging system by using a low bandwidth communications network. We obtained a security level that satisfied the system's requirements, using public code cryptography, with a code space of 2192, which guarantees privacy between "secret" and "ultra secret" levels (according to NSA).

The messaging system developed guarantees privacy, integrity, certification, authenticity, and non-repudiation of the information transmitted and of the factors intervening in Exchange processes of such.

Finally, it must be highlighted that the messaging system contemplates mechanisms to support the asynchrony of the military reports made.

References

HUTCHERSON, N. (1994). C*ommand & Control Warfare: Putting another tool in the war-fighters database.* Alabama: Air University Press.

MCCABE, J. D. (2007). *Network analysis, architecture, and design*. Burlington: Morgan Kauffman.

MICHAEL J. RYAN, M. R. (2002). *Tactical communications for the digitized battlefield*. Norwood: Arthec House, Inc.

New York: Institute of Electrical and Electronics Engineers, Inc. Teare, D. (2007). Designing for Cisco Internetwork Solutions (DESGN). Indianapolis: Cisco press.

RUSSELL, M. (10/08/2004). http://www.ibm.com/. Recovered 07/07/2010, from Quality busters: Forget the environment. The importance of non-functional and operational requirements: http://www.ibm.com/developerworks/web/library/wa-qualbust1/

SNYDER, F. (1993). *Command and Control: The Literature and Commentaries*. Washington D.C: National Defense University Press Publications.

Software Engineering Standards Committee of the IEEE Computer Society. (1998). IEEE Guide for Developing System Requirements Specifications.

United States Department of Defense. (2003). MIL-STD-961E, Defense and program-unique specifications format and content.

Information of the Volume 4

Información del Volúmen 4

Author Index

Técnicas para el desarrollo de metamodelos aplicadas a problemas multidimensionales en el diseño de barcos
In: Volume 4 Number 7; pp 55-64.

Tascón, Oscar
CFD modeling of 2D impact with symmetric entry
Modelado CFD del impacto 2D con entrada simétrica
In: Volume 4 Number 8; pp 25-30.

Yang, Qing
SPH Boundary Deficiency Correction for Improved Boundary Conditionsat Deformable Surfaces
SPH Corrección de la deficiencia de límites para la mejora de condiciones de contornos en superficies deformables
In: Volume 4 Number 7; pp 31-42.

Editorial Regulations for Authors

Thematic

The *Ship Science and Technology* Journal accepts for publication original engineering contributions in English language on ship design, hydrodynamics, dynamics of ships, structures and materials, vibrations and noise, technology of ship construction, marine engineering, standards and regulations, ocean engineering and port infrastructure, results of scientific and technological researches. Every article shall be subject to consideration of the Editorial Council of *The Ship Science and Technology* Journal deciding on pertinence of its publication.

Typology

The *Ship Science and Technology* Journal accepts publishing articles classified within following typology (Colciencias 2006):

- *Scientific and technological research article*. Document presenting detailed original results of finished research projects. Generally, the structure used contains for important parts: introduction, methodology, results and conclusions.
- *Reflection Article*. Document presenting results of a finished research as of an analytical, interpretative or critical perspective of author, on a specific theme, resorting to original sources.
- *Revision Article*. Document resulting from a finished research in the field of science or technology in which published or unpublished results are analyzed, systemized and integrated in order to present advances and development trends. It is characterized for presenting an attentive bibliographic revision of at least 50 references.

Format

All articles must be sent to editor of *The Ship Science and Technology* Journal accompanied by a letter from authors requesting its publication. Every article must be written in *Microsoft Word* processor in single space and sent in magnetic form. Articles must not exceed 10,000 words (9 pages). File must contain all text and any tabulation and mathematical equations.
All mathematical equations must be written in *Microsoft Word Equation Editor*. This file must contain graphs and figures; additionally, they must be sent in a modifiable format file (soft copy). Also, abbreviations and acronyms have to be defined the first time they appear in the text.

Content

All articles must contain following elements that must appear in the same order as follows:

Title
It must be concise (no more than 25 words) with appropriate words so as to give reader a slight idea of content. It must be sent in English and Spanish language.

Author and Affiliations
Author's name must be written as follows: name, initial of second name and surnames. Affiliations of author must be specified in following way and order:

- Business or institution (including department or division to which he/she belongs).
- Mail address.
- City (Province/State/Department).
- Country.
- Telephone.

Abstract
Short essay of no more than one hundred fifty (150) words specifying content of work, scope and results. It must be written in such a way so as to contain key ideas of document. It must be sent in English and Spanish language.

Key Words
Identify words and/or phrases (at least three) that recovers relevant ideas in an index. They must be sent in English and Spanish language.

Introduction
Text must be explanatory, clear, simple, precise and original in presenting ideas. Likewise, it must be organized in a logic sequence of parts or sections, with clear subtitles that guide reader. The first part of document is the introduction. Its objective is to present the theme, objectives and justification of why it was elected. Likewise, it must contain sources consulted and methodology used as well as a short explanation of status of research if it were the case and form in which the rest of article is structured.

Body Article
It is made up of the theoretical framework supporting the study, statement of theme, status of its analysis, results obtained and conclusions.

Equations, Tables, Charts ang Graphs
All of these elements must be numbered in order of appearance according to its type and have at the foot, that is, exactly underneath of chart, graph or picture, the source from where data was taken and who made it.

Equations must be numbered on the right hand side of column containing it, in the same line and in parenthesis. Body of text must make reference of it as "(Equation x)". When the reference starts a sentence it must be made as follows: "Equation x".

Equations must be written so that capital letters can be clearly differenced from small letters. Avoid confusions between letter "l" and number one or between zero and small letter "o". All subindexes, superindexes, Greek letters and other symbols must be clearly indicated.

All expressions and mathematical analysis must explain all symbols (and unit in which it is measured) that have not been previously defined in the nomenclature. If work is extremely mathematical by nature, it would be advisable to develop equations and formulas in appendixes instead of including them in body of text.

Figure/Fig. (lineal drawings, tables, pictures, figure, etc.) must be numbered according to order of appearance and should include the number of graph in parenthesis and a brief description. As with equations, in body of text, reference as "(Fig. X)", and when reference to a graph is the beginning of a sentence it must be made as follows: "Fig. x".

Charts, graphs and illustrations must be sent in modifiable vector file format (*Microsoft Excel*, *Microsoft Power Period* and/or *Microsoft Visio*). Pictures must be sent in TIF or JPG format files, separate from main document in a resolution higher than 1000 dpi.

Foot Notes
We recommend their use as required to identify additional information. They must be numbered in order of appearance along the text.

Acknowledgment
Acknowledgments may be made to persons or institutions considered to have made an important contribution and not mentioned in any other part of the article.

Bibliographic References

The bibliographic references must be included at the end of the article in alphabetical order and shall be identified across the document. For the citation of references the Journal uses ISO 690 standards, which specifies the mandatory elements

to cite references (monographs, serials, chapters, articles, and patents), and ISO 690-2, related with the citation of electronic documents.

Quotations
They must be made in two ways: at the end of text, in which case last name of author followed by a comma and year of publication followed in the following manner:

"Methods exist today by which carbon fibers and prepregs can be recycled, and the resulting recyclate retains up to 90 percent of the fibers' mechanical properties" *(Davidson, 2006)*.

The other way is:
Davidson (2006) manifests that "Methods exist today by which carbon fibers and prepregs can be recycled, and the resulting recyclate retains up to 90 percent of the fibers' mechanical properties".

List of References
Bibliographic references of original sources for cited material must be cited at the end of article in alphabetical order and according to following parameters:

In the event of more than one author, separate by commas and the last one by an "and". If there are more than three authors write the last name and initials of first author and then the abreviation "et al.".

Books
Last name of author followed by a comma, initial(s) of name followed by a period, the year of publication of book in parenthesis followed by a comma, title of publication in italics and without quotation marks followed by a comma, city where published followed by a comma and name of editorial without abbreviations such as Ltd., Inc. or the word "editorial".

Basic Form:
LAST NAME, N.I. *Title of book*. Subordinate responsibility (optional). Edition. Publication (place, publisher). Year. Extent. Series. Notes. Standard Number.
Example:
GOLDBERG, D.E. *Genetic Algorithms for Search, Optimization, and Machine Learning*. Edition 1. Reading, MA: Addison-Wesley. 412 p. 1989. ISBN 0201157675.

If a corporate author
Write complete name of entity and follow the other standards.

Basic form:
INSTITUTION NAME. *Title of publication*. Subordinate responsibility (optional). Edition. Publication (place, publisher). Year. Extent. Series. Notes. Standard Number.

Example:
AMERICAN SOCIETY FOR METALS. *Metals Handbook: Properties and Selection: Stainless Steels, Tool Materials and Special-Purpose Metals*. 9th edition. Asm Intl. December 1980. ISBN: 0871700093.

When book or any publication have as author an entity pertaining to the state, write name of country first.

Basic form:
COUNTRY, ENTITY PERTAINING TO THE STATE. *Title of publication*. Subordinate responsibility (optional). Edition. Publication (place, publisher). Year. Extent. Series. Notes. Standard Number.

Example:
UNITED STATED OF AMERICAN. EPA - U.S. Environmental Protection Agency. Profile of the Shipbuilding and Repair Industry. Washington D.C. 1997. P. 135.

Journal Article

Basic form:
Last name, N.I. Title of article, *Name of publication*. Edition. Year, issue designation, Pagination of the part.

Example:
SAVANDER, B. R. and TROESCHB. Mission Configurable Modular Craft Concept Study. S*hip Science and Technology*. Year 3, N.° 5, Vol. 1, July 2009, p. 31-56.

Graduation Work

Basic form:
Primary responsibility. *Title of the invention*. Subordinate responsibility. Notes. Document identifier: Country or issuing office. *Kind of patent document*. Number. Date of publication of cited document.

Example:
CARL ZEISS JENA, VEB. *Anordnung zur lichtelektrischen Erfassung der Mitte eines Lichtfeldes. Et-finder*: W. FEIST, C. WAHNERT, E. FEISTAUER. Int. Cl.3 : GO2 B 27/14. Schweiz Patentschrift, 608 626. 1979-01-15.

Presentation at conferences or academic or scientific event

Basic form:
LAST NAME, N.I. Title of the presentation. In: Sponsor of the event. *Name of the event*. Country, City: Publisher, year. Pagination of the part.

Example:
VALENCIA, R., et al. Simulation of the thrust forces of a ROV En: COTECMAR. P*rimer Congreso Internacional de Diseño e Ingeniería Naval CIDIN 09*. Colombia, Cartagena: COTECMAR, 2009.

Internet

Basic form:
LAST NAME, N.I. *Title of work*, [on-line]. Available at: http://www.direccion_completa.com, recovered: day of month of year.

Example:
COLOMBIA. ARMADA NACIONAL. Cotecmar gana premio nacional científico, [web on-line]. Available at: http://www.armada.mil.co/?idcategoria=545965, recovered: 5 January of 2010.

Acceptance

Articles must be sent by e-mail to editor of The *Ship Science and Technology* Journal to otascon@cotecmar.com or in CD to mail address of journal (Cotecmar Mamonal Km 9 Cartagena Colombia), accompanied of the "Declaration of Originality of Work Written "included in this journal. Author shall receive acknowledgement of receipt by e-mail. All articles will be submitted to Peer Review. Comments and evaluations made by the journal shall be kept in confidentiality. Receipt of articles by The Ship Science and Technology Journal does not necessarily constitute acceptance for publishing. If an article is not accepted it shall be returned to the respective author. The Journal only publishes one article by author in the same number of the magazine.

Opinions and declarations stated by authors in articles are of their exclusive responsibility and not of the journal. Acceptance of articles grants The Ship Science and Technology Journal the right to print and reproduce these; nevertheless, any reasonable petition by author to obtain permission to reproduce his/her contributions shall be attended.

Further information can be obtained by:
Sending an e-mail to sst.journal@cotecmar.com
Contacting Oscar Dario Tascón (Editor)
The Ship Science and Technology (Ciencia y Tecnología de Buques) office located at: Cotecmar Mamonal Km. 9 Cartagena Colombia. Phone Number: 57 - 5 - 6685377.

SHIP
SCIENCE & TECHNOLOGY
CIENCIA & TECNOLOGÍA DE BUQUES

Statement of Originality of Written Work

Title of work submitted

_____

_____

_____

I hereby certify that work submitted for publication in The *Ship Science and Technology* journal, of Science and Technology for the Development of Naval, Maritime and Riverine Industry Corporation, Cotecmar, was written by me, given that its content is product of my direct intellectual contribution. All data and references to material already published are duly identified with its respective credit and included in the bibliographic notes and quotations highlighted as such.

I therefore declare that all materials submitted for publication are completely free of copyrights; consequently, I make myself responsible for any lawsuit or claim related with Intellectual Property Rights thereof.

In the event that article is chosen for publication by The *Ship Science and Technology* journal, I hereby state that I totally transfer reproduction rights of same to Science and Technology for the Development of Naval, Maritime and Riverine Industry Corporation, Cotecmar. In retribution for present transfer I agree to receive two issues of the journal where my article is published.

In witness thereof, I sign this statement on the _____ day of the month of _____ of year _____, in the city of _____ .

Name and signature: Identification document:

_____ _____

Km. 9 Vía Mamonal - Cartagena, Colombia
www.shipjournal.co

Passenger Submarine Concept Design for Oil Production Offshore Systems

Thiago Lobão de Almeida, Victor Coracini Tonacio

CFD modeling of 2D impact with symmetric entry

Roberto Algarín, Antonio Bula, Oscar Tascón

Electric Arc Spray Coatings for the Naval Industry

Laura Marcela Dimate Castellanos, José Alfredo Morales Torres, Jhon Jairo Olaya Florez

Aid in the Design of Antenna Arrays with Electronic Phase Steering using Matlab®

Francisco José Gil Navia

Design methodology of a military messaging system

Gustavo Pérez V., Stefany Marrugo Li.

COTECMAR

www.shipjournal.co